# OXYLIPIN SIGNALS GOVERN DROUGHT AND SALT TOLERANCE AND RESISTANCE TO PATHOGENS

A Dissertation

by

PEI-CHENG HUANG

Submitted to the Office of Graduate and Professional Studies of
Texas A&M University
in partial fulfillment of the requirements for the degree of

DOCTOR OF PHILOSOPHY

| | |
|---|---|
| Chair of Committee, | Michael Kolomiets |
| Committee Members, | Libo Shan |
| | Hisashi Koiwa |
| | Seth Murray |
| Head of Department, | Leland Pierson III |

December 2017

Major Subject: Plant Pathology

## ABSTRACT

Lipid signals derived from lipoxygenases (LOX), called oxylipins, emerge as pivotal mediators in responses to environmental constraints including biotic and abiotic stresses. Anthracnose leaf blight and stalk rot caused by *Colletotrichum graminicola* are major diseases threatening corn production; drought and salinity severely devastate crop yield. The involvement of specific LOXs in defense responses to *C. graminicola* and tolerance to drought and salinity remain largely unknown. The first objective of this study was to elucidate the functions of dual-specific LOXs in defense against *C. graminicola*. The second objective aimed to test the hypothesis that LOXs regulate drought and salt stress tolerance in maize.

Transposon-insertional mutants and near-isogenic wild type of several LOXs, 12-oxophytodienoic reductase (OPR), and ACC synthase (ACS) were utilized to investigate the oxylipin-mediated responses to *C. graminicola*, drought, and salinity.

Results showed recombinant ZmLOX1 protein imparts both 13- and 9-LOX activities, a unique feature for plant LOX. Defense phytohormones, mechanical wounding, and Z-3-hexenal treatment significantly up-regulated *ZmLOX1* and *ZmLOX2* expression, suggesting roles in various stress responses. Disruption of these genes does not impair wound-induced JA biosynthesis. Genetic evidence is provided that disruption of *ZmLOX1* or *ZmLOX2* caused a significant decrease in resistance to *C. graminicola* in leaves that associated with lower benzoic acid (BA) and salicylic acid (SA) accumulation. By contrast, *lox1-3* and *lox2-1* mutants accumulated significantly higher

level of SA, but lower 10-oxo-11-phytoenoic acid (10-OPEA) in stalks upon *C. graminicola* infection, resulting in increased resistance. These findings have shed light on understanding that these rare dual specific LOXs play a role in defense against pathogens.

In this study, evidence is provided that *ZmLOX2* is required for drought tolerance via regulating transpirational water loss, while *ZmLOX4* promoted drought sensitivity. Metabolite profiling and RNA sequencing results suggest that oxylipins regulate maize drought tolerance by mediating JA biosynthesis pathway. Supporting this notion, a JA-deficient mutant *opr7-5 opr8-2* displayed dramatic reduction in stomata aperture and transpirational water loss, indicating that JA serves to open stomata. Increased ET production of *opr7-5 opr8-2* under drought stress is in agreement with higher transpiration of ET-deficient *acs2 acs6* mutant, suggesting ET enhances stomatal closure. Excessive amounts of SA and 10-OPEA accumulation in *lox1-3* correlated with increased sensitivity to salt stress. Collectively, these data suggest that oxylipin signals govern drought and salt tolerance and resistance to pathogens.

## ACKNOWLEDGEMENTS

I would like to thank my committee chair, Dr. Michael Kolomiets, and my committee members, Dr. Libo Shan, Dr. Hisashi Koiwa, and Dr. Seth Murray for their guidance and support throughout the course of this research.

Thanks also go to my friends and colleagues and the department faculty and staff for making my time at Texas A&M University a great experience. Finally, thanks to my mother, father, and sister for their encouragement and to my wife for her patience and love.

## CONTRIBUTORS AND FUNDING SOURCES

### Contributors

This work was supervised by a dissertation committee consisting of Professor Michael Kolomiets and Libo Shan of the Department of Plant Pathology and Microbiology, Professor Hisashi Koiwa of the Department of Horticultural Sciences, and Associate Professor Seth Murray of the Department of Soil and Crop Science.

The Biochemical properties of recombinant ZmLOX1 for Chapter 2 was kindly provided by Professor Ivo Feussner at the Georg-August-University (Göttingen, Germany). The Southern and Northern blotting analyses in Chapter 2 were conducted in part by Dr. Yuanxin Yan of the Department of Plant Pathology and Microbiology and have not yet been published. The phytohormone and oxylipin profiling was conducted with the help of Dr. Eli Borrego of the Department of Plant Pathology. Transpirational water loss experiments were conducted by using the growth chamber space and setup of Dr. Hisashi Koiwa of the Department of Horticultural Sciences. RNA-seq and differential expression analyses were conducted by Ms. Kai He and Dr. Xiaoning Qian of the Department of Electrical and Computer Engineering.

All other work conducted for the dissertation was completed by the student independently.

**Funding Sources**

This work was made possible in part by Agriculture and Food Research Initiative Grant under Grant Number 2015-67013-22816. Its contents are solely the responsibility of the authors and do not necessarily represent the official views of the USDA National Institute of Food and Agriculture.

## NOMENCLATURE

| | |
|---|---|
| LOX | Lipoxygenase |
| OPR | Oxo-phytodienoate reductase |
| ACS | ACC synthase |
| JA | Jasmonic acid |
| ET | Ethylene |
| ABA | Abscisic acid |
| 13-HODE | (9Z,11E,13S)-13-hydroxy-octadeca-9,11-dienoic acid |
| 9-HODE | (9S,10E,12Z)-9-hydroxy-10,12-octadecadienoic acid |
| 13-KODE | (9Z,11E)-13-oxo-octadeca-9,11-dienoic acid |
| 9-KODE | ketodiene (9S,10E,12Z)-9-oxo-10,12-octadecadienoic acid |
| 12-OPDA | (+)-12-oxo-phytodienoic acid |
| JA-Ile | Jasmonyl-isoleucine |
| SA | Salicylic acid |
| BA | Benzoic acid |
| 9-HOD | (9S, 10E, 12Z)-9-hydroxy-10, 12-octadecadienoic acid |
| 9-HOT | (9S, 10E, 12Z, 15Z)-9-hydroxy-10, 12, 15-octadecatrienoic acid |
| 9-KOD | ketodiene (9S, 10E, 12Z)-9-hydroxy-10,12-octadecadienoic acid |
| 9-KOT | ketodiene (10E, 12Z, 15Z)-9-hydroxy-10, 12, 15-octadecatrienoic acid |
| 10-OPEA | 10-oxo-11-phytoenoic acid |

| | |
|---|---|
| 13-HOD | (9Z, 11E, 13S)-13-hydroxy- 9,11-octadecadienoic acid |
| 13-HOT | (9Z, 11E, 13S, 15Z)-9-hydroxy-9,11,15-octadecatrienoic acid |
| 13-KOD | keto (9Z, 11E, 13S, 15Z)-9-hydroxy-9,11,15-octadecatrienoic acid |
| MeJA | Methyl jasmonate |
| AOS | Allene oxide synthase |
| AOC | Allene oxide cyclase |
| JAR | Jasmonic acid resistant |
| JAZ | Jasmonate ZIM domain |

## TABLE OF CONTENTS


Page

ABSTRACT ..... ii

ACKNOWLEDGEMENTS ..... iv

CONTRIBUTORS AND FUNDING SOURCES ..... v

NOMENCLATURE ..... vii

TABLE OF CONTENTS ..... ix

LIST OF FIGURES ..... x

LIST OF TABLES ..... xiii

CHAPTER I INTRODUCTION ..... 1

CHAPTER II MATERIAL AND METHODS ..... 4

Background ..... 4

CHAPTER III MAIZE DUAL POSITIONAL SPECIFIC LIPOXYGENASES REGULATE SALICYLIC ACID BIOSYNTHESIS UPON *COLLETOTRICHUM GRAMINICOLA* INFECTION IN AN ORGAN-SPECIFIC MANNER ..... 13

Introduction ..... 13
Results ..... 17
Discussion ..... 42

CHAPTER IV OXYLIPINS MEDIATE DROUGHT AND SALT TOLERANCE IN MAIZE ..... 48

Introduction ..... 48
Results ..... 52
Discussion ..... 95

CHAPTER V CONCLUSION ..... 104

REFERENCES ..... 106

## LIST OF FIGURES


Page

Figure 1. Alignment of the amino acid sequences of ZmLOX1 and ZmLOX2. .... 18

Figure 2. Biochemical properties of recombinant ZmLOX1. ..... 20

Figure 3. Characterization of *lox1* and *lox2* mutants. ..... 23

Figure 4. Organ-specific and hormone- and wound-induced expression of *ZmLOX1* and *ZmLOX2*. ..... 26

Figure 5. ZmLOX1 and ZmLOX2 are not required for wound-induced JA-biosynthesis. ..... 29

Figure 6. 9- and 13-oxylipin contents in WT, *lox1-3*, and *lox2-1* in response to wounding. ..... 30

Figure 7. *ZmLOX1* and *ZmLOX2* are essential for resistance against anthracnose leaf blight. ..... 33

Figure 8. Benzoic acid (BA), SA, JA, and JA-Ile contents in WT, *lox1-3*, and *lox2-1* leaves in response to *C. graminicola* infection. ..... 34

Figure 9. Concentration of 9-, and 13-oxylipins in leaves of WT, *lox1-3*, and *lox2-1* in response to *C. graminicola* infection. ..... 35

Figure 10. ZmLOX1 and ZmLOX2 facilitate pathogenicity of *C. graminicola*. ..... 37

Figure 11. Accumulation of 9- and 13-oxylipins in stalks of WT, *lox1-3*, and *lox2-1* in response to *C. graminicola* infection. ..... 39

Figure 12. Accumulation of jasmonates, ABA and SA in stalks of WT, *lox1-3*, and *lox2-1* in response to *C. graminicola* infection. ..... 41

Figure 13. Proposed model of *ZmLOX1* and *ZmLOX2* mediated interactions with *C. graminicola* in leaves and stems. ..... 47

Figure 14. Transpirational water loss of maize B73 inbred line and lipoxygenase genes expression in leaf and root of B73 plant in response to withholding water. ..... 54

Figure 15. *ZmLOX2* promotes drought tolerance by reducing transpirational water loss. ..... 56

Figure 16. *ZmLOX4* promotes drought sensitivity via increasing transpirational water loss. ..... 58

Figure 17. Disruption of *ZmLOX3* and *ZmLOX6* increased transpirational water loss while *ZmLOX5* is required for prolonged drought stress tolerance. 60

Figure 18. *ZmLOX4*- and *ZmLOX2*-mediated pathways interact in response to drought. ..... 62

Figure 19. Accumulation of ABA and SA in leaves and roots of WT, *lox2-1*, *lox4-7*, *lox5-3* and *lox2-1 lox4-7* mutant in response to 4 and 6 days of water deprivation. ..... 65

Figure 20. Accumulation of 12-OPDA, JA, and JA-Ile in leaves and roots of WT, *lox2-1*, *lox4-7*, *lox5-3* and *lox2-1 lox4-7* mutant in response to 4 and 6 days of water deprivation. ..... 66

Figure 21. Accumulation of 9-oxylipins in leaves and roots of WT, *lox2-1*, *lox4-7*, *lox5-3* and *lox2-1 lox4-7* mutant in response to 4 and 6 days of water deprivation. ..... 67

Figure 22. Accumulation of 13-oxylipins in leaves and roots of WT, *lox2-1*, *lox4-7*, *lox5-3* and *lox2-1 lox4-7* mutant in response to 4 and 6 days of water deprivation. ..... 68

Figure 23. Profile of gene expression in leaf and root under both well-watered and drought-stressed conditions. ..... 70

Figure 24. Profile of differentially expressed genes (DEGs) in leaf and root in response to drought stress in drought sensitive *lox2-1* and *lox5-3* mutants, intermediate WT, and drought tolerant *lox4-7* and *lox2-1 lox4-7* mutants. ..... 73

Figure 25. Expression of genes involved in JA biosynthesis pathway in response to drought in leaves. ..... 78

Figure 26. Expression of potassium channel proteins specific to guard cells and subsidiary cells. ..... 80

Figure 27. Validation of RNA-seq expression through qRT-PCR. ..... 81

Figure 28. Exogenous 12-OPDA application restored *lox2-1* transpirational water loss to WT level. ..... 83

Figure 29. JA promotes stomatal opening. ..... 85

Figure 30. Ethylene enhances stomatal closure. ..... 87

Figure 31. *ZmLOX1* promotes salt stress tolerance. ..... 89

Figure 32. Accumulation of ABA and SA in leaves and roots of WT and *lox1-3* mutant in response salt stress. ..... 91

Figure 33. Accumulation of 12-OPDA, JA and JA-Ile in leaves and roots of WT and *lox1-3* mutant in response salt stress. ..... 92

Figure 34. Accumulation of 9-oxylipins in leaves and roots of WT and *lox1-3* mutant in response salt stress. ..... 93

Figure 35. Accumulation of 13-oxylipins in leaves and roots of WT and *lox1-3* mutant in response salt stress. ..... 94

Figure 36. Proposed model of oxylipin signals mediated drought and salt stress responses in maize. ..... 103

## LIST OF TABLES

Page

Table1. List of primers used in this study ..... 12

Table 2. Enriched GO terms of candidate drought tolerance genes. ..... 74

Table 3. Enriched GO terms of candidate drought sensitivity genes. ..... 75

# CHAPTER I

# INTRODUCTION

Biotic and abiotic stresses severely impact plant growth and crop production, causing dramatic yield loss worldwide. Scientific studies predict that extreme weather, including drought incidents, may happen more frequently and intensely with global climate change in the future (Woodward et al., 2016). The world population has surpassed 7.5 billion in 2017 and is estimated to reach 9 billion or more by 2050, and food production would have to increase by 70% in order to feed the world's surging population (Fischer et al., 2005; Smith and Gregory, 2013; McKersie, 2015). Therefore, developing disease resistant and drought tolerant crops is an urgent challenge to solve the food supply problem. Maize is the number one cereal crop produced and a staple food of people in Americas and Africa and a major feed source for livestock worldwide. Maize is also used to produce a variety of food and products for industrial purposes (Ranum et al., 2014). Therefore, developing pathogen-resistant and drought-tolerant maize lines will not only help supply food in the future, but also result in other economic benefits.

Anthracnose leaf blight (ALB) and stalk rot (ASR) diseases caused by hemi-biotrophic fungal pathogen *C. graminicola* are worldwide economically important diseases on maize (Bergstrom, 1999). Both diseases combined account for a yield loss greater than one billion dollars annually, and are major threats for corn production in the US (Frey, 2011). *C. graminicola* infects plant with a brief biotrophic phase before switching into a more destructive necrotrophic lifestyle. However, the molecular details

and factors regulating the transition have yet to be identified (Dean et al., 2012). Disruption of *ZmLOX3* caused increased resistance to *C. graminicola* (Gao et al., 2007), and further studies are needed to test the interactions regulated by other *LOX* isoforms.

Drought and high soil salinity are the major abiotic stresses that can cause up to 50% yield loss or more in combination with other stressful conditions (Fita et al., 2015). Drought is the most devastating stress for agriculture, and more than 50% of land surface on earth is arid or semiarid where constant irrigation is required for agricultural production. As of now, salt stress is estimated to affect more than 20% of the irrigated cropland worldwide, leading to severe yield reduction (Owens, 2001; Flowers, 2004). However, unlike dicotyledonous model plant *Arabidopsis thaliana*, drought tolerance mechanisms remain largely unknown in monocotyledonous *Zea mays*.

In plants, lipid signaling plays a pivotal role in various biological processes, such as growth and development (Acosta et al., 2009; Yan et al., 2014), abiotic stress responses (Grebner et al., 2013; Savchenko et al., 2014), and microbe- and herbivore-induced defense responses (Yan et al., 2012; Christensen et al., 2013). Oxidized polyenoic fatty acids are collectively called oxylipins, and the majority of them are derivatives of seven downstream branches of lipoxygenase (LOX) pathways (Feussner and Wasternack, 2002). LOXs in plants incorporate molecular oxygen into linoleic acid (C18:2) and linolenic acid (C18:3) at either carbon position 9 or 13 of the 18 carbon chain and are functionally grouped into 9-LOXs and 13-LOXs (Howe and Schilmiller, 2002). Accumulating evidence suggests that oxylipins are plant signaling molecules for

both biotic and abiotic stresses (Vellosillo et al., 2007; Constantino et al., 2013; Lim et al., 2015).

This study focuses on examining the role of 9- and 13-oxylipins in defense against fungal pathogen *C. graminicola*, regulation responses to drought and salt stresses in maize and to investigate the molecular and biochemical mechanisms behind increased/decreased resistance and tolerance in response to pathogen and abiotic stresses. The knowledge obtained from this study is expected to help understand the biochemical function of oxylipins in pathogen defense response and abiotic stress tolerance. The results may also help identify genes and gene networks responsible for drought tolerance to assist scientists and plant breeders in molecular breeding and genome-wide association mapping.

# CHAPTER II

# MATERIAL AND METHODS

## BACKGROUND

### Plant material

For functional characterization of dual positional specific *ZmLOX1* and *ZmLOX2*, experiments were conducted on *lox1-3* and *lox2-1* mutants, which had been advanced to $BC_7$ stage and their WT (B73 inbred line). For transpirational water loss and prolonged drought stress survival assays, wild type, *lox1-1*, *lox1-3*, *lox1-4*, *lox2-1*, *lox3-4* (Gao et al., 2007), *lox4-1*, *lox4-7*, *lox5-3*, *lox10-3* (Christensen et al., 2013), *acs6*, *acs2 acs6* (Young et al., 2004) and *opr7-5 opr8-2* (Yan et al., 2012) were advanced to the $BC_7$ genetic stage. Mutants of *lox4-10* and near-isogenic WT were at $BC_5$ stage. Different mutants in W438 genetic background were also evaluated for the phenotype. Mutant of *lox2-1* and its near-isogenic WT in W438 genetic background were at the $BC_5$ genetic stage. Mutants of *lox6-1*, *lox6-2*, and *lox6-3* and their near-isogenic WT in the W438 genetic background were at $BC_3$ genetic stage. Mutants of *lox10-3* in the B73 and W438 genetic background were at the $BC_7$ genetic stage. For salt stress tolerance screening, maize WT (B73 inbred line) and near-isogenic *lox1-3*, *lox2-1*, *lox4-7*, and *lox5-3* were at $BC_7$ genetic stage. For the study of resistance against anthracnose leaf blight and stalk rot caused by *Colletotrichum graminicola*, maize WT and near-isogenic *lox1-3* and *lox2-1* in the B73 genetic background were at the $BC_7$ genetic stage. For genotyping plant materials, polymerase chain reaction (PCR) was conducted as described in (Gao et al., 2007) using gene-specific primers listed in Table 1.

**Southern and Northern blot analyses**

Southern and Northern blot analyses were conducted following the protocol described by Gao et al., 2007. DNA for Southern blot was extracted using urea-based extraction protocol and RNA for Northern blot was isolated using TRI reagent. The gene-specific probes for *ZmLOX1* and *ZmLOX2* were amplified by PCR from the 3'-UTR region with gene-specific primers.

**Biochemical property of recombinant ZmLOX1**

Over-expression vector containing open reading frame (ORF) of *ZmLOX1* was constructed as described by Nemchenko et al., 2006 to produce recombinant ZmLOX1 protein in *E. coli*. The *E. coli* cultures were grown in LB broth media at 37°C overnight until cell density reach $A_{600}$=0.7 and then 1mM of IPTG was added to induce the expression of the construct at 15°C for 48 hours. Cell cultures were then centrifuged and re-suspended in 30ml lysis buffer (50mM Tris-HCl, pH7.5) containing 10% (v/v) glycerol, 0.5 M NaCl, and 0.1% Tween-20 and disrupted by sonication. After centrifugation at 12,000*g* for 15 minutes, cell debris and membranes were removed and supernatant was incubated with linoleic acid as substrate (120 µM final concentration) in 1 ml of 0.1 M sodium phosphate buffer (pH 5.7-7.0) or 0.1 M Tris buffer (pH 7.7-8.6) for 20 minutes at room temperature. Then 100 µl of glacial acetic acid was added to terminate the reaction. Solvent from organic phase was vacuum dried and remaining lipids were re-suspended in 0.1 ml of high-performance liquid chromatography (HPLC) solvent. The oxidation products were measured by HPLC as described in (Nemchenko et al., 2006).

**Anthracnose leaf blight and stalk rot assays**

Anthracnose leaf blight and stalk rot assays were performed following the protocol from (Gao et al., 2007). For anthracnose leaf blight assay, *lox* mutants and WT plants were grown in conical pots (20.5 by 4 cm) in commercial potting mix for 2 to 3 weeks to reach V3 stages (three fully expanded leaves) as the same condition described above. Plants were laid down on sterile paper towel in the trays (78.5 x 63 x 7 $cm^3$). Conidial suspension of *C. graminicola* strain 1.001 was prepared from a potato dextrose agar plate and the third leaves of each plant were drop inoculated with 10 $\mu$l of conidial suspension ($10^6$ conidia/ml), with six droplets per leaf. Sterile water was subsequently added, and the tray was sealed with Press'n Seal Saran wrap (The Glad Products Company, Oakland, CA, U. S. A.) to form a humid growth chamber. The plants were returned to an upright position 24 hours after inoculation and grown under the same condition prior to inoculation. The disease symptoms were scanned and lesion areas were measured using ImageJ software (ImageJ 1.50i; Wayne Rasband, NIH, Bethesda, MD, USA) 5 days post inoculation.

For stalk rot assays, stalks of mid-silking plants (about 10-weeks old) grown in a green house with a temperature of 22 to 28°C were wounded using a sterile needle (1 cm in depth) and then infected with conidial suspension of *C. graminicola*. A sterile Q-tip cotton swab soaked with the conidia suspension (about 150 µl of $10^6$ spores/ml) was placed on the wound site and subsequently sealed with Parafilm to form a humidity chamber. Three internodes around the brace roots were infected on each plant. Stalks

were split longitudinally and scanned. The lesion areas were scanned and measured by ImageJ software.

**Phytohormone and oxylipin profiling**

Phytohormone extraction was performed following the protocol from (Christensen et al., 2013) with modifications. Leaf or root tissues were harvested in liquid $N_2$ and ground into power by using a mortar and pestle. About 100 mg of ground plant tissues were placed in a 2 ml screw-cap Fast-Prep tube (Qbiogene, Carlsbad, CA, U. S. A.) with the standard dihydro JA (10-50ng) and shaken for 30 minutes at 4 °C. Each tube was then added with 500 µl dichloromethane and shaken for 30 minutes at 4°C and centrifuged for 5 minutes at 13,000 rpm. The bottom organic phase was transferred into 1.8 ml glass vials (VWR International, West Chester, PA, USA), evaporated by continuous $N_2$ gas, and then dissolved in 150 µl methanol. Then the dissolved sample were transferred into 1.5 ml tube and centrifuged at 13,000 rpm for 5 minutes and 100 µl of the sample was transferred into auto-sampler vials. Phytohormone and oxylipin measurements were performed by using a QTrap 2000 (Applied Biosystems, Foster, CA, USA) LC/MS with a Discovery C18 HPLC column (5 cm X 2.1, 5 µm particle size; Supelco, Bellefonte, PA, USA) and a flow rate of 100 µl $min^{-1}$.

**Transpirational water loss and prolonged drought stress screening**

Transpirational water loss measurements were performed with slight modification following the protocol from (Ruggiero et al., 2004). Maize WT and mutant seeds were grown in conical pots (15 by 3 cm) in same amount (dry weight) of filtered sterile (autoclaved) commercial potting mix (Metro-Mix 366; Scotts-Sierra Horticultural

products, Marysville, OH, U. S. A.) at 22°C under a 14 hours day length, 50% humidity, 200 $\mu$mol $m^{-2}$ $s^{-1}$ of light in laboratory. Fourteen days after sowing, pots with seedlings (at V2 stage) were soaked in deionized water for more than 30 minutes to reach 100% water content in soil and then each pot was covered with Parafilm to avoid water loss from the soil surface. Three plants were then placed on an electronic balance under a 12 hours day length with light intensity of 140 $\mu$mol $m^{-2}$ $s^{-1}$ at 27°C, and the weight was automatically measured every twenty minutes for 7 days using WinWedge software. Water loss through transpiration was normalized for plant dry weight taken at the end of the experiment. For prolonged drought stress survival, two-weeks old plants were well-watered, which involved soaking them in water to reach 100% water content in soil and then placing them on a plant light shelf and withholding additional water. Re-watering was done when either WT or mutant plants were wilted and collapsed. Survival phenotypes were recorded three to seven days after re-watering (Meeks et al., 2013).

**Salt stress tolerance screening**

WT and *lox* mutant seeds were grown in conical pots (20.5 by 4 cm) in same amount (dry weight) of sterile (autoclaved) commercial potting mix (Metro-Mix 366; Scotts-Sierra Horticultural products, Marysville, OH, USA) at 22°C under a 14 hours day length, 50% humidity, 200 $\mu$mol $m^{-2}$ $s^{-1}$ of light in laboratory. Five days after sowing, each conical pot with seedlings was given 10 ml of sterile deionized water (mock) or 200 mM NaCl (salt stress) every day. Fourteen days after treatment, soil was gently rinsed away and growth phenotypes such as shoot length, shoot dry weight, root length, and root dry weight were recorded at the end of the experiment.

**Ethylene measurement**

Ethylene measurements were performed by using the fourth leaves of plants that have been well-watered every day (control) or withholding water for six days following the protocol from (Gao et al., 2008b) with modifications. The fourth leaves were excised from the plants and subsequently transferred into a 15 ml syringe with 2 ml headspace. After incubation for 30 minutes, 1 ml volume of headspace gas was injected into a digital gas chromatograph (Photovac 10 plus; Perkin-Elmer, Inc., Norwalk, CT, USA) with a photo detector and compressed air (ultra zero grade; Praxair, Inc., Danbury, CT, USA) as carrier gas.

**RNA isolation and qRT-PCR**

Maize leaf and root tissues were frozen in liquid $N_2$, and ground into powder by mortar and pestle. About 150 to 200 mg of plant tissue were used for RNA extraction. Total RNA was extracted using TRI reagent (Molecular Research Center Inc., Cincinnati, OH, USA) according to the manufacturer's protocol. For RNA sequencing sample preparation, total RNA was extracted using TRI reagent and then cleanup was done by using QIAGEN RNeasy Mini Kit column (RNeasy Mini Kit; Qiagen, Valencia, CA, U. S. A.). A total 2 µg of RNA sample each sample was sent out for RNA-sequencing at AgriLife Genomics and Bioinformatics Service. For a quantitative reverse transcription-PCR (qRT-PCR) assay, a one-step qPCR procedure was performed using Thermo Scientific Verso One-Step RT-qPCR Kits (Thermo Scientific, Waltha, MA, USA) with a reaction optimized following the protocol described in (Constantino et al., 2013).

**RNA-sequencing and processing and mapping of illumina reads**

Total RNA was extracted using the method described above and the cDNA library construction and sequencing were conducted by AgriLife Genomics and Sequencing Service. TruSeq Stranded Total RNA Library Prep Kit was used to construct the cDNA library and the cDNA library was sequenced on the Illuminia Hiseq 2500 platform with 50bp single-end sequencing. After preprocessed reads were mapped to Zea_mays.AGPv3 release 22 (downloaded from ftp://ftp.ensemblgenomes.org/pub/plants/release-22), and Tophat 2.1.1, a fast splice junction mapper for RNA-Seq reads, was used as the aligner in this study.

**Transcript assembly and differential expression analysis**

The aligned reads were quantified by Cufflinks 2.2.1. FPKM in Fragments Per Kilobase of transcript per Million mapped reads, as the unit of measurement for the transcript abundance. After assembling mapped reads to transcript fragments, differential expression analysis was performed by Cuffdiff 2.2.1. Genes were considered as significantly differentially expressed genes (DEGs) only if the adjusted *p*-value (*q*-value) is smaller than 0.05 and the absolute value of $\log_2$ (fold Change) was larger than 0.58.

**Gene ontology (GO) analysis of selected DEGs**

Agrigo (GO analysis toolkit and database for the agriculture community; http://bioinfo.cau.edu.cn/agriGO/index.php) was used for conducting GO analysis. Candidate DEGs were submitted to agriGO and enriched GO terms were selected using Singular Enriched Analysis (SEA) with the maize reference genome B73 as the

background (Schnable et al., 2009). The GO analysis results shown in this study had FDR less than 0.05.

**Stomatal aperture measurement**

Epidermal strips of decent size were peeled from the 1st true leaf of plants at V2 stage and placed into a petri dish with 25 ml stomatal opening buffer (10mM MES-KOH, 50mM KCl, pH6.2). The peels were incubated in the petri dish with $CO_2$-free air being directly bubbled in for 1 and ¾ hours under growth lights. The peels were then transferred into a new petri dish with fresh 25 ml stomatal opening buffer containing 0.001% FDA with 100 μM MeJA and incubated for an additional hour with $CO_2$-free air under growth lights. Then, photos were taken from at least 100 stomata from at least eight peels per treatment and stomatal aperture was measured using ImageJ.

**Data analysis**

JMP® Pro 12.0.1 (SAS Institute, Inc) statistical package was used for data analysis. Differences between values were calculated using one-way analysis of ANOVA with Students' *t*-test at a significance level of 0.05.

Table1. List of primers used in this study

| Primer Name | Primer sequence | Purpose |
|---|---|---|
| LOX1 3'UTR F | TCTGTCTGAGCTGAGGACGTA | LOX1 probe |
| LOX1 3' UTR R | TCCTCAATAATGAAGTTACTTTGTG | LOX1 probe |
| LOX2 3' UTR F | TTCCATCTGATTCGATCGAG | LOX2 probe |
| LOX2 3' UTR R | GTTGGTTTCCCAATAATAATGTG | LOX2 probe |
| 9242 | AGAGAAGCCAACGCCAWCGCCTCYA | *Mutator* transposon |
| LOX1-1 F | AGATGTTCGGGAACATCGGAAAG | *lox1-1* genotyping |
| 51469 R | TACTTGGACTGCGGGTAGATCCATGAGT | *lox1-1* genotyping |
| LOX1 intro F | CTCAGCTCAGCTGTGCACTGAA | *lox1-3* and *lox1-4* genotyping |
| LOX1-3 gspR | CTGCTCTGTGAAGTTCCAGTCCTT | *lox1-3* genotyping |
| LOX1-4 gspR | ACGAACACCTTCTCCGGCTTGCG | *lox1-4* genotyping |
| LOX2-1 gspF | TGATCGAGGTCAACAGCCTGAAC | *lox2-1* genotyping |
| LOX2-1 gspR | GAAGTTCCAGCTGCCGTAGACTTT | *lox2-1* genotyping |
| LOX3-4F | CTCGCCAAGGCCTATGTCGCCGTC | *lox3-4* genotyping |
| LOX3-4R | GGATCTGGCTCGTGATGGTGTGGAT | *lox3-4* genotyping |
| LOX4-1F | CTTTGCTCGCCGCCACATCACATT | *lox4-1* genotyping |
| LOX4-1R | GGGAGTAGAGATTGTGCGGGTAGAT | *lox4-1* genotyping |
| LOX4-7F | GTTCCTCAGAAGCATTCTGCCCGAT | *lox4-7* genotyping |
| LOX4-7R | CAAGTTGCCAGACGTGGCCCTCAG | *lox4-7* genotyping |
| LOX4-10F | GCCGGACCAGTCAAGCCCCTAC | *lox4-10* genotyping |
| LOX4-10R | ATCTACAAACCATCCGCTCAGGC | *lox4-10* genotyping |
| LOX5-3F | TGCCGGACCAGTCAAGCCCATAT | *lox5-3* genotyping |
| LOX5-3R | GGCCCCTTCCGGTTCTTCAAGTC | *lox5-3* genotyping |
| 51499 | CTGTACAACGACCTGGGGAACCCA | *lox6-2* genotyping |
| LOX6-2gspF | TGTGTCAAGGAAGAAACGCCGAG | *lox6-2* genotyping |
| LOX6-2gspR | GTCGTGCCTCAGGTCATTTCAGGTGC | *lox6-2* genotyping |
| 61562 | GGAAGCGCAGATCCTTCTTGTTGATGAG | *lox10-3* genotyping |
| 61568 | CGGCTGTTCATCCTGGACTACCAC | *lox10-3* genotyping |
| OPR7F | AGTGGCGATTCGCTTTCGAACC | *opr7-5* genotyping |
| OPR7R(in) | ACCAGTCGCAGTCAAGAGGACCAT | *opr7-5* genotyping |
| OPR8F | ACCTCGACGCGTACGACTCCAA | *opr8-2* genotyping |
| OPR8R(supp) | GAGATGACTGCTGATTGCTGTGCA | *opr8-2* genotyping |
| ACCF1 | CCAGATGGGCCTCGCCGAGAAC | *acs2* and *acs6* genotyping |
| ACC1 | GTTGGCGTAGCAGACGCGGAACCA | *acs2* and *acs6* genotyping |

# CHAPTER III

# MAIZE DUAL POSITIONAL SPECIFIC LIPOXYGENASES REGULATE SALICYLIC ACID BIOSYNTHESIS UPON *COLLETOTRICHUM GRAMINICOLA* INFECTION IN AN ORGAN-SPECIFIC MANNER

## INTRODUCTION

Plants produce an array of small signaling molecules to mediate defense against pathogens and the best studied are defense phytohormones, such as SA, JA, and ET. In response to pathogen infection, phytohormones interact with each other synergistically and antagonistically. SA has been extensively investigated in the plant-pathogen interaction (Kumar, 2014) and acts as a plant defensive molecule against biotrophic and hemi-biotrophic pathogens (Boatwright and Pajerowska-Mukhtar, 2013). JA/ET play important roles synergistically in resistance against necrotrophic pathogens (Glazebrook, 2005). Both JA and SA contents are accumulated in response to *C. graminicola* infection implicated for plant immunity (Balmer et al., 2013; Miranda et al., 2017). Exogenous or biotroph-induced SA accumulation abolishes JA-dependent defense against necrotrophic pathogen *Alternaria brassicicola* (Spoel et al., 2007). Coronatine secreted by virulent *Pseudomonas syringae* strains acts as a molecular mimic of bioactive JA-Isoleucine conjugate (JA-Ile) to overcome SA-mediated stomatal closure (Wasternack, 2017). A newly emerging group of poorly understood defense mediators are lipid-derived small molecules called oxylipins. While in mammalian systems many oxylipins are recognized as major hormones that regulate central processes of immunity, inflammation, allergy,

and reproductive development (Funk, 2001), in plants, research into their roles in diverse physiological responses has only recently begun.

Oxylipins constitute a family of oxidized polyenoic fatty acids that mostly derive from lipoxygenases (LOX) and seven downstream sub-branch pathways. LOX isoforms in plants are functionally grouped into 9- and 13-LOXs which incorporate molecular oxygen into either carbon position 9 or 13 of the 18 carbon chain of the substrate linoleic (18:2) or linolenic acid (18:3). The resulting products are therefore named 9- or 13-oxylipins with each group containing hundreds of known molecules with hypothesized unique functions (Borrego and Kolomiets, 2016). The only well investigated small group of 13-oxylipins derived from 13-LOX pathway are jasmonates comprising JA-precursor, 12-oxo-phytodienoic acid (12-OPDA), jasmonic acid (JA) and JA-Ile, and derivatives of JA. Jasmonates are involved in reproductive development, wound response, abiotic stress tolerance, and defense against herbivores and necrotrophic pathogens (Wasternack, 2007) including recent advances made in maize (Borrego and Kolomiets, 2016).

In contrast to jasmonates, which have been studied for decades, little is known about the function of a vast array of 9-oxylipins downstream of non-JA producing 9-LOX pathway. 9-LOXs play important roles in the interaction between host and pathogens and can either promote resistance or in specific instances, even facilitate pathogenicity of specific pathogens (Gao et al., 2007; Gao et al., 2009; Marcos et al., 2015). In addition to 9- or 13-LOXs, non-traditional LOXs possessing dual positional specific enzymatic activities have been reported in plants including apple, barley,

cucumber, maize, lentil, pea, peanut, potato, and rice (Feussner and Wasternack, 2002; Porta and Rocha-Sosa, 2002; Kim et al., 2003; Schiller et al., 2015), but not in the model plant, *Arabidopsis thaliana* and related Brassicaceae. The function of these enigmatic enzymes has not yet been clearly characterized. Apple dual positional specific MdLOX1a is responsible for the majority of the LOXs activity in intact apple fruit and contributes to the generation of C6-aldehydes during apple ripening (Schiller et al., 2015). Maize LOX1 has been reported to possess both 9- and 13-LOX activities (Kim et al., 2003). It mainly localizes in cytoplasm when transgenically expressed in rice but can be associated with chloroplast *in vitro* with increased concentrations of $Ca^{2+}$ (Cho et al., 2011).

Accumulating evidence suggests that 9-oxylipins are key determinants of the outcomes of diverse plant-pathogen interaction systems. Disruption of the maize 9-LOX, LOX3, results in increased resistance against *Fusarium verticillioides, Cochliobolus heterostrophus* and *Colletotrichum graminicola* but increased susceptibility to *Aspergillus spp.* (Gao et al., 2007; Gao et al., 2009). Also, *ZmLOX12*, another predominant 9-LOX, is required for resistance against *F. verticillioides* via activation of JA-mediated defense (Christensen et al., 2014). Transgenic rice expressing maize *LOX1* under a constitutive 35S-promoter increased resistance against fungal pathogen *Magnaporthe grisea* (Cho et al., 2012). Arabidopsis 9-LOXs, *LOX1* and *LOX5*, have also been reported to modulate plant defense against an obligate biotrophic pathogen, *Golovinomyces cichoracearum*, through activation of brassinosteroid signaling (Marcos et al., 2015). Therefore, various 9-oxylipins produced by different LOXs mediate

interaction with pathogen via regulating phytohormone pathways. Because the physiological functions of the mixed function 9/13-LOXs are not understood in any plant species, in this study, we aimed to decipher the functions of these genes and to test the hypothesis that two maize dual positional specific lipoxygenases, *ZmLOX1* and *ZmLOX2*, are involved in the interaction of maize leaves and stalks with *C. graminicola*.

Using reverse genetic approach, this study provide evidence that two dual positional specific lipoxygenases, *ZmLOX1* and *ZmLOX2*, regulate SA biosynthesis upon *C. graminicola* infection in an organ-dependent manner. Despite recombinant ZmLOX1 protein has both 13- and 9-LOX activities *in vitro*, neither ZmLOX1 nor ZmLOX2 are directly involved in wound-induced JA biosynthesis *in vivo*. Stress-related phytohormones including JA, ET, and ABA and mechanical wounding and Z-3-hexenal significantly up-regulate both *ZmLOX1* and *ZmLOX2* expression. Disruption of *ZmLOX1* or *ZmLOX2* caused a significant decrease in resistance to *C. graminicola* in maize leaves associated with lower BA and SA accumulation. In contrast to that, *lox1-3* and *lox2-1* mutants accumulated significantly higher SA but lower 10-OPEA in stalks upon *C. graminicola* infection resulting in increased resistance. These findings have shed light on understanding these rare dual specific LOXs have unique functions.

## RESULTS

### Amino acid sequence analysis of ZmLOX1 and ZmLOX2

Full-length cDNA sequences of *ZmLOX1* and *ZmLOX2* have been identified by sequence analyses of the DuPont/Pioneer and publicly available EST collection from *Zea mays* cultivar B73 as described in (Nemchenko et al., 2006). Full-length cDNA of *ZmLOX1* (GenBank accession numbers: mRNA DQ335760, protein ABC59685) is 2,912 bp long containing a complete ORF of 2,622 bp which encodes a predicted 873 amino acid residues with the estimated molecular weight of 98.2 kDa. *ZmLOX2* (GenBank accession number: mRNA DQ335761, Protein ABC59686) harbors a full-length cDNA of 2,949 bp containing an ORF of 2615 bp. The predicted ZmLOX2 amino acid residues is 871 with a molecular mass of 98.4 kDa. The deduced amino acid sequences share more than 83% identity and 90% homology with each other (Figure 1). Both ZmLOX1 and ZmLOX2 harbors all five canonical residues for iron binding and enzymatic activity as described in (Gao et al., 2008a).

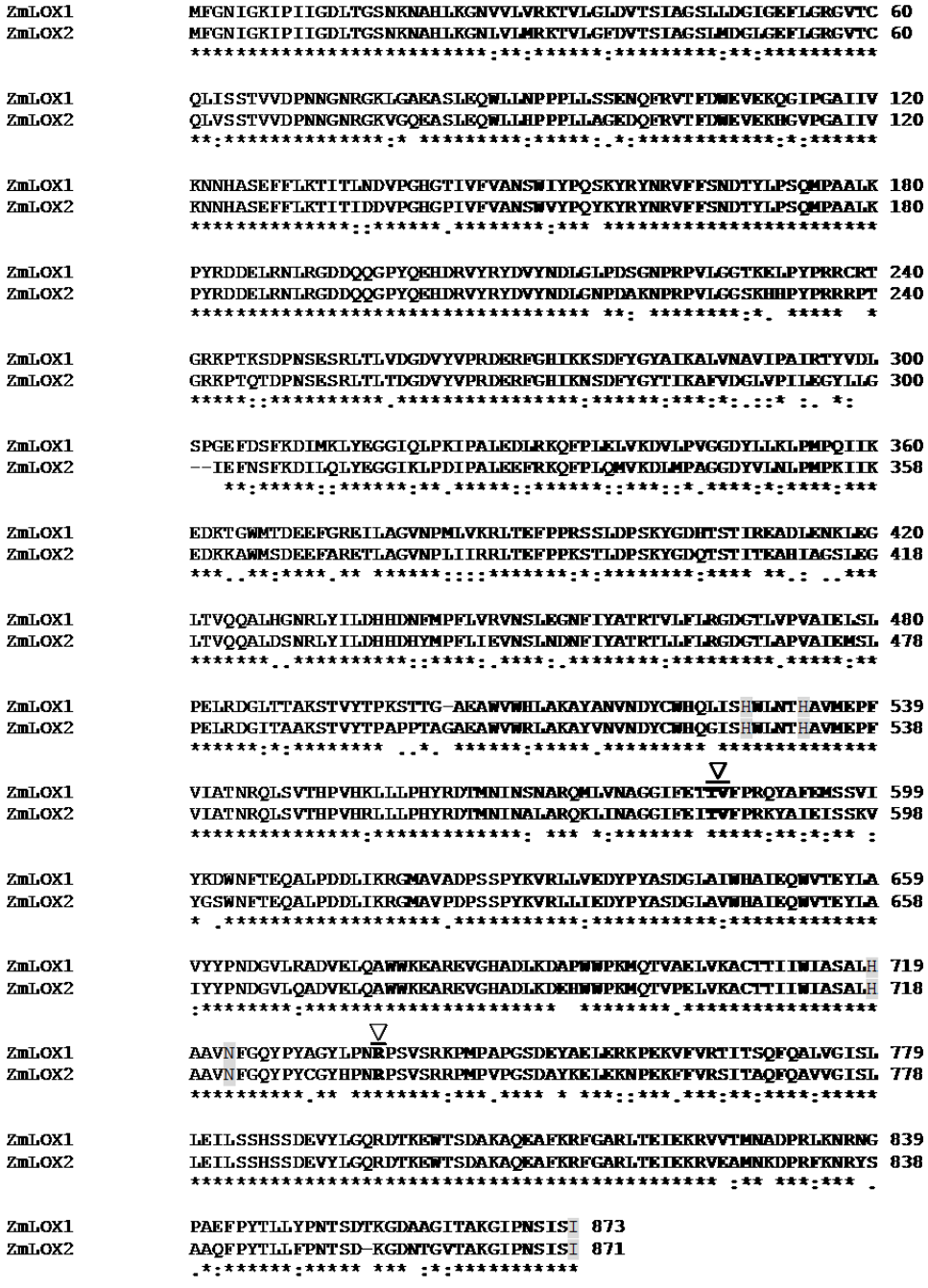

Figure 1. Alignment of the amino acid sequences of ZmLOX1 and ZmLOX2. Alignment was performed using ClustalW. Identical residues are indicated by asterisks; conservation between groups of strongly similar properties are indicated by colons; conservation between groups of weakly similar properties are indicated by periods. The conserved amino acid residues required for iron binding and catalytic activity are indicated by gray background as described in (Gao et al., 2008a). Presumed motifs (TV/R) responsible for 9-LOX positional specificities are in bold face and indicated by reverse triangles as described in (Kim et al., 2003).

**Biochemical properties of recombinant ZmLOX1**

To characterize biochemical properties of ZmLOX1 for which a full length cDNA was available, ZmLOX1 recombinant protein was overexpressed in *E. coli* to characterize its enzymatic activity by using linoleic acid as a substrate. The recombinant ZmLOX1 showed enzymatic activity at both pH 6.7 and 7.6 with a slightly higher activity at pH 7.6 (Figure 2). 13-oxylipins and 9-oxylipins comprised approximately 70% and 30%, respectively, of total products of recombinant ZmLOX1 under both pH conditions and these oxylipins were predominantly *S*-enantiomers suggesting the conversion is a result of enzymatic activity. Together, these data suggest that recombinant ZmLOX1 protein has both 13- and 9-LOX activities. Since amino acid sequences of ZmLOX2 showed more than 83% identity with ZmLOX1 and had the conserved residues for positional specificity, the data imply that ZmLOX2 is also a dual-positional specific enzyme.

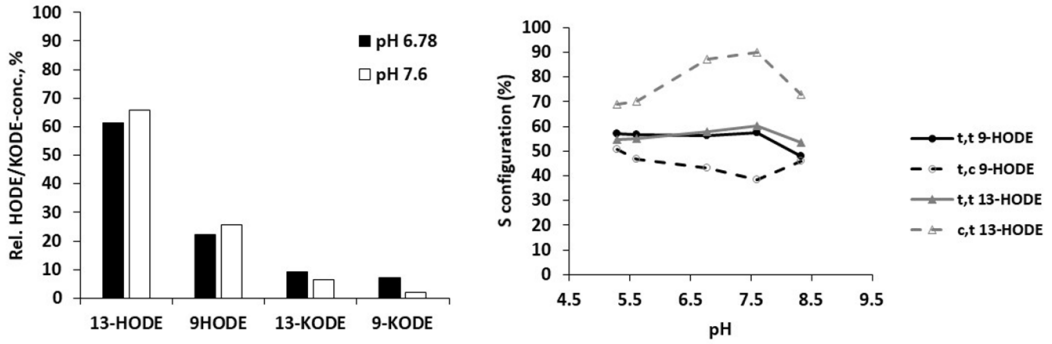


| pH | c,t 13-HODE | t,t 13-HODE | t,c 9-HODE | t,t 9-HODE | c,t 13-KODE | t,t 13-KODE | t,c 9-KODE | t,t 9-KODE |
|---|---|---|---|---|---|---|---|---|
| 7.6 | 59.7% | 6.2% | 18.6% | 7.0% | 5.2% | 1.3% | 1.4% | 0.5% |

Figure 2. Biochemical properties of recombinant ZmLOX1. Analysis of lipoxygenase regio-specificity was conducted at various pH values using linoleic acid as a substrate. This fatty acid was converted by the recombinant ZmLOX1 into correspondent 13-HODE, (9Z,11E,13S)-13-hydroxy-octadeca-9,11-dienoic acid; 9-HODE, (9S,10E,12Z)-9-hydroxy-10,12-octadecadienoic acid; 13-KODE, (9Z,11E)-13-oxo-octadeca-9,11-dienoic acid; and 9-KODE, ketodiene (9S,10E,12Z)-9-oxo-10,12-octadecadienoic acid. Relative concentration of LOX products (y axis) is presented as a portion of the sum of all isomers which was set as 100%. Ratios of (*S*)-enantiomers were also presented as a portion of sum of all isomers which as set as 100% and the result showed the products are converted by enzymatic activity. c and t represent cis- and trans-isomerism.

**Generation of *lox1* and *lox2* mutants**

Both *ZmLOX1* and *ZmLOX2* are on chromosome 3 in maize inbred line B73 genome, approximately 138 kb apart (Figure 3A). With such high amino acid identity and close proximity, *ZmLOX1* and *ZmLOX2* are predicted to arise by a tandem duplication in maize ancient ancestors. Full-length cDNA of *ZmLOX1* and *ZmLOX2* was aligned with the corresponding genomic DNA sequences from NCBI and MaizeGDB. Both *ZmLOX1* and *ZmLOX2* contain seven exons and six introns. A transposon insertional reverse genetics approach was used to generate *lox1* and *lox2* mutants. Approximately 42,000 *Mutator* (*Mu*)-insertional individual plants (Meeley, 1995) available at DuPont-Pioneer (Johnston, IA, USA) was screened by using *ZmLOX1*- and *ZmLOX2*-specific primers and *Mu* terminal inverted repeat-specific primers. Three alleles with *Mu* elements inserted in *ZmLOX1* exons and two in introns were identified by polymerase chain reaction (PCR)-based screening named *lox1-1*, *lox1-2*, *lox1-3*, *lox1-4* and *lox1-5* while only one insertional allele was found for *ZmLOX2*, named *lox2-1* (Figure 3B). Subsequent analyses of segregating populations failed to recover *lox1-2* and *lox1-5* alleles; therefore, no further work with these alleles were conducted. Sequence analysis of the adjoining sequences on both sides of the insertion site showed that *lox1-1* had a *Mu*-element inserted in exon II, *lox1-3* had insertion in exon VI, *lox1-4* in intron VI, and *lox2-1* has insertion in exon VI (Figure 3). All four alleles were then introgressed into maize inbred line B73. To test whether *Mu*-insertions impair gene expression for following functional characterization of ZmLOX1 and ZmLOX2, Northern blotting was conducted by using RNA extracted from individual plants in

segregating families of *lox1-1*, *lox1-3*, and *lox1-4*, and hybridized with the *ZmLOX1* gene specific probe. The result showed that *lox1-3* is a transcriptional null, knockout mutant, while *lox1-1* and *lox1-4* are knockdown mutant alleles. Reverse transcription-PCR (RT-PCR) was conducted using *ZmLOX2* gene-specific primers to detect *ZmLOX2* gene expression in the *lox2-1* mutant and in the B73 inbred line. The result showed that *Mu*-insertion in ZmLOX2 exon VI resulted in complete lack of detectable transcripts and thus, *lox2-1* represents a knockout mutant allele. To eliminate unrelated mutations, all *lox1-1*, *lox1-3*, *lox1-4*, and *lox2-1* alleles was backcrossed 7 times into B73 genetic background and self-pollinated, and mutants and near-isogenic WT lines most suitable for functional analyses presented in this study.

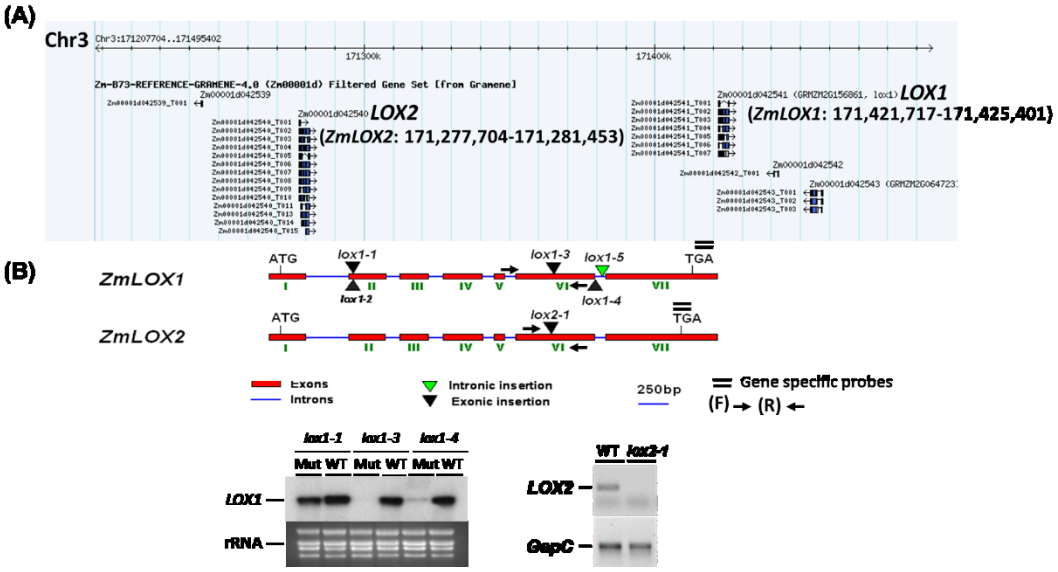


Figure 3. Characterization of *lox1* and *lox2* mutants. (A) A snapshot from MaizeGDB of *ZmLOX1* and *ZmLOX2*. The locus of ZmLOX1 is between 171,421,717 and 171,425,401 while ZmLOX2 is between 171,277,704 and 171,281,453 on chromosome 3 using AGPV3. *ZmLOX1* and *ZmLOX2* are approximately 138 kb apart and no other transcript was found between these two genes. (B) Genomic structure of *ZmLOX1* and *ZmLOX2* showing the *Mutator* (*Mu*)-element insertion site. RNA extracted from individual plant of segregating families for *lox1-1*, *lox1-3*, and *lox1-4* and near-isogenic WT was hybridized with the *ZmLOX1* gene-specific probe. Reverse transcription-PCR was conducted to measure the *ZmLOX2* gene expression in *lox2-1* mutant and the wild-type recurrent parent, B73 inbred line. The results showed that *lox1-3* and *lox2-1* are both knockout mutant alleles while *lox1-1* and *lox1-4* are knockdown alleles. Ethidium bromide staining of gels confirmed equal loading of RNA samples. GapC represents a reference gene for RT-PCR.

**Organ-specific and hormone- and wound-induced expression of *ZmLOX1* and *ZmLOX2***

Organ-specific expression of *ZmLOX1* and *ZmLOX2* was measured by using massively parallel signature sequencing (MPSS) technology (Zhang et al., 2005) in various maize organs (Fig. 4a). *ZmLOX1* transcripts were present at relatively high levels in mesocotyls (approximately 1,800 part per million [ppm]) and at lower levels in root and stem (approximately 200 ppm) and kernel (approximately 100 ppm). Transcript abundance of *ZmLOX2* was exceptionally high in mesocotyls (more than 10,000 ppm), high in pericarp, root, stem, and kernel (from approximately 1,000 to 2,300 ppm), and level in leaf, apical meristem, silk, and tassel (about 30 ppm).

Maize *LOX* genes are induced by stress-related hormones and by wounding (Nemchenko et al., 2006; Gao et al., 2008a; Park et al., 2010; Christensen et al., 2014). To gain an understanding of the potential functions of *ZmLOX1* and *ZmLOX2* in stress-induced responses, transcriptional activation of *ZmLOX1* and *ZmLOX2* in leaves by stress-related hormones (JA, ET, and ABA) and wounding was measured by Northern blotting. Both *ZmLOX1* and *ZmLOX2* expression was strongly induced by JA at 3 hours post treatment (hpt) and was maintained at the highest level at 6 and 12 hpt and then reduced to a lower level at 24 hpt. *ZmLOX1*, but not *ZmLOX2*, was transcriptionally induced by ethylene and reached the highest level at 6 hpt. ABA activated *ZmLOX1* and *ZmLOX2* expression at 3 hpt and then reduced to a steady state level (Figure 4B). Wounding also highly induced the expression of *ZmLOX1* and *ZmLOX2* starting 1 hpt. *ZmLOX2* expression in response to wounding reached the highest level at 2 and 4 hpt

followed by gradual reduction of expression at 8 and 16 hpt (Fig. 4C). Wound-induced *ZmLOX1* expression was maintained at the highest levels at 2, 4, and 8 hpt and reduced to a resting level before 16 hpt. Expression of *ZmLOX1* and *ZmLOX2* were also highly induced by Z-3-hexenal, which is a major component of the plant green leaf volatile mixture emitted in response to wounding, exhibiting a response similar to that of wounding (Fig. 4C).

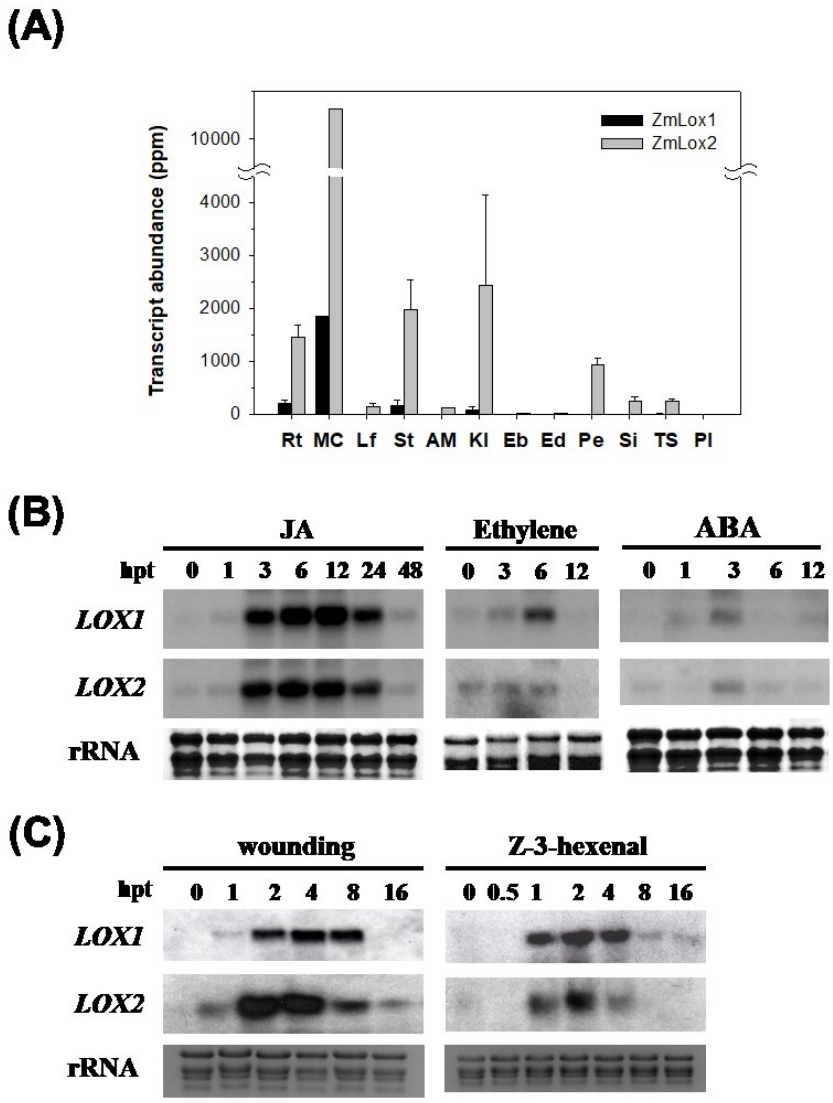


Figure 4. Organ-specific and hormone- and wound-induced expression of *ZmLOX1* and *ZmLOX2*. (A) Massively parallel signature sequencing (MPSS) expression profile of both *ZmLOX1* and *ZmLOX2* in different maize organs (Brenner et al., 2000). Expression of *ZmLOX1* and *ZmLOX2* in root (Rt), mesocotyl (MC), leaf (Lf), stalk (St), apical meristem (AM), kernel (Kl), embryo (Eb), endosperm (Ed), pericarp (Pe), silk (Si), tassel (TS), and pollen (Pl) is plotted in parts per million (ppm) of transcript abundance. (B) Maize B73 seedlings at the V2 stage were used in this experiment. Northern blot analysis of gene expression levels of *ZmLOX1* and *ZmLOX2* in leaves in response to 200 µM jasmonic acid (JA), 10 µL/L ethylene,100 µM abscisic acid (ABA), (C) mechanical wounding and 200 µM Z-3-hexenal. Total RNA (15 µg per lane) was used for all blots and hybridized with *ZmLOX1*- and *ZmLOX2*-specific probes. Ethidium bromide staining of gels confirmed equal loading of RNA samples.

**ZmLOX1 and ZmLOX2 are not involved in wound-induced JA biosynthesis**

Subcellular localization study by overexpressing *ZmLOX2*-GFP in maize protoplast showed that ZmLOX2 does not localize in chloroplasts where JA biosynthesis is initiated by 13-LOXs (Tolley and Koiwa, under review). ZmLOX1 was shown to localize in cytosol in transgenic rice, but was able to associate with chloroplasts isolated from pea *in vitro* (Cho et al., 2011). Because ZmLOX1 has both 13- and 9-LOX activities and ZmLOX2 is predicted to contain the same enzymatic activities and both genes showing strong induction by wounding, it was necessary to test whether these isoforms are directly involved in JA-biosynthesis. To test this, leaves of WT, *lox1-3*, and *lox2-1* were wounded by a hemostat as previously described (Christensen et al., 2013), and oxylipin contents were measured at 0 (control), 1, and 2 hours after wounding. Concentration of JA precursor, 12-OPDA, increased 1.6-fold in WT 1 hour after mechanical wounding and slightly reduced to 1.4-fold at 2 h, while *lox2-1* accumulated higher concentration (1.6-fold) of 12-OPDA compared to WT (Figure 5A). JA (Figure 5B) and JA-Ile (Figure 5C) contents in WT increased rapidly and significantly (approximately 88- and 300-folds, respectively) at 1 hour post wounding and started to decrease at 2 hours. No dramatic difference of JA and JA-Ile content was observed among *lox1-3*, *lox2-1*, and WT plant, except for slightly lower JA content in *lox1-3* and higher JA-Ile in *lox2-1* at 1 hour post wounding. These data suggest ZmLOX1 and ZmLOX2 are not required for wound-induced JA biosynthesis.

To identify other potential oxylipin products of ZmLOX1 and ZmLOX2, following oxylipins were quantified in response to wounding: 9-HOD, (9S, 10E, 12Z)-9-

hydroxy-10, 12-octadecadienoic acid; 9-HOT, ((9S, 10E, 12Z, 15Z)-9-hydroxy-10, 12, 15-octadecatrienoic acid; 9-KOD, ketodiene (9S, 10E, 12Z)-9-hydroxy-10,12-octadecadienoic acid; 9-KOT, ketodiene (10E, 12Z, 15Z)-9-hydroxy-10, 12, 15-octadecatrienoic acid; 13-HOD, (9Z, 11E, 13S)-13-hydroxy- 9,11-octadecadienoic acid; 13-HOT, (9Z, 11E, 13S, 15Z)-9-hydroxy-9,11,15-octadecatrienoic acid; 13-KOD, keto (9Z, 11E, 13S, 15Z)-9-hydroxy-9,11,15-octadecatrienoic acid were also measured in *lox1-3*, *lox2-1*, and WT. Upon wounding, 9-HOD, 9-HOT, and 9-KOT contents gradually increased in WT while 9-KOD content was not changed (Figure 6A). 9-HOD, 9-HOT, and 9-KOT all accumulated to a higher level in *lox2-1* mutant 2 hours post wounding compared to WT. 13-HOD and 13-HOT accumulated to a higher level and maintained similar level at 1 and 2 hours post wounding while 13-KOD content increased about 3-folds at 1-hour post wounding and reduced to resting level at 2 hours post wounding in WT (Figure 6B). Unlike in WT, 13-HOD and 13-HOT contents in *lox1-3* did not change in response to wounding suggesting that *ZmLOX1* is essential for 13-HOD and 13-HOT synthesis upon wounding. In *lox2-1* mutant, concentrations of all three 13-oxylipins were accumulated to a higher level than WT plant, especially 2 hours after wounding. Taken together, except for ZmLOX1 relevance to 13-HOD/T synthesis, wound-induced oxylipin profiling did not reveal molecular species of oxylipins produced by ZmLOX2 isoform. This is likely due to potential functional redundancy of these two isoforms in the biosynthesis of specific oxylipins.

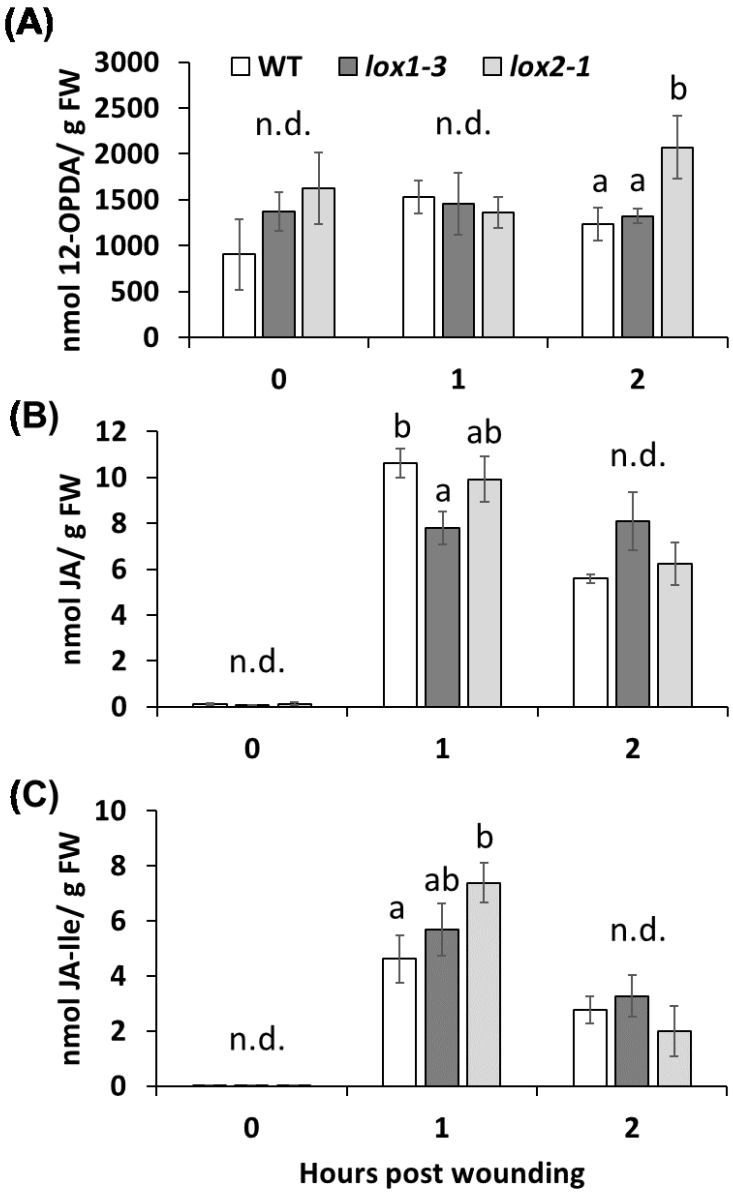


Figure 5. ZmLOX1 and ZmLOX2 are not required for wound-induced JA-biosynthesis. Fourth leaves of V4 stage seedlings were wounded following the protocol described in Christensen et al., 2013. Contents of JA-precursor (+)-12-oxo phytodienoic acid (12-OPDA), jasmonic acid (JA), and JA-isoleucine (JA-Ile) were shown here. No dramatic difference of jasmonate contents was observed at 0, 1, 2 hours post wounding among *lox1-3*, *lox2-1* mutants and WT plants. Bars are means ± SE. Unconnected letters indicate statistically significant differences among the samples within the same time-point (ANOVA followed by post hoc of Student's *t*-test, $p < 0.05$).

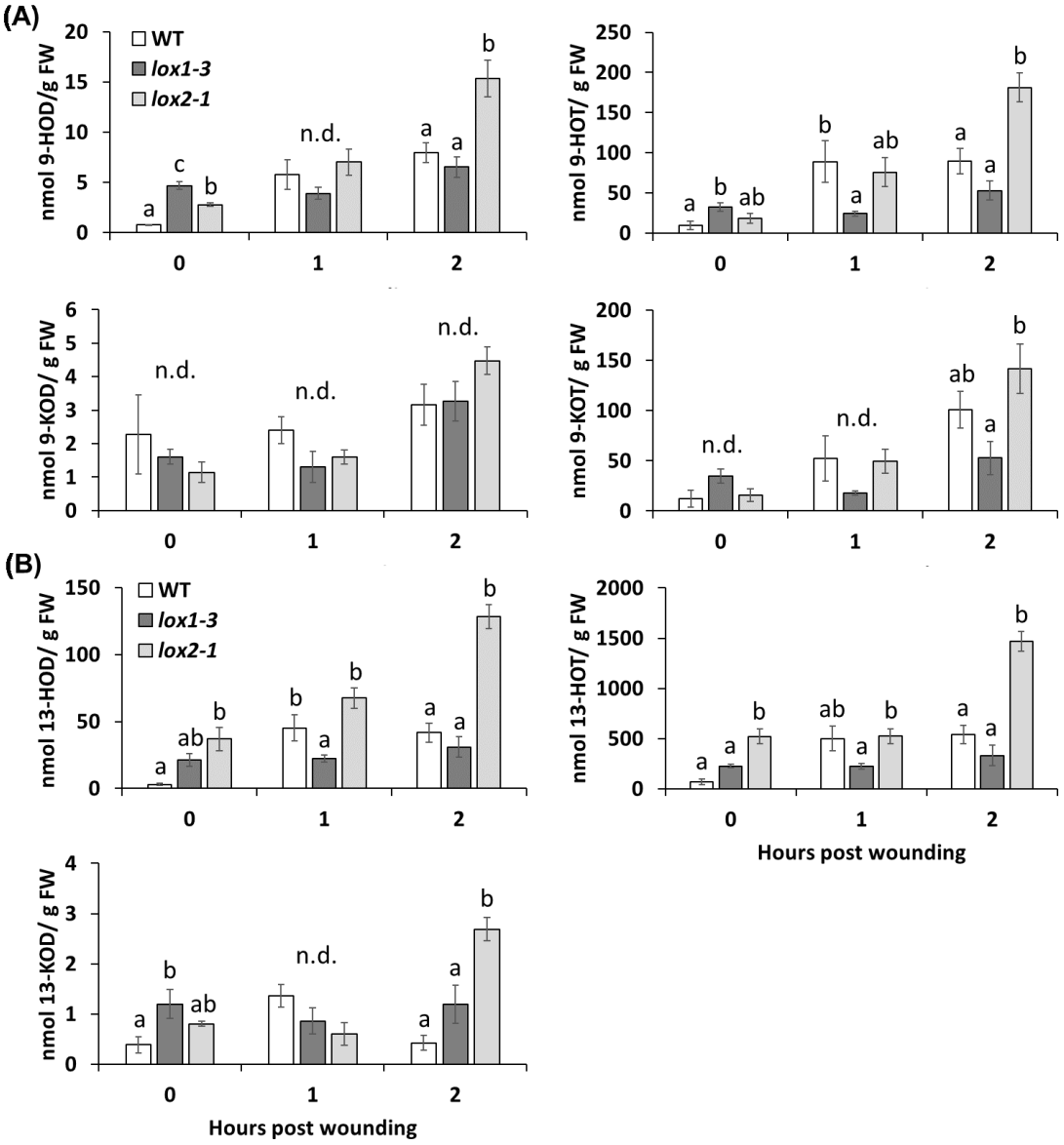


Figure 6. 9- and 13-oxylipin contents in WT, *lox1-3*, and *lox2-1* in response to wounding. Oxylipins included 9-HOD, (9S, 10E, 12Z)-9-hydroxy-10, 12-octadecadienoic acid; 9-HOT, (9S, 10E, 12Z, 15Z)-9-hydroxy-10, 12, 15-octadecatrienoic acid; 9KOD, ketodiene (9S, 10E, 12Z)-9-hydroxy-10,12-octadecadienoic acid; 9-KOT, ketodiene (10E, 12Z, 15Z)-9-hydroxy-10, 12, 15-octadecatrienoic acid (A); 13-HOD, (9Z, 11E, 13S)-13-hydroxy- 9,11-octadecadienoic acid; 13-HOT, (9Z, 11E, 13S, 15Z)-9-hydroxy-9,11,15-octadecatrienoic acid; 13KOD, keto (9Z, 11E, 13S, 15Z)-9-hydroxy-9,11,15-octadecatrienoic acid (B) were shown here. Bars are means ± SE. Unconnected letters indicate statistically significant differences among the samples within the same time-point (ANOVA followed by post hoc of Student's *t*-test, $p < 0.05$).

***ZmLOX1* and *ZmLOX2* are essential for resistance against anthracnose leaf blight caused by *C. graminicola***

Overexpression of maize *LOX1* in rice increased resistance against a hemibiotrophic fungal pathogen *Pyricularia grisea* (Cho et al., 2012). Therefore, *ZmLOX1* and/or *ZmLOX2* were hypothesized to play a role in maize interactions with the maize hemibiotrophic pahtogen *C. graminicola*. To test this hypothesis, seedlings ofWT, *lox1-3*, and *lox2-1* were infected with conidia suspension of *C. graminicola*. Disease symptoms (lesion area) were measured 5 days post inoculation. The leaves of *lox1-3* and *lox2-1* were more susceptible to anthracnose leaf blight caused by *C. graminicola* (Figure 7A) with lesion areas approximately twice as large on the mutants compared to WT (Figure 7B). To gain insight into potential biochemical mechanisms underlying the *ZmLOX1* and *ZmLOX2*-mediated defense against *C. graminicola* in leaves, a range of oxylipins and phytohormones were quantified at 0, 6, 12, and 24 hours post infection. Among the metabolites measured, we found that concentration of benzoic acid (BA), one of the salicylic acid (SA) precursors (Yalpani et al., 1993; Leon et al., 1995), increased approximately three-folds at 6 hpi and was maintained at a higher level at 12 and 24 hpi in WT plants. SA content in WT plants increased about 1.8-fold at 24 hours after infection. Both BA and SA accumulated at a significantly lower level in *lox1-3* and *lox2-1* compared to WT throughout the experiment (Figure 8). Also, WT plants showed increased concentrations of JA and JA-Ile in response to *C. graminicola* infection at 24 hpi but lower concentrations of JA and JA-Ile were observed in *lox1-3* and JA-Ile in *lox2-1* at 24 hours post infection. Collectively, these results suggest that *ZmLOX1* and

*ZmLOX2* have positive roles in regulating pathogen-induced SA and JA biosynthesis in leaves.

To identify 9- or 13-oxylipins produced by ZmLOX1 and ZmLOX2 isoforms and potentially responsible for the regulation of SA and JA biosynthesis during early plant response to infection, we profiled several other 9- and 13-oxylipins in WT, *lox1-3*, *lox2-1* plants. Unfortunately, no clear difference was observed at the time points after infection tested among all three genotypes except for moderately lower 13-KOD and 12-OPDA content in both *lox1-3* and *lox2-1* mutants at 24 hpi (Figure 9). These results suggest that some other unknown oxylipins are produced by these two LOXs.

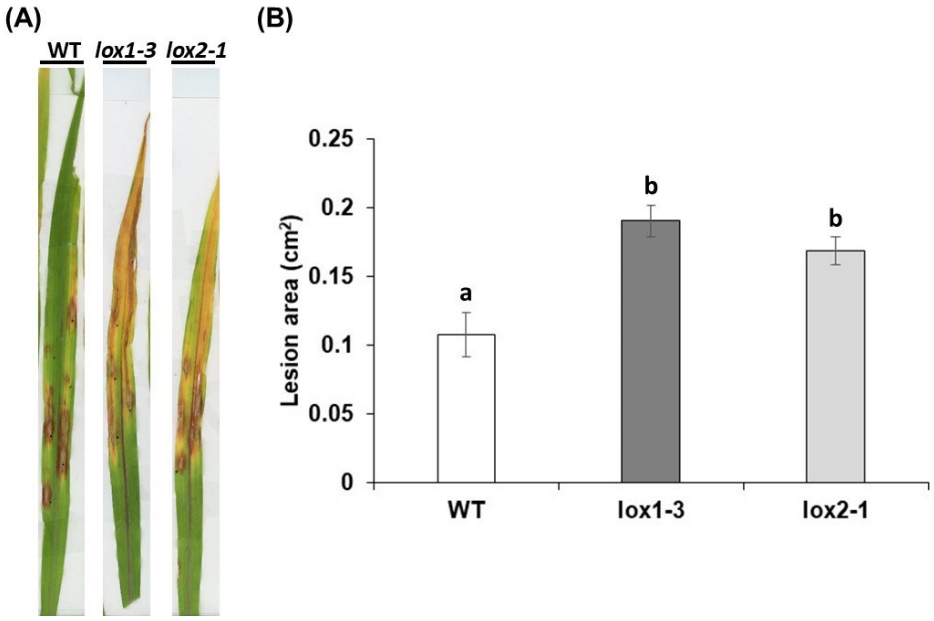


Figure 7. *ZmLOX1* and *ZmLOX2* are essential for resistance against anthracnose leaf blight. (A) Disease symptom of WT, *lox1-3*, and *lox2-1* mutants 5 days after inoculation with *C. graminicola* and lesion area was measured by using ImageJ software (B). *lox1-3* and *lox2-1* mutants are clearly more susceptible to anthracnose leaf blight caused by *C. graminicola*. Bars are means ± SE. Unconnected letters indicate statistically significant differences among the samples (Student's *t*-test, $p < 0.05$).

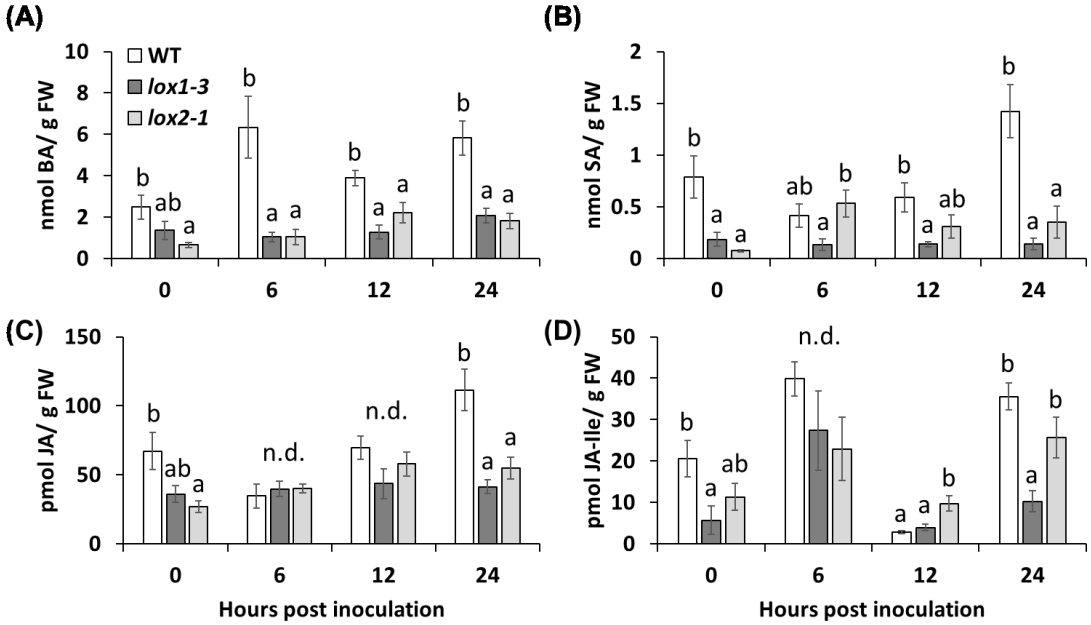


Figure 8. Benzoic acid (BA), SA, JA, and JA-Ile contents in WT, *lox1-3*, and *lox2-1* leaves in response to *C. graminicola* infection. Metabolites including BA (A), SA (B), JA (C), and JA-Ile (D) were shown here. Bars are means ± SE. Unconnected letters indicate statistically significant differences among the samples (ANOVA followed by post hoc of Student's *t*-test, $p < 0.05$). n.d. (not statistically different).

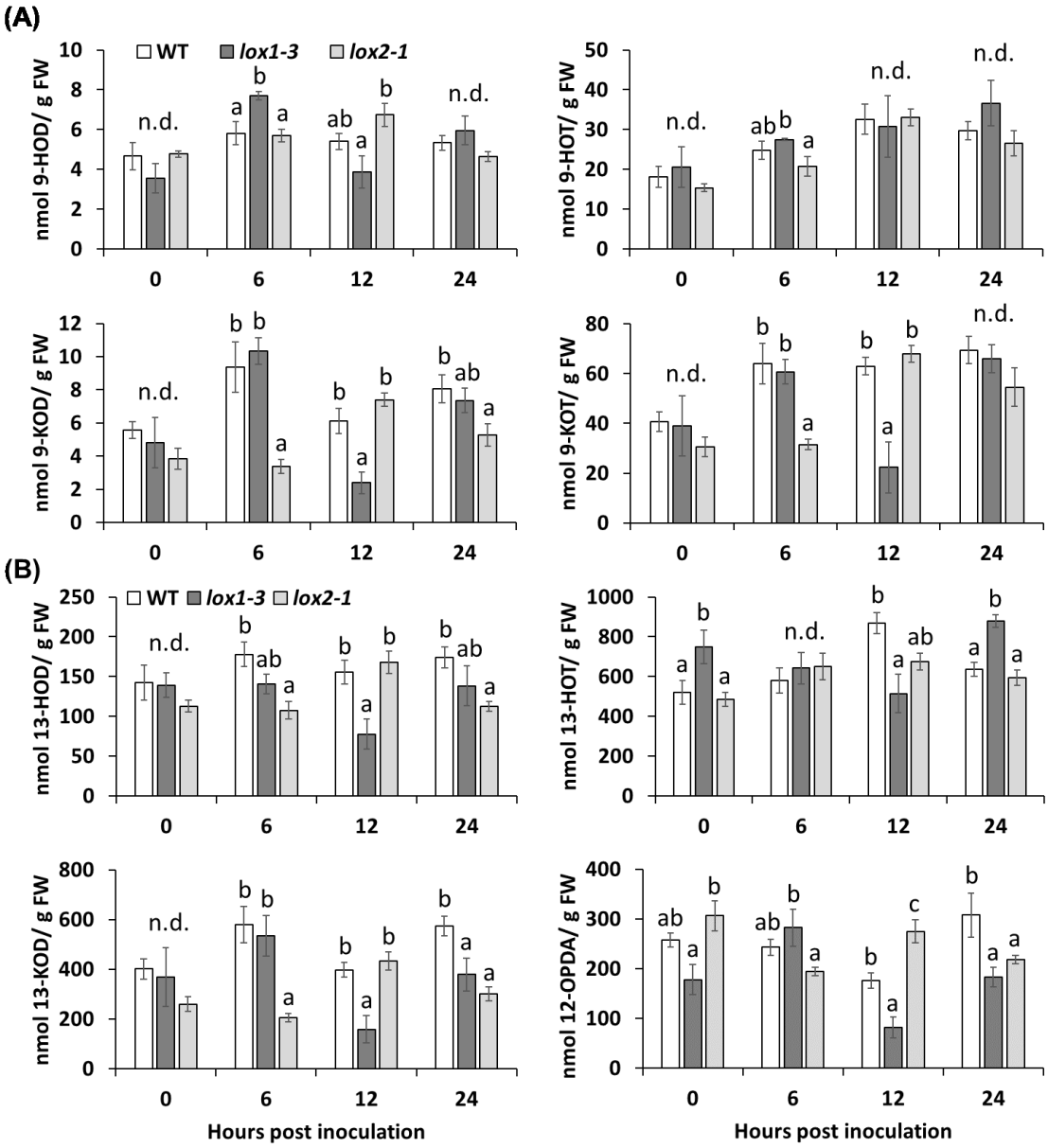


Figure 9. Concentration of 9-, and 13-oxylipins in leaves of WT, *lox1-3*, and *lox2-1* in response to *C. graminicola* infection. Oxylipins included 9-HOD, 9-HOT, 9-KOD, 9-KOT (A), 13-HOD, 13-HOT, 13-KOD, and 12-OPDA (B) were shown here Bars are means ± SE. Unconnected letters indicate statistically significant differences among the samples within the same time-point (ANOVA followed by post hoc of Student's *t*-test, $p < 0.05$). n.d. (not statistically different).

**ZmLOX1 and ZmLOX2 facilitate pathogenicity of *C. graminicola* in stalk**

WT and *lox1-3* and *lox2-1* mutant stalks were infected with *C. graminicola* to test whether these two genes are also required for resistance against *C. graminicola* in maize stem as shown for leaves. Three internodes above brace roots of WT, *lox1-3*, and *lox2-1* were wounded with a needle and then infected by using cotton swab soaked in conidia suspension of *C. graminicola*. Eight days after infection, internodes were split and scanned and disease symptoms (lesion area) were measured by using ImageJ software. Surprisingly, *lox1-3* and *lox2-1* were much more resistant to *C. graminicola* in stalk (Figure 10A). Forty percent of lesions in WT stalks caused by *C. graminicola* were larger than 200 $mm^2$ and about 20% of the lesions were between 150-200 $mm^2$, while both *lox1-3* and *lox2-1* had no lesions larger than 200 $mm^2$ and only 8% of the lesions between 150-200 $mm^2$ showing that *lox1-3* and *lox2-1* are both more resistant to *C. graminicola* than the WT in stalk. (Figure 10B). Fungal biomass and colonization were measured by quantification of the membrane fungal-specific lipid, ergosterol. In agreement with lesion area distribution, the results showed that there was indeed less fungal colonization in *lox1-3* and *lox2-1* compared to WT suggesting that ZmLOX1 and ZmLOX2 facilitate pathogenicity of *C. graminicola* in stalk (Figure 10C).

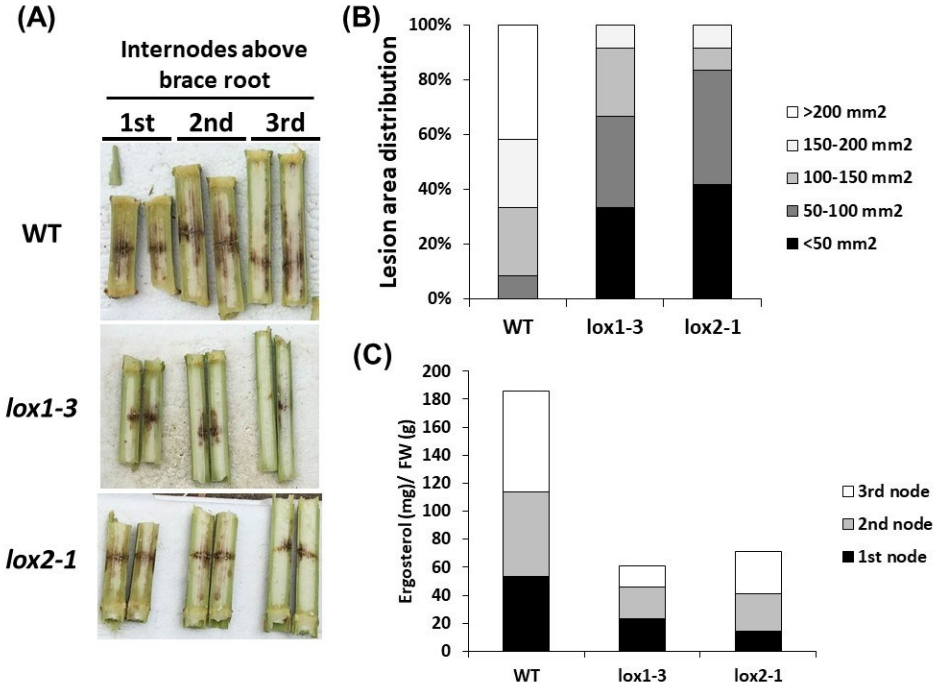


Figure 10. ZmLOX1 and ZmLOX2 facilitate pathogenicity of *C. graminicola*. Eight days after infection, internodes were split and scanned, and disease symptoms (lesion area) was measured by using ImageJ software. (A) Disease symptom of WT plants, *lox1-3*, and *lox2-1* mutants 8 days after inoculated with *C. graminicola* (B). Scoring of lesion areas. Lesions were grouped in five classes: <50, 50 to100, 100 to 150, 150 to 200, and >200 $mm^2$. *lox1-3* and *lox2-1* mutants are more susceptible to *C. graminicola* in terms of lesion distribution scores. (C) Fungal biomass and colonization was measured by quantification of fungal membrane specific lipid ergosterol. Bars are means.

To test whether the mutations resulted in altered oxylipin and hormone profiles, the infected internodes were harvested for select hormone analyses and comprehensive oxylipin profiling 0, 2, 4, and 8 days after *C. graminicola* inoculation. Following *C. graminicola* inoculation, concentration of all most abundant oxylipins, 9-HOD, 9-HOT, 9KOD, 9-KOT (Figure 11A), 13-HOD, 13-HOT, and 13-KOD (Figure 11B) was increased in WT stalks starting as early as 2 days after inoculation, whereas *lox1-3* and *lox2-1* failed to accumulate these 9- and 13-oxylipins to a level found in WT, especially 13-oxylipins. Interestingly, 10-OPEA, one of the so called dead acids, which has been shown to induce programmed cell death (Christensen et al., 2015), accumulated to a higher level in WT stalks and was associated with more rapid disease progression and reached the highest level at 8 days after inoculation (Figure 11A). Much lower 10-OPEA content was observed in both *lox1-3* and *lox2-1* mutants, which was also in coincident with smaller lesions developed in the mutants.

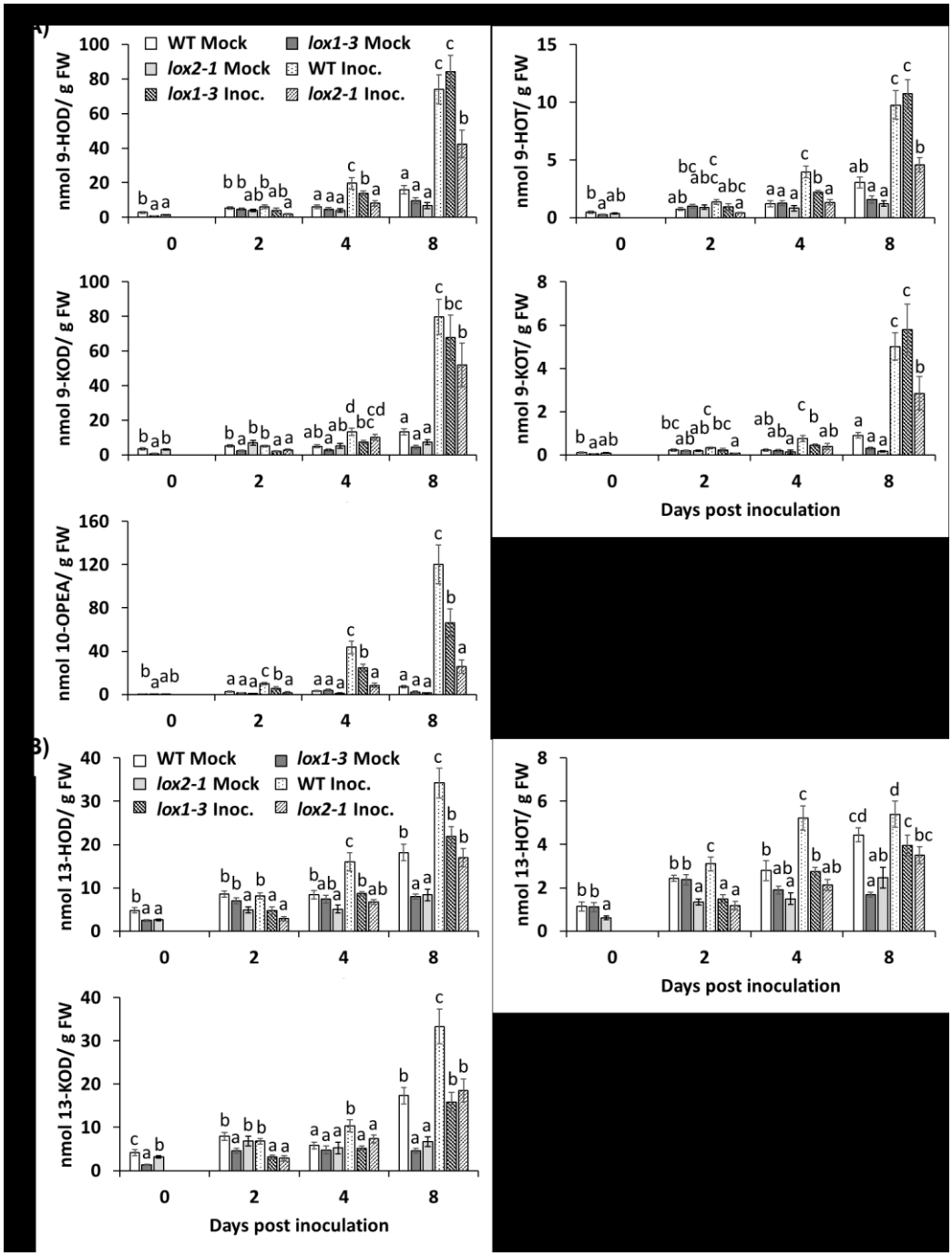


Figure 11. Accumulation of 9- and 13-oxylipins in stalks of WT, *lox1-3*, and *lox2-1* in response to *C. graminicola* infection. Internodes at 0, 2, 4, and 8 days after inoculation were harvested for metabolite and hormone quantification. (A) 9-oxylipins shown here: 9-HOD, 9HOT, 9KOD, 9KOT, and 10-OPEA (10-oxo-11-phytoenoic acid); (B) 13-oxylipins: 13-HOD, 13-HOT, and 13-KOD. Bars are means ± SE. Unconnected letters indicate statistically significant differences among the samples within the same time-point (ANOVA followed by post hoc of Student's *t*-test, $p < 0.05$).

Stress-related jasmonates including 12-OPDA, JA, JA-Ile and hormones SA and ABA were also measured. In response to infection, 12-OPDA content increased approximately three-fold and was maintained at high concentration for 8 days after inoculation; *lox1-3* and *lox2-1* stalks accumulated lower concentration of 12-OPDA compared to WT. OPDA downstream products, JA and JA-Ile, content also increased in WT in response to *C. graminicola* inoculation. While JA accumulated to the highest level at 8 days and JA-Ile reached the highest concentration at 4 dpi (Figure 12A). Similar to lower 12-OPDA, overall lower amounts of JA and JA-Ile were also observed in *lox1-3* and *lox2-1* stalks in response to infection except for 4 dpi and *lox2-1* at 8 days with a higher level of JA. ABA accumulated at a lower level in *lox2-1* regardless of infection, but no difference was observed in *lox1-3* compared to WT (Figure 12B). Supporting the major role of SA in resistance against hemibiotrophic pathogens like *C. graminicola*, SA levels correlated closely with increased resistance levels observed for the two mutants. Specifically, SA rapidly accumulated twice as much in *lox2-1* stalks as WT stalks at 2 dpi and remained at a higher level at 4 dpi; *lox1-3* also accumulated higher amount of SA at 4 dpi. Collectively, these data suggest *ZmLOX1* and *ZmLOX2* may negatively regulate the biosynthesis of SA and 10-OPEA in stalks in response to *C. graminicola* infection.

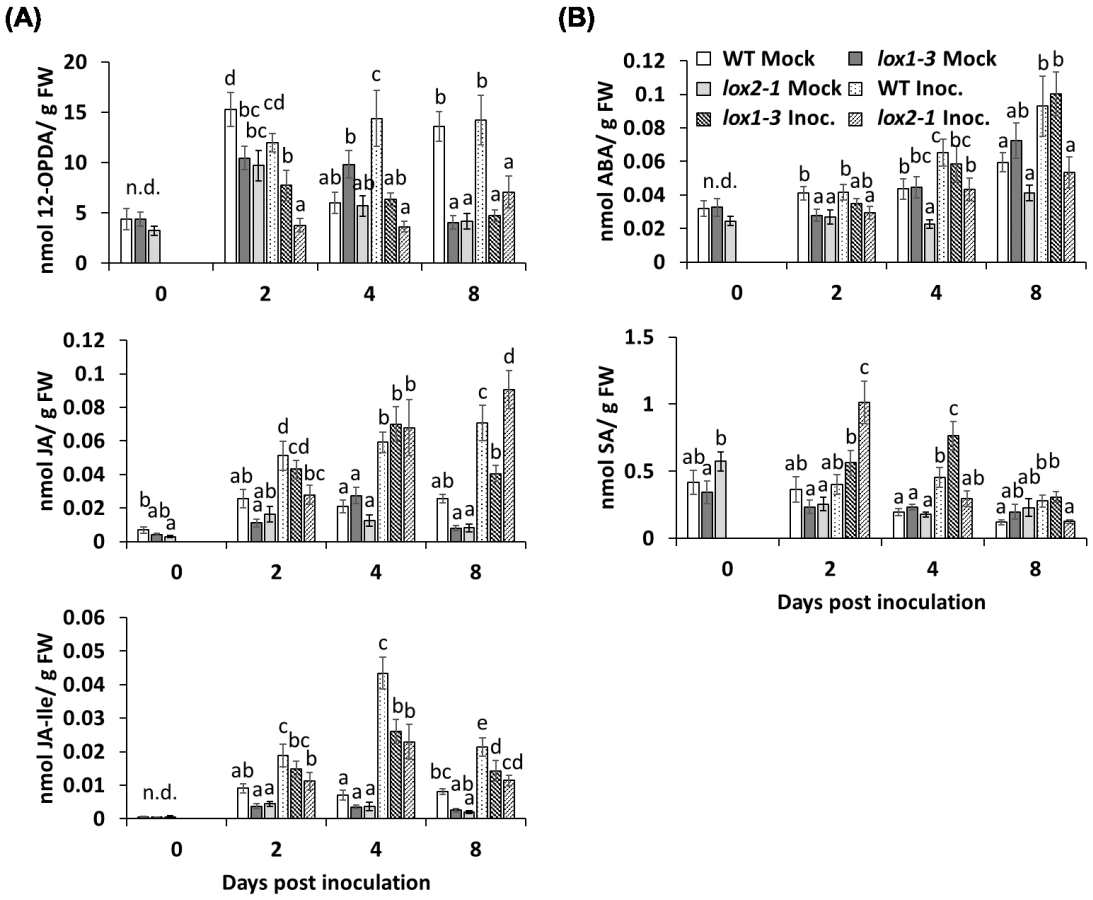


Figure 12. Accumulation of jasmonates, ABA and SA in stalks of WT, *lox1-3*, and *lox2-1* in response to *C. graminicola* infection. Stalk tissues were harvested at 0, 2, 4, and 8 days after inoculation. (A) Jasmonates included 12-OPDA, JA, and JA-Ile and (B) ABA and SA were shown here. Bars are means ± SE. Unconnected letters indicate statistically significant differences among the samples within the same time-point (ANOVA followed by post hoc of Student's *t*-test, $p < 0.05$). n.d. (not statistically different).

## DISCUSSION

### ZmLOX1 and ZmLOX2 possess unique 13- and 9-LOX activities

The results of this showed that maize genome encodes two dual positional specific LOXs, ZmLOX1 and ZmLOX2. Although *ZmLOX1* and *ZmLOX2* are phylogenetically classified into type I 9-LOXs (Nemchenko et al., 2006; Andreou and Feussner, 2009), recombinant ZmLOX1 converted linoleic acid into approximately 70% 13-oxylipins and 30% 9-oxylipins suggesting they possess greater 13-LOX rather than 9-LOX activity. Unlike maize and several other monocot species, the model plant *Arabidopsis thaliana* and most studied dicots do not possess LOX isoforms with such unusual promiscuity in the carbon position being oxygenated. Biological functions of 13/9-LOXs are poorly understood in all plant species studied thus far. Constitutive expression of maize *LOX1* in rice enhanced ROS scavenging enzyme activities and expression of defense-related, antioxidative, hypersensitive response, and cell wall modifying genes, leading to increase resistance against fungal pathogen *Magnaporthe grisea* (Cho et al., 2012). To my knowledge, this study represents the first functional analyses of these atypical plant LOXs using the reverse genetic approach.

### Disruption of ZmLOX1 and ZmLOX2 does not impair wound-induced JA biosynthesis

Most known 13-LOXs carry a chloroplast transit peptide and localize in plastids, where they are implicated in the initial steps of JA biosynthesis (Andreou and Feussner, 2009). However, no clear transit peptide was found in ZmLOX1 and ZmLOX2, and overexpression of *ZmLOX2*-GFP fusion protein in maize protoplast showed that

ZmLOX2 localizes in cytoplasm (Tolley and Koiwa, under review). Because *ZmLOX1* and *ZmLOX2* are both highly induced by mechanical wounding, I hypothesized that they have potential roles in regulating JA biosynthesis. Oxylipin profiling revealed that neither *lox1-3* nor *lox2-1* single mutant accumulate abnormal levels of OPDA, JA or JA-Ile in response to wounding. The slight perturbations in the levels of jasmonates were only observed at either 1 or 2 hours after the treatment depending on the mutant, suggesting that the two enzymes may be in part of fine-tuning levels of JA biosynthesis upon wounding. In line with this, accumulation of JA in response to wounding also shifted in rice transgenically overexpressing maize *LOX1* (Cho et al., 2012). Overall, these results and cytosolic localization of these proteins suggest that despite their predominant 13-LOX activity, ZmLOX1 and ZmLOX2 are not involved in wound-induced JA biosynthesis. Therefore, any biological significance of strong wound-inducibility of transcription of *ZmLOX1* and *ZmLOX2* genes is not clear at this moment. Interestingly, wound-inducibility of *ZmLOX1* and ZmLOX2 were found to be completely dependent on functional JA signaling because the JA-deficient *opr7-5 opr8-2* mutant was unable to induce these genes upon wounding (Yan et al., 2012). Therefore, it is reasonable to suggest that these two genes are downstream of JA and their function in JA-mediated defense responses need to be further investigated by direct testing of resistance levels of the mutants against insect herbivory.

**Oxylipin products of ZmLOX1 and ZmLOX2 remain elusive**

Surprisingly, oxylipin profiling of the tissues and treatments tested in this study were unable to identify any oxylipins that are produced specifically by ZmLOX1 and ZmLOX2. Several technical reasons could explain this failure. First, due to shortage of commercially available oxylipin standards, only about 60 oxylipins can be quantified by LC-MS/MS currently in our laboratory, which is approximately one tenth of the 600 or more oxylipins identified in plants (Borrego and Kolomiets, 2016). Second, 9/13-HPODE/HPOTE, the direct products of LOX-catalyzed oxidation of fatty acids, could not be quantified by available LC-MS/MS protocols. Third, these LOX isoforms may be involved in the biosynthesis of only recently characterized novel class of oxylipins produced LOX-mediated oxidation of *N*-linoleoylethanolamine (NAE 18:2) and *N*-linolenoylethanolamine (NAE 18:3) resulting in the biosynthesis of various NAE-oxylipins (Shrestha et al., 2002; Kilaru et al., 2011). It also has been reported that membrane bound LOXs can use phospholipids as substrates (Droillard et al., 1993), although no membrane associated pattern has been found in maize protoplast over-expressing *ZmLOX2*-GFP. Fourth, since ZmLOX1 and ZmLOX2 share high amino acid homology and have similar stress-related phytomorne responses, we cannot rule out the possibility of gene redundancy between *ZmLOX1* and *ZmLOX2*. In order to generate double knockout mutations in both genes with such close proximity, the technology of genome editing like CRISPR would need to be used to modify *ZmLOX1* in *lox2-1* mutant and vice versa. Disruption of both *ZmLOX1* and *ZmLOX2* may be one of the approaches to identify the products of ZmLOX1 and ZmLOX2.

**Oxylipin signals produced by ZmLOX1 and ZmLOX2 regulate SA biosynthesis upon *C. graminicola* infection in an organ-specific manner**

Several non-JA biosynthesis LOXs have been found to be required for resistance to pathogens. *ZmLOX3* is required for resistance to *Aspergillus* species (Gao et al., 2009) and *ZmLOX12* regulates JA-mediated defense against another seed colonizing fungal pathogen, *F. verticillioides* (Christensen et al., 2014). The pepper 9-LOX gene *CaLOX1* is required for defense against *Xanthomonas campestris* pv. *vesicatoria* infection and also enhances resistance to *Pseudomonas syringae* pv. *tomato* and other pathogens when overexpressed in Arabidopsis (Hwang and Hwang, 2010). Surprisingly, functional analyses of *lox1* and *lox2* mutants revealed that they have complete opposite function in leaves and stems in response to *C. graminicola* infection. While both mutants are more susceptible to anthracnose leaf blight, they are significantly more resistant to anthracnose stalk rot disease. Perhaps the most intriguing were the results that these phenotypes most consistently correlated with the levels of SA. Decreased resistance to *C. graminicola* in leaves of both mutants was accompanied with lower SA accumulation compared to WT. However, both *lox1-3* and *lox2-1* mutant alleles showed increased resistance to *C. graminicola* in stalks with higher SA accumulation during the early infection period. SA is the major defense hormone for defense against biotrophic and hemi-biotrophic pathogens (Boatwright and Pajerowska-Mukhtar, 2013). These results provided evidence that 13/9-LOXs and their products regulate pathogen-induced SA biosynthesis differentially in leaves and stalks. As with the wounding experiment, precise oxylipins produced by these two isoforms were not identified that have such a

potent effect on SA biosynthesis. Therefore, the link between LOX1/2-dependent oxylipin metabolism and SA biosynthesis could not be established here. Also, it is not clear why these two genes regulate SA biosynthesis positively or negatively in tissue-specific manner. It is possible that immediate hydroperoxide products of ZmLOX1 and ZmLOX2 in different organs is channeled into different sub-branches of the LOX pathway in a tissue-specific manner to eventually synthesize vastly different subsets of oxylipin signals. In addition to that, different substrates for these two LOXs may determine what final oxylipin products may be produced in leaves and stems, since leaf tissue contains more linolenic acid than linoleic acid, whereas stem contain substantially greater proportion of linoleic acid (Skibbe et al., 2010).

In summary, this is the first study providing strong genetic evidence that maize dual positional specific LOXs, *ZmLOX1* and *ZmLOX2*, play a central role in maize interaction with *C. graminicola* via differential regulation of SA biosynthesis in an organ-specific manner in response to *C. graminicola* infection (Figure 13).

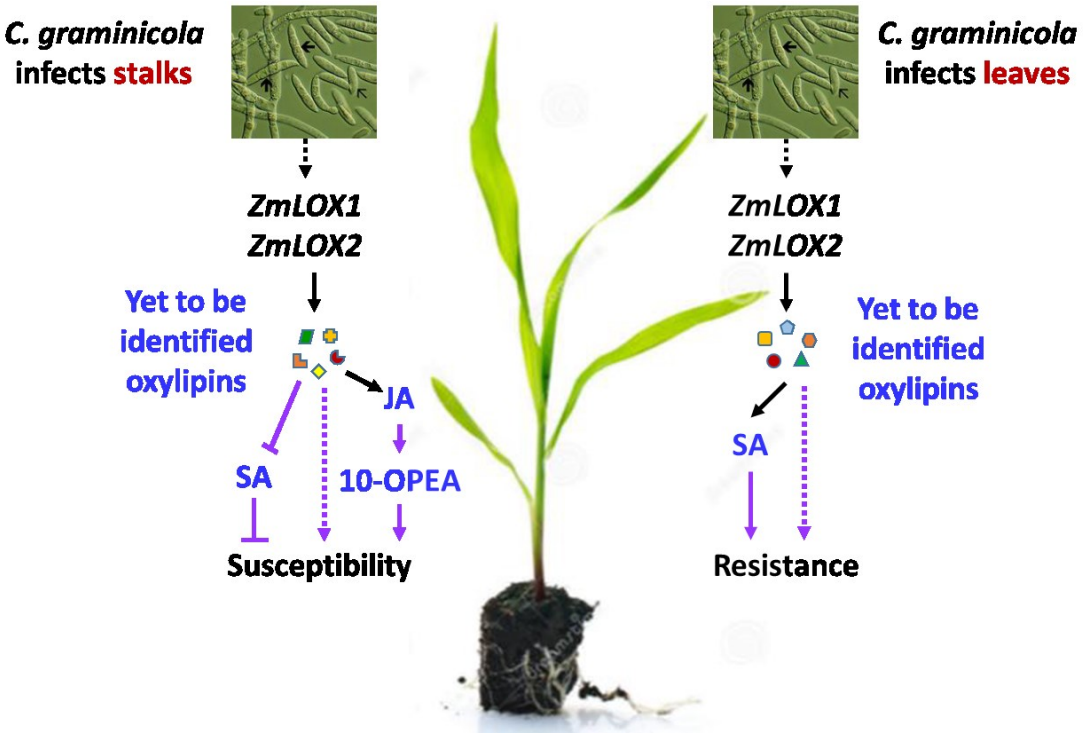


Figure 13. Proposed model of *ZmLOX1* and *ZmLOX2* mediated interactions with *C. graminicola* in leaves and stems.

# CHAPTER IV

# OXYLIPINS MEDIATE DROUGHT AND SALT TOLERANCE IN MAIZE

## INTRODUCTION

Environmental constraints restrict plant growth and productivity. Drought and salt stresses are two of the major abiotic stresses devastating crop yield worldwide and the situation has aggravated due to global climate change (Woodward et al., 2016). Recent studies have reported that drought stress caused up to 21% and 40% yield loss in wheat and maize, respectively, on a global scale (Daryanto et al., 2016; Fahad et al., 2017). Salt stress causes enormous problems in the arid and semi-arid regions of the world, where water and soil salinity are elevated from the constant irrigation required (Shrivastava and Kumar, 2015). The global population is estimated to increase to 9 billion or more by 2050, and 70% or more food production is required to keep up the pace of the surging population's food demand (Fischer et al., 2005; Smith and Gregory, 2013; McKersie, 2015). Maize, the most widely grown crop worldwide and the most important feed grain in the United States, is used to produce a variety of food and industrial products (Ranum et al., 2014). Therefore, developing drought and salt stress tolerant maize lines will not only alleviate future food needs but also will have economic implications. However, the mechanisms underpinning maize drought and salt tolerance remain largely unknown.

One of the major rapid changes to occur during abiotic stress is production of reactive oxygen species (ROS). During abiotic stresses, ROS, play a dual role in the abiotic stress responses depending on the concentration. Low levels of ROS are required

for signal transduction contributing to stress acclimation. However, excess amounts of ROS production cause an oxidative burst that leads to lipid peroxidation and cell death (Cruz de Carvalho, 2008). LOX activity is one source of ROS generation as a by-product of the LOX-mediated lipid peroxidation is production of the highly reactive singlet oxygen. The primary products of the LOX reaction on the fatty acid substrates are hydroperoxy fatty acids, which are highly reactive compounds and must be further converted to a variety of more stable oxylipins including JA, conjugate dienoic acids, volatile aldehydes such as green leaf volatiles, pentenol, and malondialdehyde (MDA) (Sofo et al., 2004). MDA levels have been widely used as a marker to evaluate the level of cellular damage caused by stress. Multiple studies in drought stressed maize showed that increased activity of ROS scavenging enzymes correlated with lower MDA accumulation and improved drought tolerance (Lu et al., 2013; Anjum et al., 2016; Gou et al., 2017). These studies indicate that improved control of drought-mediated lipid peroxidation can increase drought tolerance in maize.

In plants, lipid signaling plays a pivotal role in various biological processes such as growth and development (Acosta et al., 2009; Yan et al., 2014), abiotic stress responses (Grebner et al., 2013; Savchenko et al., 2014), and microbe- and herbivore-induced defense responses (Yan et al., 2012; Christensen et al., 2013). Oxidized fatty acids are collectively called oxylipins and the majority of them are derivatives of seven downstream branches of lipoxygenase (LOX) pathways (Feussner and Wasternack, 2002). LOXs in plants incorporate molecular oxygen into linoleic acid (C18:2) and linolenic acid (C18:3) at either carbon position 9 or 13 of the 18 carbon chain and are

functionally grouped into 9-LOXs and 13-LOXs (Howe and Schilmiller, 2002). The only well investigated small group of 13-oxylipins derived from the 13-LOX pathway are jasmonates comprising phytohormone jasmonic acid (JA), JA-precursor, 12-oxo-phytodienoic acid (12-OPDA), and derivatives of JA. Jasmonates are involved in wound response, abiotic stress tolerance, and defense against herbivores and necrotrophic pathogens (Wasternack, 2007). 12-OPDA has been reported to promote stomatal closure and functions additively with ABA (Savchenko et al., 2014). The role of JA in stomatal regulation is still controversial. Methyl jasmonic acid (MeJA) promotes stomatal closure by promoting $H_2O_2$ production in guard cells (Suhita et al., 2004; Munemasa et al., 2007). However, the phytotoxin coronatine, a JA-Ile functional and structural mimic, secreted by bacterial pathogen *Pseudomonas syringae,* re-opens stomata (Zheng et al., 2012; Wasternack, 2017). Therefore, the endogenous biological function of JA in stomatal regulation remains unclear.

Unlike jasmonates which have been well-studied, the function of 9-oxylipins downstream of 9-LOX pathway remains largely unknown. Accumulating evidence suggests that the 9-LOX pathways may play important roles in defense response to diverse pathogens and abiotic stresses (Gao et al., 2007; Gao et al., 2008b; Park et al., 2010; Christensen et al., 2014; Christensen et al., 2015; Marcos et al., 2015; Nalam et al., 2015). However, there is a lack of convincing genetic evidence showing LOXs are required for drought and salt tolerance. Furthermore, the identity and function of specific oxylipins or the mechanisms of their involvement in the regulation of drought and salt tolerance is unexplored. This study aims to test the hypothesis that LOXs are required

for drought and salt stress tolerance in maize and to understand the mechanisms regulated by LOXs in response to drought and salt stresses.

This study provides evidence that *ZmLOX2* is an essential component of processes leading to drought tolerance via regulating transpirational water loss. This is in sharp contrast to the function of *ZmLOX4*, which promotes drought sensitivity by increasing water loss through transpiration. Metabolite profiling and RNA sequencing results suggest that *ZmLOX2* and *ZmLOX4* regulate maize drought responses in opposite manners by mediating the JA biosynthesis pathway and JA signaling to regulate stomatal aperture. To test the hypothesis that JA negatively regulates the stomatal aperture, JA-deficient *opr7-5 opr8-2* mutant was analyzed for drought-relevant physiological traits. JA-deficient *opr7-5 opr8-2* mutant reduced transpirational water loss and was restored by exogenous MeJA application and stomatal aperture measured from the epidermal peels supported these results that JA promotes stomatal opening. Higher level of ET was produced in drought stressed JA-deficient *opr7-5 opr8-2*; in line with that, ET-deficient mutant *acs2 acs6* had significantly higher water loss suggesting ET enhances stomatal closure. In contrast to the role of ZmLOX2 in drought tolerance, its tandem duplicated paralogue, *ZmLOX1,* was found to be required for salt stress tolerance via regulating SA and 10-OPEA biosynthesis in roots. Collectively, these data suggest that oxylipin signals from diverse biosynthetic branches govern drought and salt tolerance in maize.

## RESULTS

### Lipoxygenase genes expression in response to withholding water

To establish the dynamics of transpirational water loss by maize seedlings in response to withholding water, two-weeks old seedlings the inbred line B73 at V2 developmental stage grown in conical pots with same amount of sterile potting mix from were placed on electronic balances within an environmentally controlled growth chamber and the weights of the pots were recorded using a WinWedge software after well-watered to reach 100% water content in soil. Water loss via transpiration was normalized for the plant above-ground dry weight taken at the end of the experiment. The B73 inbred showed slight increase in transpirational water loss during the first three days after withholding water and then dramatically reduced water loss towards the end of the time-course (Figure 14A). The plants displayed noticeable wilting symptoms at the tip of the third leaf approximately four days after withholding water. In order to investigate whether *LOXs* are responsive to drought stress, gene expression analysis of *ZmLOX1*, *ZmLOX2*, *ZmLOX3*, *ZmLOX4*, *ZmLOX5*, *ZmLOX6*, and *ZmLOX10* in leaves and roots in response to withholding water was performed by conducting quantitative reverse transcription polymerase chain reaction (qRT-PCR) using gene-specific primers. In leaves, expression of *ZmLOX2*, *ZmLOX5*, and *ZmLOX6* was significantly up-regulated at three and four days with the highest expression levels as 3.6-, 5.8-, and 2.8-folds; *ZmLOX4* was up-regulated one day after withholding water and maintained elevated expression with the highest level as 5.2-folds observed at the third day while expression of *ZmLOX1*, *ZmLOX3*, and *ZmLOX10* did not change (Figure 14B). In roots,

*ZmLOX10* was significantly up-regulated to 3.4-folds in response to withholding water starting at the first day and maintained elevated expression level. Expression of *ZmLOX2* was suppressed at day 3 and day 4 after withholding water. *ZmLOX4* was significantly down-regulated starting at day 3 and even further reduced at day 4 as 0.3-fold compared to well-watered day 0. *ZmLOX5* expression was only suppressed at 4 days (0.6-fold) and *ZmLOX6* was down-regulated only at 3 days (0.5-fold) after withholding water. Expression of *ZmLOX1* and *ZmLOX3* did not change throughout the four days of water deprivation. Collectively, the dynamic and differential expression pattern of maize *LOXs* in response to water deprivation suggest that they serve specialized roles in the normal maize drought response.

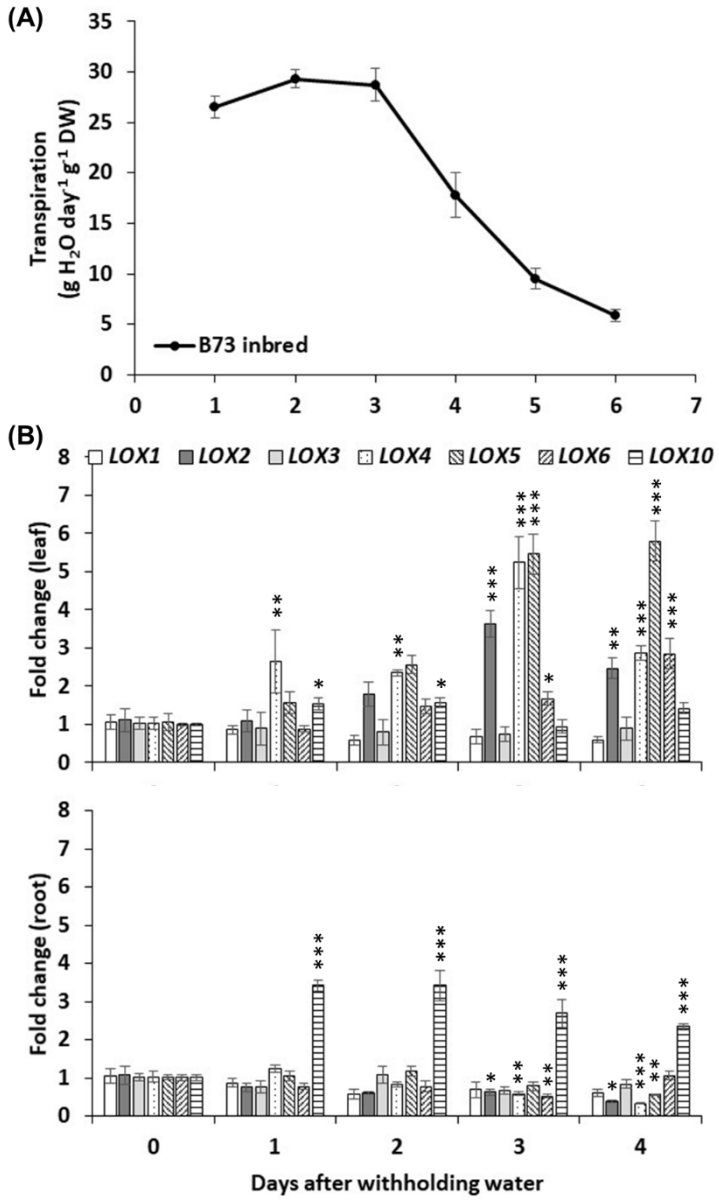


Figure 14. Transpirational water loss of maize B73 inbred line and lipoxygenase genes expression in leaf and root of B73 plant in response to withholding water. (A) B73 seedlings at V2 stage had slightly increased transpiration during the first three days and then significantly reduced transpirational water loss to the end of the experiment. (B) Average fold changes of *LOXs* gene expression over time in B73 leaves and roots in response to withholding water compared to well-watered day 0. Asterisks represent statistically significant differences from gene expression at day 0 (Student's *t*-test, * $0.01 < p < 0.05$, ** $0.001 < p < 0.01$, *** $p < 0.001$).

### *ZmLOX2* promotes drought tolerance through regulating transpirational water loss

To test the hypothesis that maize *LOXs* serve different roles in response to water deprivation at seedling stage, transposon-insertional knockout mutants and near-isogenic WT maize lines were assessed for water loss and recovery after prolonged drought stress. The results showed *lox2-1* had significantly increased transpirational water loss during water deprivation (Figure 15A) and failed to recover after 16 days of prolonged drought stress (Figure 15B). To test the context dependency and background epistasis of *ZmLOX2* during drought stress, *lox2-1* was introgressed into the W438 genetic background, an inbred line diverse from B73, and advanced to the $BC_5$ stage. In the W438 background, the *lox2-1* mutant also displayed increased transpirational water loss compared to its near-isogenic WT (Figure 15C) and the tip of the third and fourth leaves of *lox2-1* mutant showed more severe drought-induced leaf senescence seven days after water deprivation than WT (Figure 15D). These results provide strong genetic evidence that *ZmLOX2* promotes drought tolerance through the regulation of transpirational water loss at seedling stage in these inbred lines.

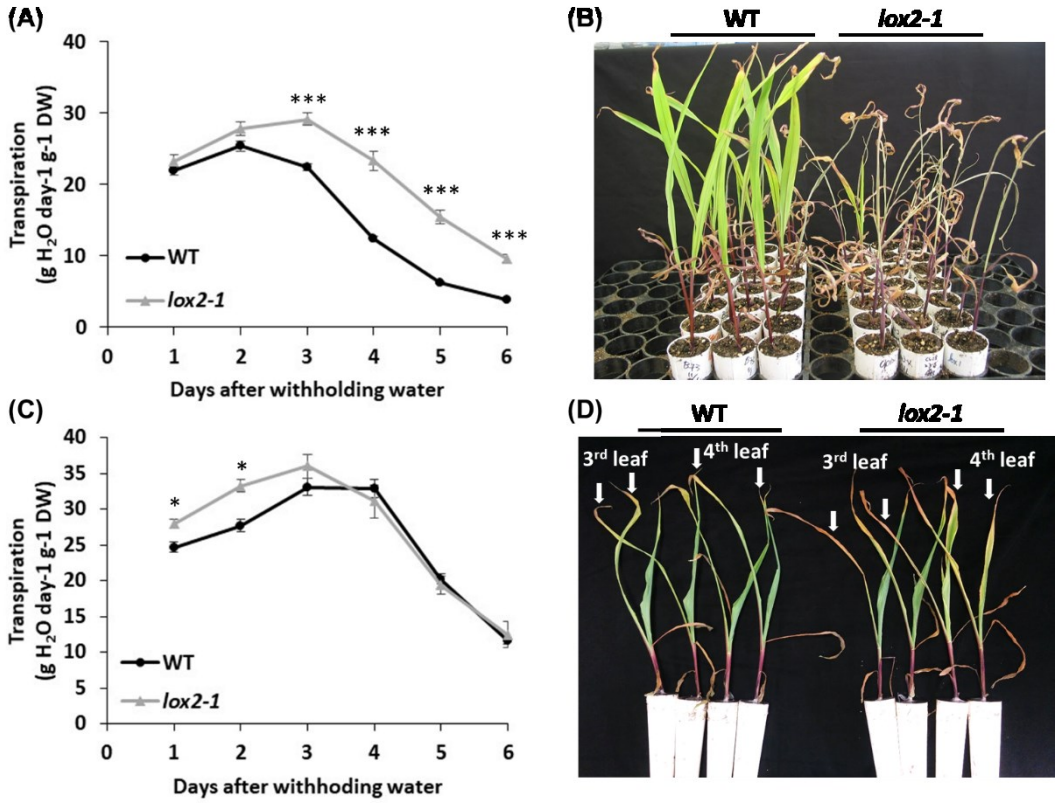


Figure 15. *ZmLOX2* promotes drought tolerance by reducing transpirational water loss. (A) *lox2-1* mutant lost more water through transpiration compared to WT (B73 inbred line) during water deprivation, and (B) failed to recover from 16 days of prolonged drought stress followed by rewatering. (C) *lox2-1* mutant in the W438 genetic background displayed greater transpirational water loss than its near-isogenic WT plant at the $BC_5$ genetic stage and (D) arrows indicate drought-induced leaf senescence was more severe in *lox2-1* mutant in the W438 genetic background. The Y-axis represents transpirational water loss (g $H_2O$ $day^{-1}$ $g^{-1}$ DW) and the X-axis represents the days after withholding water. Bars are means ± SE. Black line depicts WT and gray line depicts *lox2-1* mutant. Asterisks represent statistically significant differences between WT and *lox2-1* mutant within the same time-point (Student's *t*-test, * $0.01 < p < 0.05$, ** $0.001 < p < 0.01$, *** $p < 0.001$).

**Disruption of *ZmLOX4* resulted in reduced transpiration and increased drought tolerance**

In sharp contrast to *lox2-1,* the *lox4-7* mutant had significantly reduced water loss through transpiration than WT (Figure 16A) and recovered more successfully after 14 days of prolonged drought stress (Figure 16B), suggesting that *ZmLOX4* functions in promoting transpirational water loss. To further test this hypothesis by using other independent knock-out alleles of *ZmLOX4*, transpirational water loss of *lox4-1* (at the $BC_7$ stage) and *lox4-10* (at $BC_5$ stage) mutant alleles in the B73 background was measured. Similar to *lox4-7*, both *lox4-1* (Figure 16C) and *lox4-10* (Figure 16D) mutants showed significantly reduced transpirational water loss compared to WT. Together, these results provide strong genetic evidence that *ZmLOX4* reduces drought tolerance via increasing transpirational water loss at seedling stage.

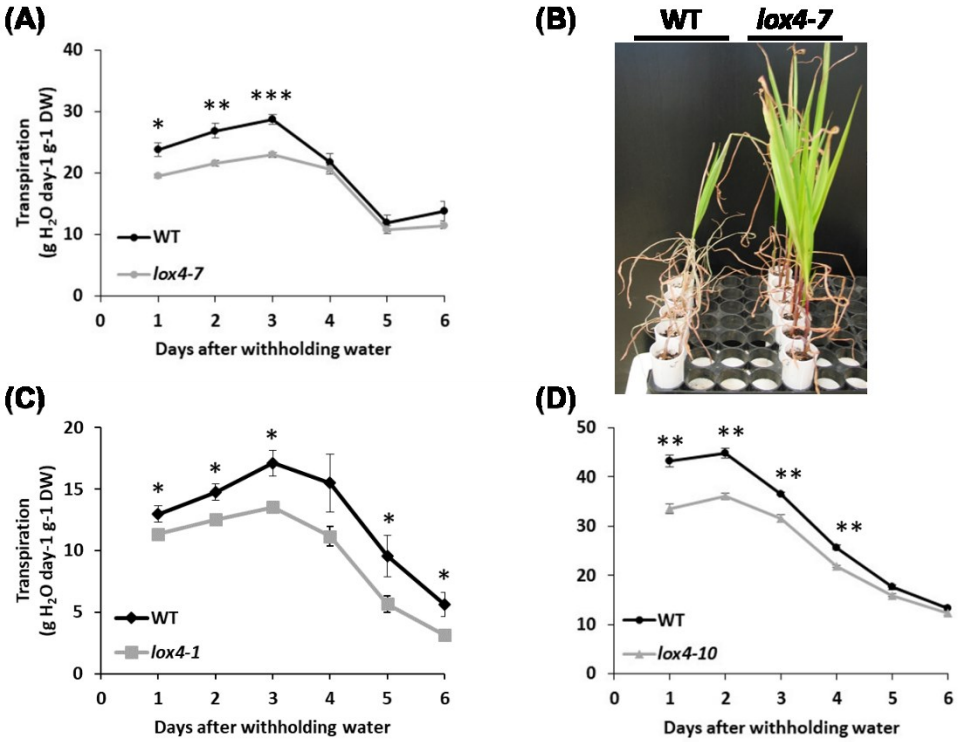


Figure 16. *ZmLOX4* promotes drought sensitivity via increasing transpirational water loss. *lox4-7* mutant lost less water through transpiration than WT (B73 inbred line) during water deprivation (A) and recovered more successfully from 14 days of prolonged drought stress (B). *lox4-1*(C) and *lox4-10* (D) mutants displayed reduced transpirational water loss compared to WT. The Y-axis represents transpirational water loss (g $H_2O$ $day^{-1}$ $g^{-1}$ DW) and the X-axis represents the days after withholding water. Bars are means ± SE. Black line depicts WT and gray line depicts *lox4* mutants. Asterisks represent statistically significant differences between WT and *lox4* mutants within the same time-point (Student's *t*-test, * $0.01 < p < 0.05$, ** $0.001 < p < 0.01$, *** $p < 0.001$).

**Disruption of *ZmLOX3* and *ZmLOX6* increases transpirational water loss while *ZmLOX5* is required for prolonged drought stress tolerance**

Transpirational water loss experiment was also conducted on the *lox3-4, lox5-3,* and *lox6-2* mutants. The *lox3-4* mutant showed increased water loss compared to WT but recovered more successfully from 14 days of prolonged drought stress (Figure 17A). One plausible explanation for better recovery after rewatering of the lox3-4 mutant compared to WT is that *lox3* are smaller in size (Gao et al., 2007). Decreased plant size may lead to decreased net water lost through transpiration by the mutant and allowed more water to remain in soil after prolonged drought stress and subsequently better recovery. The *lox5-3* mutant lost a similar amount of water via transpiration compared to WT, but failed to recover after 14 days of prolonged drought stress (Figure 17B). The *lox6-2* mutant displayed dramatically increased transpirational water loss compared to WT and the drought-induced leaf senescence was more severe on 2$^{nd}$ and 3$^{rd}$ leaves in *lox6-2* mutant seven days after withholding water (Figure 17C). The expression of *ZmLOX1* and *ZmLOX10* did not change in response to water deprivation in the leaves of the B73 inbred line, suggesting these two *LOX* isoforms are not likely involved in transpirational water loss. Indeed, no difference was observed between WT and knockout mutant lines in terms of transpirational water loss (data not shown). Together, these results implicate *ZmLOX3* and *ZmLOX6* in addition to *ZmLOX2* in the regulation of transpirational water loss and *ZmLOX5* is specifically associated with the ability of seedlings to recover severe drought stress but not transpirational water loss.

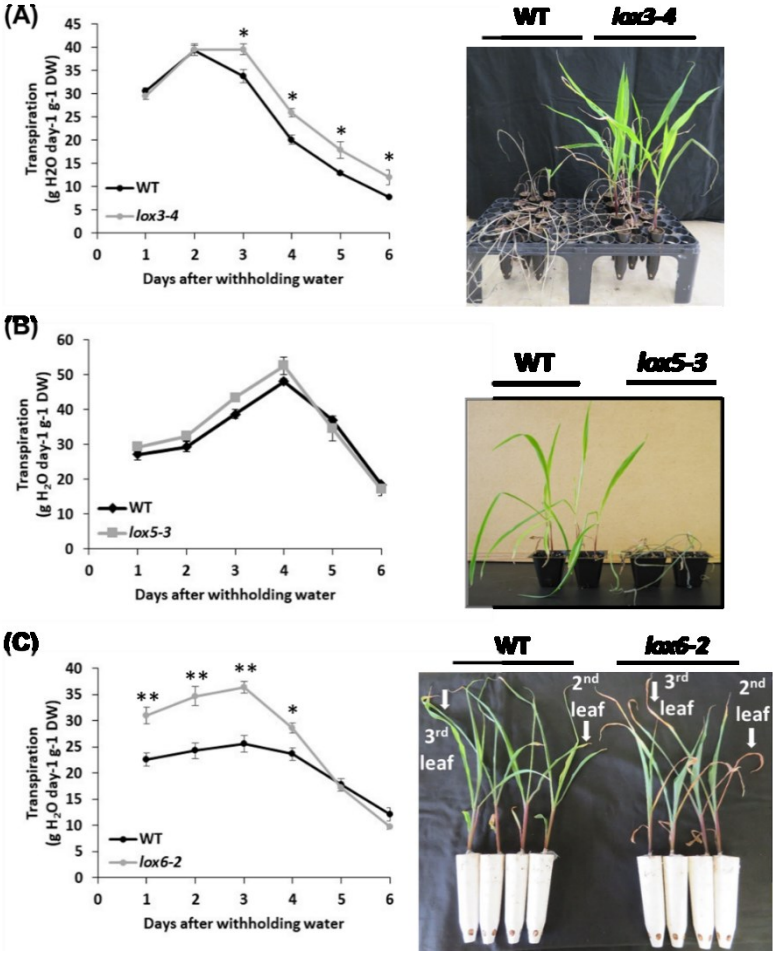


Figure 17. Disruption of *ZmLOX3* and *ZmLOX6* increased transpirational water loss while *ZmLOX5* is required for prolonged drought stress tolerance. *lox3-4* mutant lost more water through transpiration compared to WT (B73 inbred line) during water deprivation but had better recovery from 14 days of prolonged drought stress (A). *lox5-3* mutant had similar amount of transpirational water loss compared to WT but failed to recover from 14-day–long drought stress (B). *lox6-2* mutant showed dramatically higher transpirational water loss than its near-isogenic WT (WT-NIL at $BC_2$ genetic stage in the W438 genetic background) plant and arrows clearly indicate drought-induced leaf senescence was more severe in the *lox6-2* mutant than WT plant after seven days of water deprivation (C). The Y-axis represents transpirational water loss (g $H_2O$ $day^{-1}$ $g^{-1}$ DW) and the X-axis represents the days after withholding water. Bars are means ± SE. Black line depicts WT and gray line depicts *lox* mutants. Asterisks represent statistically significant differences between WT and *lox* mutants within the same time-point (Student's *t*-test, * $0.01 < p < 0.05$, ** $0.001 < p < 0.01$, *** $p < 0.001$).

### *ZmLOX4* is upstream of *ZmLOX2* during drought responses

While both *ZmLOX2* and *ZmLOX4* regulate transpirational water loss and prolonged drought tolerance, these two genes function in opposing manners. To elucidate whether there is an interaction between these two *LOX* isoforms, double mutants of *ZmLOX2* and *ZmLOX4* were generated. Transpirational water loss measurement was conducted and no difference was found between *lox2-1 lox4-7* and WT; however, *lox2-1 lox4-7* recovered after 14 days of prolonged drought stress more successfully (Figure 18A). To investigate whether disruption of the LOX genes affects expression of other LOXs, transcript accumulation of the drought-responsive *LOX* genes was tested in *lox2-1* and *lox4-7* leaves and roots under well-watered (WW) and drought-stressed (DS) conditions by quantitative reverse transcription polymerase chain reaction (qRT-PCR). In *lox2-1* leaves (Figure 18B), *ZmLOX5* and *ZmLOX10* were significantly up-regulated in response to water deprivation while expression of *ZmLOX4* and *ZmLOX6* did not change; *ZmLOX4* was down-regulated in *lox2-1* roots. In *lox4-7* leaves, *ZmLOX2* and *ZmLOX5* were significantly up-regulated by withholding water while expression of *ZmLOX6* and *ZmLOX10* was not altered. *ZmLOX2* and *ZmLOX5* were both down-regulated in *lox4-7* roots. In line with the observation that *ZmLOX2* and *ZmLOX5* play a role in drought tolerance, up-regulation of both *LOX* genes in *lox4-7* leaves was associated with its reduced transpiration and enhanced tolerance to severe drought stress. Because expression of *ZmLOX4* was found unaffected in the *lox2-1* under drought stress and since the *lox2-1 lox4-7* displayed increased survival from prolonged drought stress, these results indicate that *ZmLOX4* acts upstream of *ZmLOX2*.

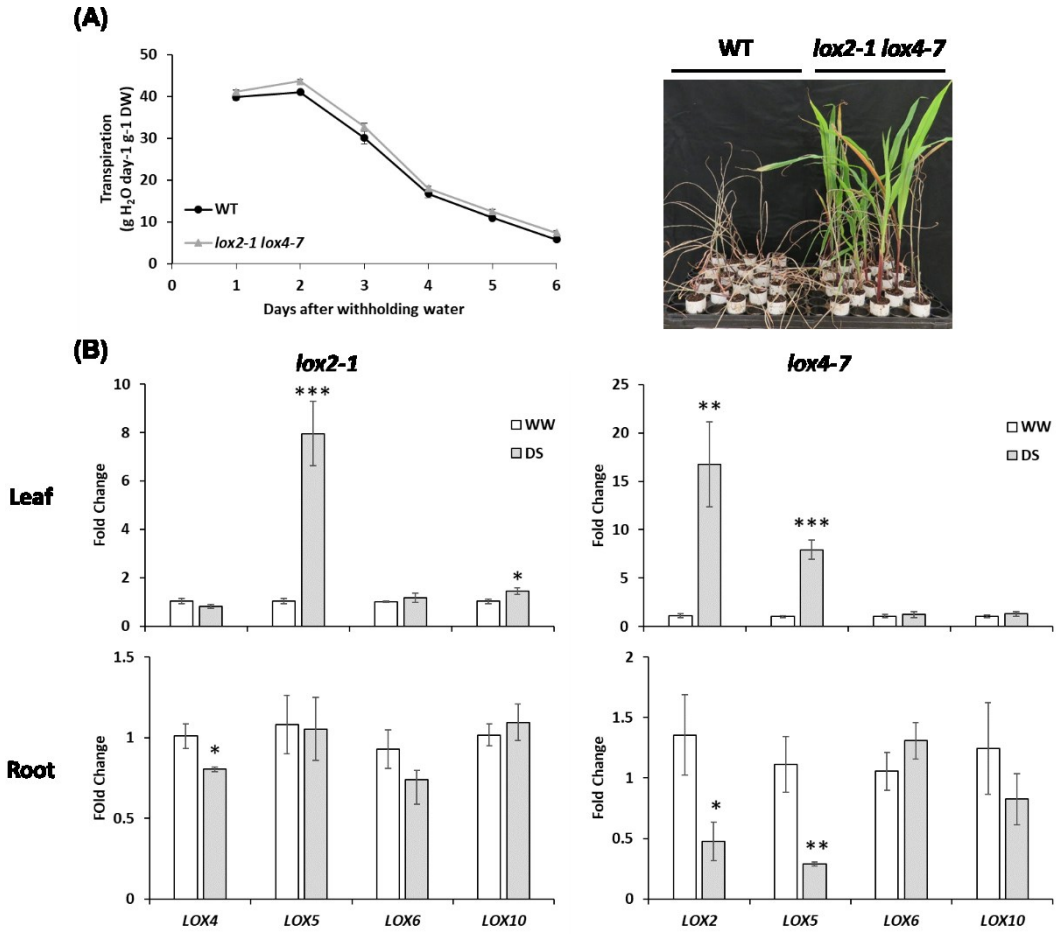


Figure 18. *ZmLOX4*- and *ZmLOX2*-mediated pathways interact in response to drought. *lox2-1 lox4-7* had similar amount of transpirational water loss during water deprivation but recovered more successfully from 14 days of prolonged drought stress (A). The Y-axis represents transpirational water loss (g $H_2O$ $day^{-1}$ $g^{-1}$ DW) and the X-axis represents the days after withholding water. The black line depicts WT and gray line depicts the *lox2-1 lox4-7* mutant. (B) *ZmLOX5*, and *ZmLOX10* were up-regulated by approximately 8 and 1.5-folds, respectively, in response to withholding water in *lox2-1* leaf while *ZmLOX4* was down-regulated about 0.8-fold in root. *ZmLOX2*, and *ZmLOX5* are up-regulated in the *lox4-7* leaves approximately 16.7 and 8 folds, respectively, in response to water deprivation. *ZmLOX2* and *ZmLOX5* were down-regulated about 0.5 and 0.3-fold, respectively, of in the *lox4-7* root. Bars are means ± SE. Asterisks represent statistically significant differences between well-watered (WW) and drought-stressed (DS) conditions. (Student's *t*-test, * $0.01 < p < 0.05$, ** $0.001 < p < 0.01$, *** $p < 0.001$).

**Phytohormone and oxylipin profiling in *lox2-1*, *lox4-7*, *lox5-3*, and *lox2-1 lox4-7* mutants in response to drought stress**

To gain a better understanding of the LOX-mediated drought tolerance mechanisms, a range of oxylipins and phytohormones were measured in leaves and roots of WT and the mutants in response to withholding water. Two-week old maize seedlings were soaked in water to reach 100% soil water content and then water was withheld. The tips of the 3rd and 4th leaves and roots were harvested at 0 (control), 4, and 6 days after withholding water for oxylipin and phytohormone profiling. The results showed that stress-related phytohomone ABA accumulated to a significantly higher level in WT, *lox2-1*, and *lox2-1 lox4-7* after 4 and 6 days of water deprivation in both leaves and roots while *lox4-7* and *lox5-3* mutant had significantly lower ABA content in both leaves and roots (Figure 19). *lox2-1* accumulated significantly higher SA levels in response to withholding water at day 4 and 6, while lower SA content was found in *lox4-7* compared to WT at day 6. No difference was observed in *lox5-3* and *lox2-1 lox4-7* mutants. Quantified jasmonates included JA-precursor, 12-OPDA, JA, and JA-Ile. Overall, *lox2-1* accumulated significantly higher levels of 12-OPDA and JA-Ile while *lox4-7* had much lower JA and JA-Ile contents in leaves but had higher levels of both molecules in roots after 6 days of water deprivation (Figure 20). No clear difference was found in both *lox5-3* and *lox2-1 lox4-7* mutants. *lox2-1* had higher content of 9-oxylipins including 9-HOD, 9-HOT, 9-KOD, 9-KOT, and 10-OPEA in leaves at both day 0 and day 6 after withholding water, whereas *lox4-7* and *lox2-1 lox4-7* accumulated lower contents of these 9-oxylipins in roots after water deprivation. *lox5-3* had lower 9-HOD, 9-HOT, 9-

KOD, and 10-OPEA contents in roots at 6 days of withholding water (Figure 21). No clear difference of 13-oxylipins was observed among WT and *lox* mutants except for lower 13-HOD and 13-KOD in *lox4-7* roots at day 6 (Figure 22). Collectively, these results suggest that *ZmLOX2* and *ZmLOX4* regulate maize drought tolerance by mediating synthesis of various oxylipins and stress-related phytohormones, especially jasmonates. Previously 12-OPDA has been reported to promote stomatal closure (Savchenko et al., 2014) while the role of JA remains controversial. In leaves, significantly higher level of JA-Ile accumulated in *lox2-1* while *lox4-7* had significantly lower JA-Ile content at six days of water deprivation correlated with water loss phenotypes of these two mutants. These observations prompt the hypothesis that the JA functions to open stomata in B73 seedlings.

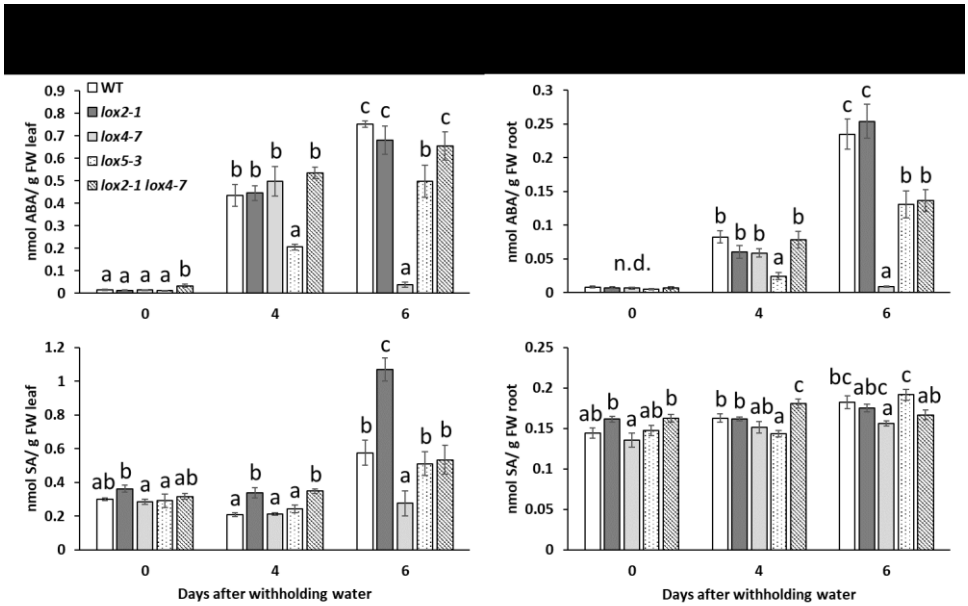


Figure 19. Accumulation of ABA and SA in leaves and roots of WT, *lox2-1*, *lox4-7*, *lox5-3* and *lox2-1 lox4-7* mutant in response to 4 and 6 days of water deprivation. Leaves and roots were harvested at 0 (control), 4, and 6 days after withholding water for metabolite and hormone measurement. Bars are means ± SE. Unconnected letters indicate statistically significant differences among the samples within the same time-point (ANOVA followed by post hoc of Student's *t*-test, $p < 0.05$). n.d. (not statistically different).

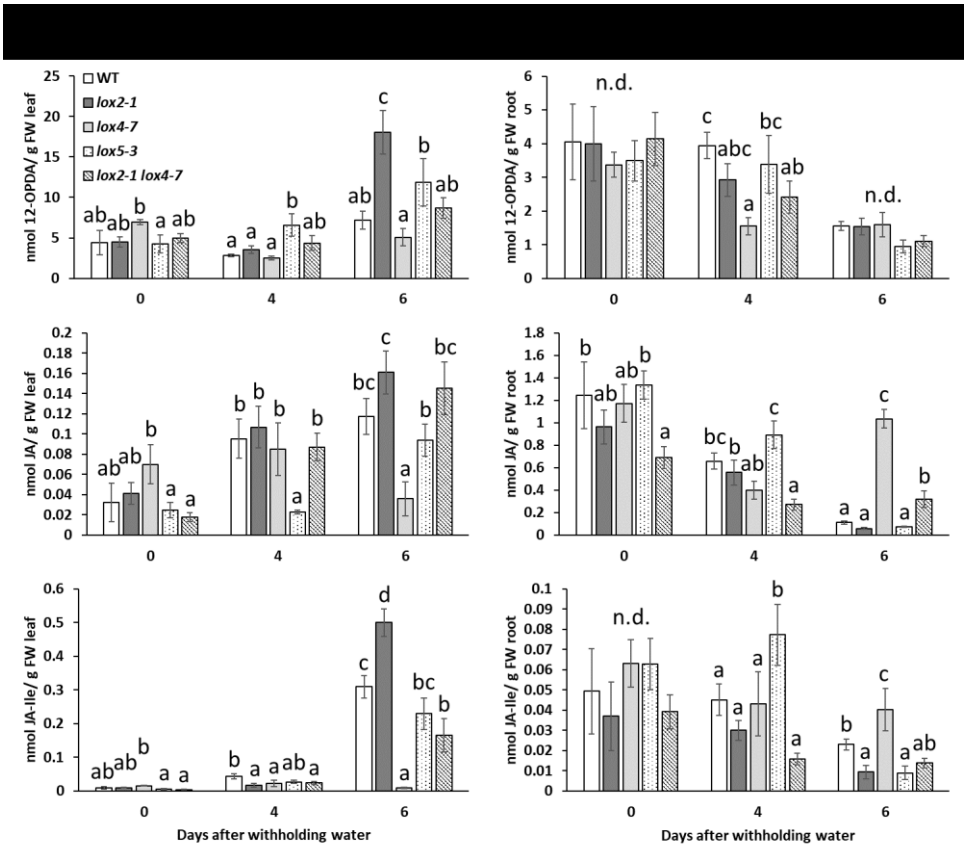


Figure 20. Accumulation of 12-OPDA, JA, and JA-Ile in leaves and roots of WT, *lox2-1*, *lox4-7*, *lox5-3* and *lox2-1 lox4-7* mutant in response to 4 and 6 days of water deprivation. Leaves and roots were harvested at 0 (control), 4, and 6 days after withholding water for metabolite and hormone measurement. Bars are means ± SE. Unconnected letters indicate statistically significant differences among the samples within the same time-point (ANOVA followed by post hoc of Student's *t*-test, $p < 0.05$). n.d. (not statistically different).

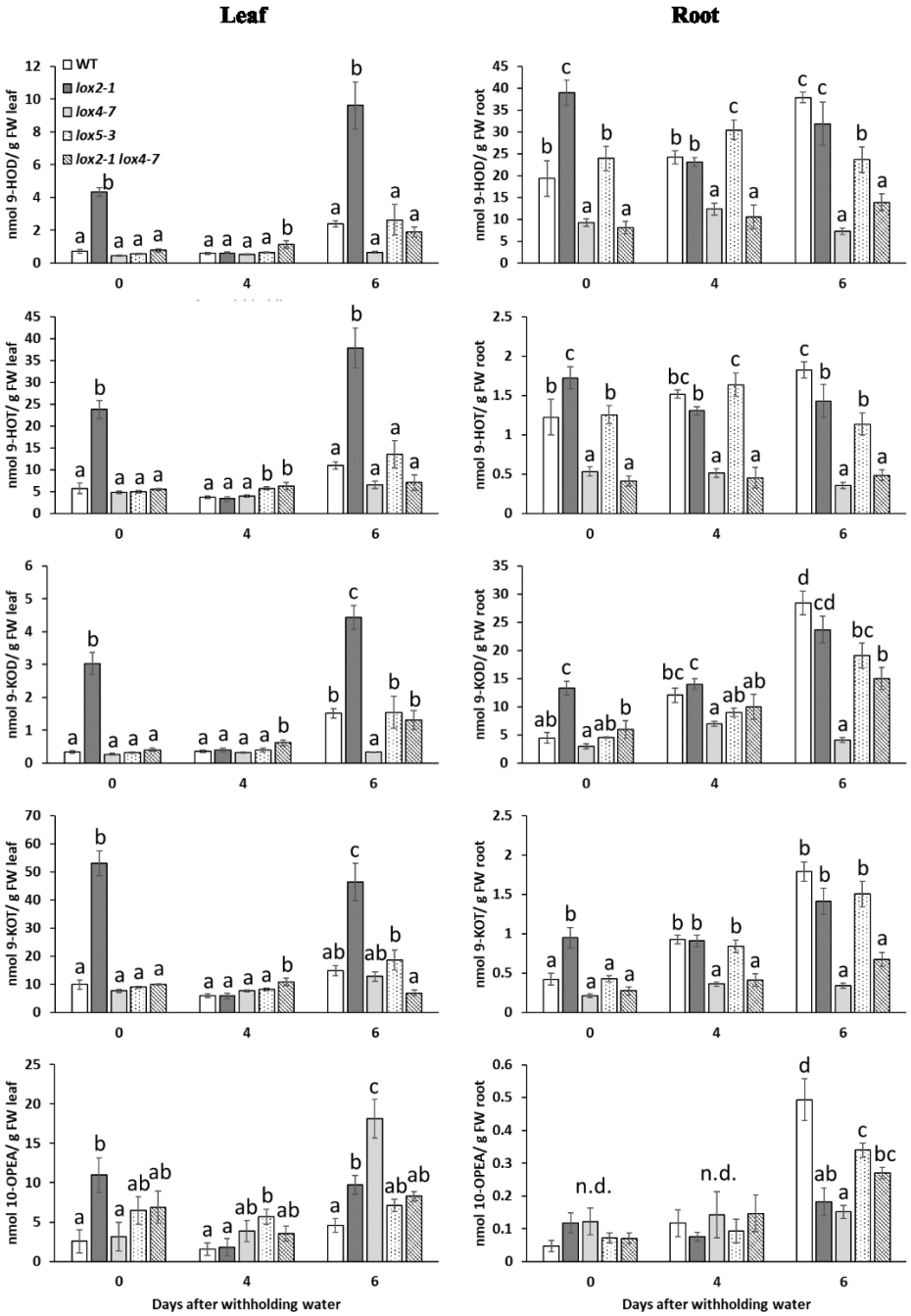


Figure 21. Accumulation of 9-oxylipins in leaves and roots of WT, *lox2-1*, *lox4-7*, *lox5-3* and *lox2-1 lox4-7* mutant in response to 4 and 6 days of water deprivation. Leaves and roots were harvested at 0 (control), 4, and 6 days after withholding water for metabolite and hormone measurement. Bars are means ± SE. Unconnected letters indicate statistically significant differences among the samples within the same time-point (ANOVA followed by post hoc of Student's *t*-test, $p < 0.05$). n.d. (not statistically different).

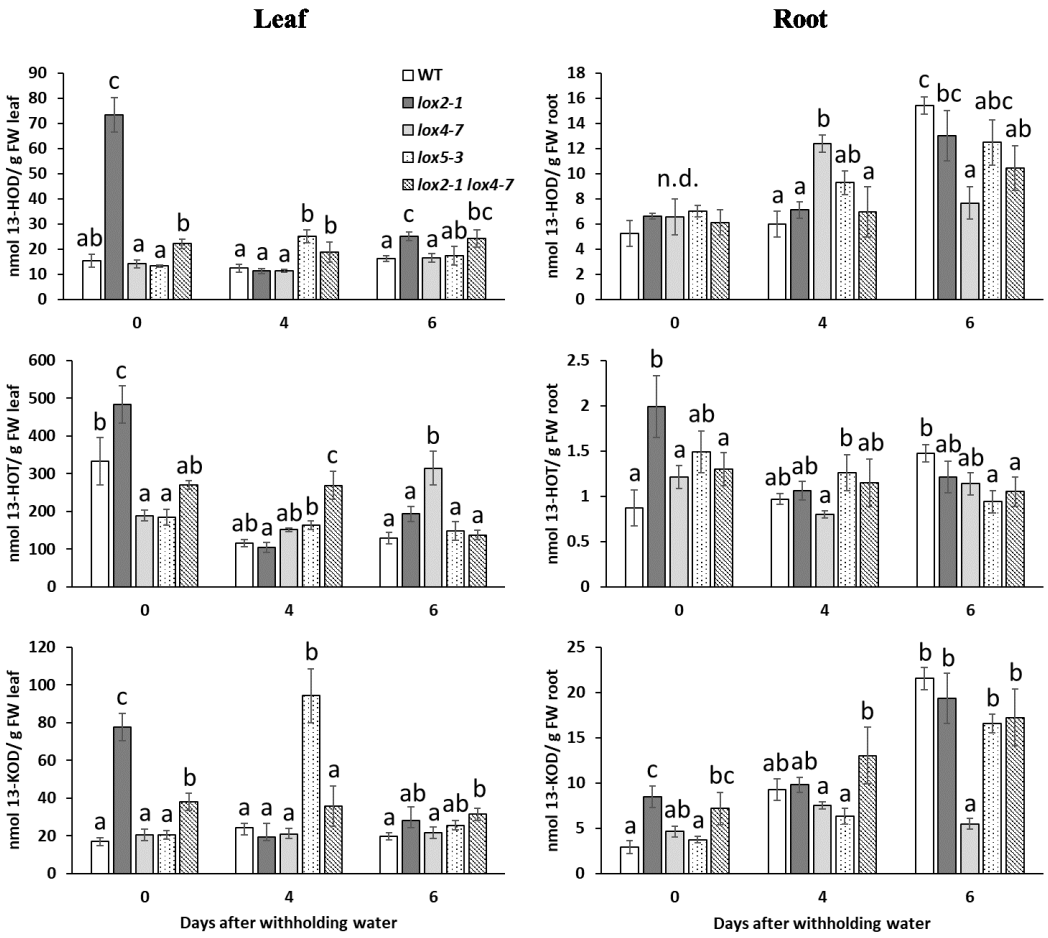


Figure 22. Accumulation of 13-oxylipins in leaves and roots of WT, *lox2-1*, *lox4-7*, *lox5-3* and *lox2-1 lox4-7* mutant in response to 4 and 6 days of water deprivation. Leaves and roots were harvested at 0 (control), 4, and 6 days after withholding water for metabolite measurement. Bars are means ± SE. Unconnected letters indicate statistically significant differences among the samples within the same time-point (ANOVA followed by post hoc of Student's *t*-test, $p < 0.05$). n.d. (not statistically different).

**RNA-seq analysis and transcriptome responses**

To identify the genes and gene-networks mediated by LOXs in response to drought stress, we analyzed the transcriptomes of the drought sensitive mutants, *lox2-1* and *lox5-3*, the intermediate WT (B73 inbred line), and the drought tolerant mutants *lox4-7* and *lox2-1 lox4-7* under both well-watered and drought stressed conditions at 4 days after withholding water with three biological replicates for each condition. Total RNA was prepared from both leaves and roots of each sample and then subjected to RNA-seq profiling using Illumina Hiseq 2500 platform at Texas A&M AgriLife Genomics and Bioinformatics Service. The RNA-seq analysis yielded approximately 6 million pair-ended reads per biological replicate with length of 50 bp. Approximately 95% overall read mapping rate was achieved when mapping reads to the Zea_mays_Ensembl_AGPv3. The normalized reads were used to measure the transcript abundance in each sample and presented as FPKM (Fragments Per Kilo base of transcript per Million mapped reads).

A gene is considered expressed if its FPKM is greater than 1. A total of 28,497 genes were found to be expressed in the treatments from the 41,799 annotated genes in Zea_mays.AGPv3. Among these genes, 13,368 genes were expressed in leaf samples and 19,978 genes were expressed in samples of root (Figure 23). There were 12,131 genes expressed in all treatments. A total of 1,601 genes were expressed in leaf samples and 4,855 genes were expressed in root samples, exclusively. In leaf samples, 22% (5,240) of the genes were expressed while only 4.9% (1,180) of the genes were expressed in response to drought stress in root samples.

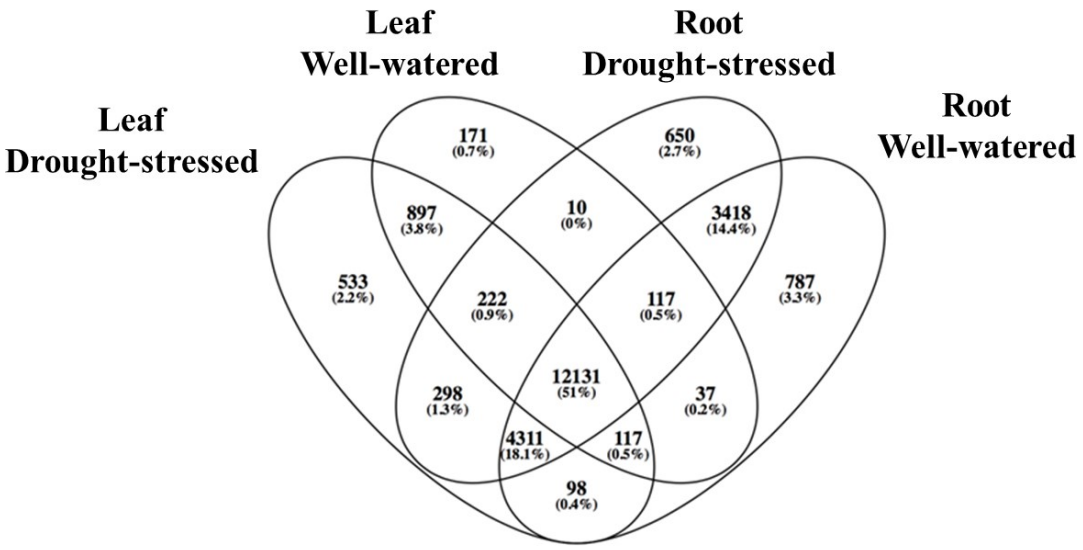


Figure 23. Profile of gene expression in leaf and root under both well-watered and drought-stressed conditions. A venn diagram is used to show the gene expression profile as the number of transcriptomic responses. A total of 28,497 genes were expressed in the treatments from the 41,799 annotated genes in Zea_mays.AGPv3. Among these genes, 13,368 genes were expressed in leaf samples, 19,978 genes were expressed in root samples. There were 12,131 genes expressed in all treatments. A total of 1,601 genes were expressed in leaf samples and 4,855 genes were expressed in root samples, exclusively. In leaf samples, 22% (5,240) of the genes were expressed while only 4.9% (1,180) of the genes were expressed in response to drought stress in root samples.

**Differential expression analysis**

After assembling mapped reads to transcript fragments, differential expression analysis was performed by Cuffdiff 2.2.1. Genes were considered as significantly differentially expressed genes (DEGs) only if the adjusted *p*-value was smaller than 0.05 and the absolute value of $\log_2$ (fold change) was larger than 0.58. A total of 7,366, 6,797, 4,909, and 6,179 DEGs were identified as up-regulated in leaf, down-regulated in leaf, up-regulated in root, and down-regulated in root in response to drought stress, respectively (Figure 24). Since *lox2-1* and *lox5-3* mutants are more sensitive to drought and *lox4-7* and *lox2-1 lox4-7* mutants are more drought tolerant, down-regulated genes shared by *lox2-1* and *lox5-3* and up-regulated genes shared by *lox4-7* and *lox2-1 lox4-7* in response to drought stress can be considered as candidate drought tolerance genes, these total 450 genes are circled by red dashed line. Up-regulated genes shared by *lox2-1* and *lox5-3* and down-regulated genes shared by *lox4-7* and *lox2-1 lox4-7* can be considered as candidate drought sensitivity genes, which total 529 genes as circled by blue dashed line.

To investigate the biological function of these candidate drought tolerance and sensitivity genes, GO enrichment analysis was performed with agriGO (Du et al., 2010). The 450 candidate drought tolerance genes were enriched in 37 GO terms in the biological process and cellular component categories (Table 2). Cellular component organization (GO:0016043), cellular component biogenesis (GO:0044085), macromolecular complex assembly (GO:0065003), cellular component assembly (GO:0022607), and macromolecular complex subunit organization (GO:0034621) are

the five major terms in biological process category, while cell (GO:0005623), cell part (GO:0044464), intracellular (GO:0005622), organelle (GO:0043226), and intracellular (GO:0005622) are the five most dominant terms in the cellular component category. The 529 candidate drought tolerance genes were enriched in 18 GO terms in the biological process, molecular function, and cellular component categories (Table 3). Interestingly, only five GO terms including nucleosome organization (GO:0034728), chromatin assembly (GO:0031497), nucleosome assembly (GO:0006334), DNA packaging (GO:0006323), nucleosome (GO:0000786), and protein-DNA complex (GO:0032993) are shared by the enriched GO terms of candidate drought tolerance and sensitivity genes. Macromolecule modification (GO:0043412), post-translation protein modification (GO:0043687), protein modification process (GO:0006464), phosphate metabolic process (GO:0006796), phosphorus metabolic process (GO: 0006793) are the five most dominant terms in the biological process category. The molecular function category contains protein serine/threonine kinase activity (GO:0004674), protein kinase activity (GO:0004672), phosphotransferase activity, alcohol group as acceptor (GO:0016773), and kinase activity (GO:0016301). These categories do not exist in the analysis of candidate drought tolerance genes. Collectively, these results suggest drought tolerant LOX mutants maintain better cell and membrane integrity under water deficit condition while kinases and protein modifications are more active in drought sensitive LOX mutants.

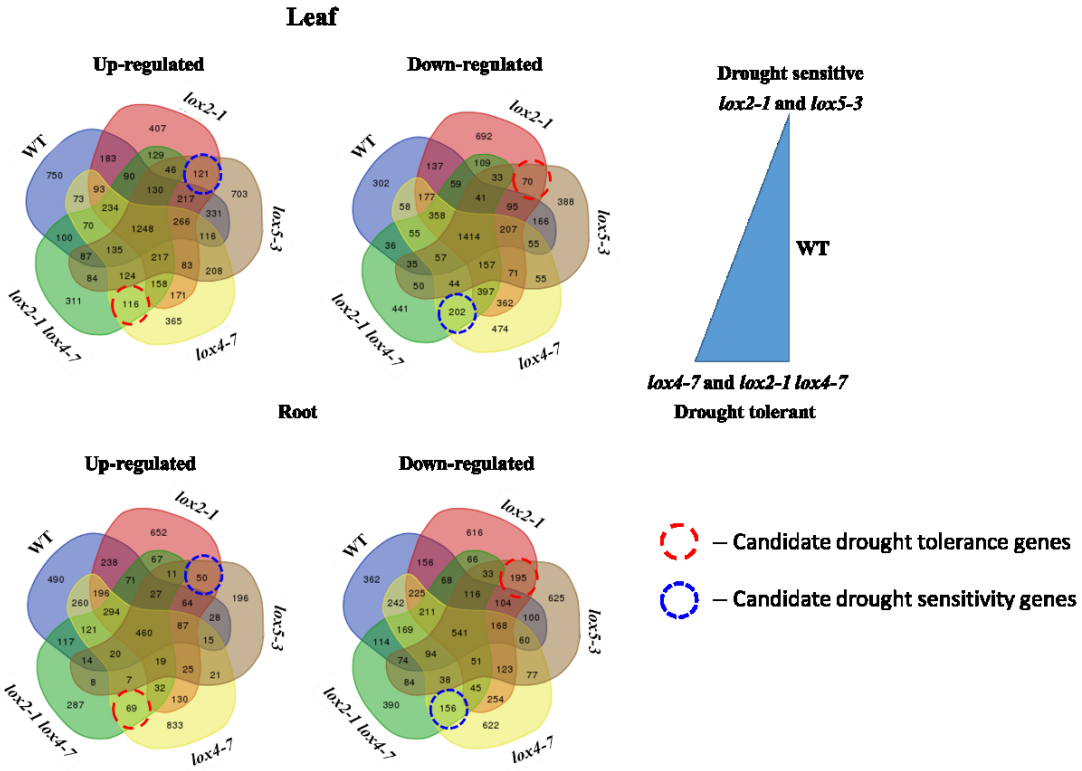


Figure 24. Profile of differentially expressed genes (DEGs) in leaf and root in response to drought stress in drought sensitive *lox2-1* and *lox5-3* mutants, intermediate WT, and drought tolerant *lox4-7* and *lox2-1 lox4-7* mutants. The gene expression profile is illustrated as the number of transcriptomic responses by using a Venn diagram. A total of 7,366, 6,797, 4,909, and 6,179 DEGs were identified as up-regulated in leaf, down-regulated in leaf, up-regulated in root, and down-regulated in root in response to drought stress, respectively. Genes circled by red dashed line represent candidate drought tolerance genes and genes circled by blue dashed line represent candidate drought sensitivity genes.

Table 2. Enriched GO terms of candidate drought tolerance genes.

| GO term | Ontology* | Description | Number of genes | p-value | FDR |
|---|---|---|---|---|---|
| GO:0071103 | P | DNA conformation change | 18 | 1.40E-09 | 1.50E-07 |
| GO:0065004 | P | protein-DNA complex assembly | 16 | 1.20E-09 | 1.50E-07 |
| GO:0034728 | P | nucleosome organization | 16 | 1.20E-09 | 1.50E-07 |
| GO:0031497 | P | chromatin assembly | 16 | 1.20E-09 | 1.50E-07 |
| GO:0006334 | P | nucleosome assembly | 16 | 1.20E-09 | 1.50E-07 |
| GO:0006323 | P | DNA packaging | 16 | 1.30E-09 | 1.50E-07 |
| GO:0006333 | P | chromatin assembly or disassembly | 16 | 8.70E-09 | 8.20E-07 |
| GO:0034622 | P | cellular macromolecular complex assembly | 18 | 6.30E-08 | 5.10E-06 |
| GO:0006325 | P | chromatin organization | 16 | 7.20E-08 | 5.30E-06 |
| GO:0051276 | P | chromosome organization | 16 | 9.70E-08 | 6.40E-06 |
| GO:0034621 | P | cellular macromolecular complex subunit organization | 18 | 2.00E-07 | 1.20E-05 |
| GO:0065003 | P | macromolecular complex assembly | 21 | 7.80E-07 | 4.30E-05 |
| GO:0022607 | P | cellular component assembly | 21 | 1.20E-06 | 6.30E-05 |
| GO:0043933 | P | macromolecular complex subunit organization | 21 | 1.70E-06 | 8.10E-05 |
| GO:0006996 | P | organelle organization | 17 | 3.10E-06 | 0.00014 |
| GO:0044085 | P | cellular component biogenesis | 21 | 9.00E-06 | 0.00037 |
| GO:0016043 | P | cellular component organization | 22 | 7.00E-05 | 0.0027 |
| GO:0007017 | P | microtubule-based process | 9 | 0.00051 | 0.019 |
| GO:0000786 | C | nucleosome | 16 | 1.10E-09 | 7.30E-08 |
| GO:0032993 | C | protein-DNA complex | 16 | 1.10E-09 | 7.30E-08 |
| GO:0044427 | C | chromosomal part | 18 | 4.70E-08 | 8.70E-07 |
| GO:0044422 | C | organelle part | 34 | 4.10E-08 | 8.70E-07 |
| GO:0000785 | C | chromatin | 18 | 3.00E-08 | 8.70E-07 |
| GO:0005694 | C | chromosome | 20 | 3.60E-08 | 8.70E-07 |
| GO:0044446 | C | intracellular organelle part | 34 | 4.10E-08 | 8.70E-07 |
| GO:0043232 | C | intracellular non-membrane-bounded organelle | 32 | 0.00065 | 0.0095 |
| GO:0043228 | C | non-membrane-bounded organelle | 32 | 0.00065 | 0.0095 |
| GO:0043227 | C | membrane-bounded organelle | 43 | 0.0022 | 0.026 |
| GO:0015630 | C | microtubule cytoskeleton | 6 | 0.0021 | 0.026 |
| GO:0043231 | C | intracellular membrane-bounded organelle | 42 | 0.0033 | 0.036 |
| GO:0005622 | C | intracellular | 82 | 0.0039 | 0.039 |
| GO:0044430 | C | cytoskeletal part | 6 | 0.0049 | 0.043 |
| GO:0005634 | C | nucleus | 34 | 0.0052 | 0.043 |
| GO:0044464 | C | cell part | 113 | 0.0057 | 0.043 |
| GO:0005623 | C | cell | 113 | 0.0057 | 0.043 |
| GO:0043229 | C | intracellular organelle | 57 | 0.0071 | 0.049 |
| GO:0043226 | C | organelle | 57 | 0.0071 | 0.049 |

* Biological Process (P) and Cellular Component (C)

Table 3. Enriched GO terms of candidate drought sensitivity genes.

| GO term | Ontology* | Description | Number of genes | p-value | FDR |
|---|---|---|---|---|---|
| GO:0006468 | P | protein amino acid phosphorylation | 43 | 1.80E-06 | 0.0012 |
| GO:0043687 | P | post-translational protein modification | 48 | 5.50E-06 | 0.0019 |
| GO:0043412 | P | macromolecule modification | 49 | 3.80E-05 | 0.0042 |
| GO:0016310 | P | phosphorylation | 44 | 2.40E-05 | 0.0042 |
| GO:0006464 | P | protein modification process | 48 | 2.60E-05 | 0.0042 |
| GO:0006796 | P | phosphate metabolic process | 46 | 4.30E-05 | 0.0042 |
| GO:0006793 | P | phosphorus metabolic process | 46 | 4.30E-05 | 0.0042 |
| GO:0065004 | P | protein-DNA complex assembly | 10 | 0.00046 | 0.026 |
| GO:0034728 | P | nucleosome organization | 10 | 0.00046 | 0.026 |
| GO:0031497 | P | chromatin assembly | 10 | 0.00046 | 0.026 |
| GO:0006334 | P | nucleosome assembly | 10 | 0.00046 | 0.026 |
| GO:0006323 | P | DNA packaging | 10 | 0.00047 | 0.026 |
| GO:0004674 | F | protein serine/threonine kinase activity | 42 | 9.70E-07 | 0.00037 |
| GO:0004672 | F | protein kinase activity | 43 | 2.60E-06 | 0.00051 |
| GO:0016773 | F | phosphotransferase activity, alcohol group as acceptor | 44 | 6.10E-05 | 0.0078 |
| GO:0016301 | F | kinase activity | 45 | 9.50E-05 | 0.0091 |
| GO:0000786 | C | nucleosome | 10 | 0.00044 | 0.026 |
| GO:0032993 | C | protein-DNA complex | 10 | 0.00044 | 0.026 |

* Biological Process (P), Molecular Function (F), and Cellular Component (C)

### *ZmLOX2* and *ZmLOX4* regulate maize transpirational water loss via modulating JA biosynthesis pathway

Increased levels of 12-OPDA correlated with decreased JA levels five days after withholding water in Arabidopsis have been reported to promote stomatal closure (Savchenko et al., 2014). This study has reported also that exogenous application of 12-OPDA has the strongest effect among tested molecules in reducing stomatal aperture especially in combinaiton with ABA (Savchenko et al., 2014). In the *lox2-1* mutant, both 12-OPDA and JA-Ile contents in leaves were significantly elevated after six days of water deprivation while similar amount of 12-OPDA and significantly lower JA-Ile accumulated in *lox4-7* leaves. Thus, we hypothesized that JA functions to open stomata and the content of JA is controlled through *ZmLOX2* and *ZmLOX4* during drought stress.

To test the hypothesis that LOX2 and LOX4 regulate JA production at the transcriptional level, expression of genes of JA biosynthesis pathway were analyzed from the RNA-seq results of the LOX mutants in response to drought stress. First, maize genes predicted to be involved in JA biosynthesis as described in Borrego and Kolomiets (2016) are listed in Figure 25A. The expression of the genes involved in the 12-OPDA biosynthesis (Figure 25B), the genes involved in the conversion of 12-OPDA into JA and JA-Ile (Figure 25C) and repressors of JA signaling, *JAZ*s, (Figure 25D) were examined from the RNA-seq results from leaf samples. Based on the analysis, *lox2-1* clustered the farthest from the WT, suggesting that 12-OPDA and JA synthesis pathway was not as active as WT. Although the drought tolerant *lox4-7* mutant clustered closer to WT than *lox2-1*, the key gene, *ZmJAR1a*, responsible for converting JA into the

bioactive form of JA, JA-Ile, was significantly down-regulated in *lox4-7*, which correlated well with reduced amount of JA-Ile in *lox4-7* leaves at 6 days after withholding water. Analyses of expression of repressors of JA signaling, *JAZs,* showed substantial differential regulation among these genotypes. With similar amount of JA and JA-Ile accumulation, *lox2-1* had reduced transcript accumulation of several *JAZ* genes, which presumably resulted in more active JA signaling. Expression of *ZmJAZ5* and *ZmJAZ7* were significantly up-regulated in all three genotypes that show similar water loss phenotype, WT, *lox5-3*, and *lox2-1 lox4-7* in response to drought stress. Interestingly, these genes were not responsive to drought in  in *lox2-1*, and even significantly down-regulated in *lox4-7* suggesting these two *JAZ* isoforms may potentially function in negative regulation of JA signaling in guard cell to enhance stomatal closure under drought stress. It is important to note that reduced expression of several JAZ genes in *lox4-7* mutant may be a consequence of this mutant not experiencing water deficit to the same level as other genotypes as evidenced by lower level of ABA compared to other genotypes.

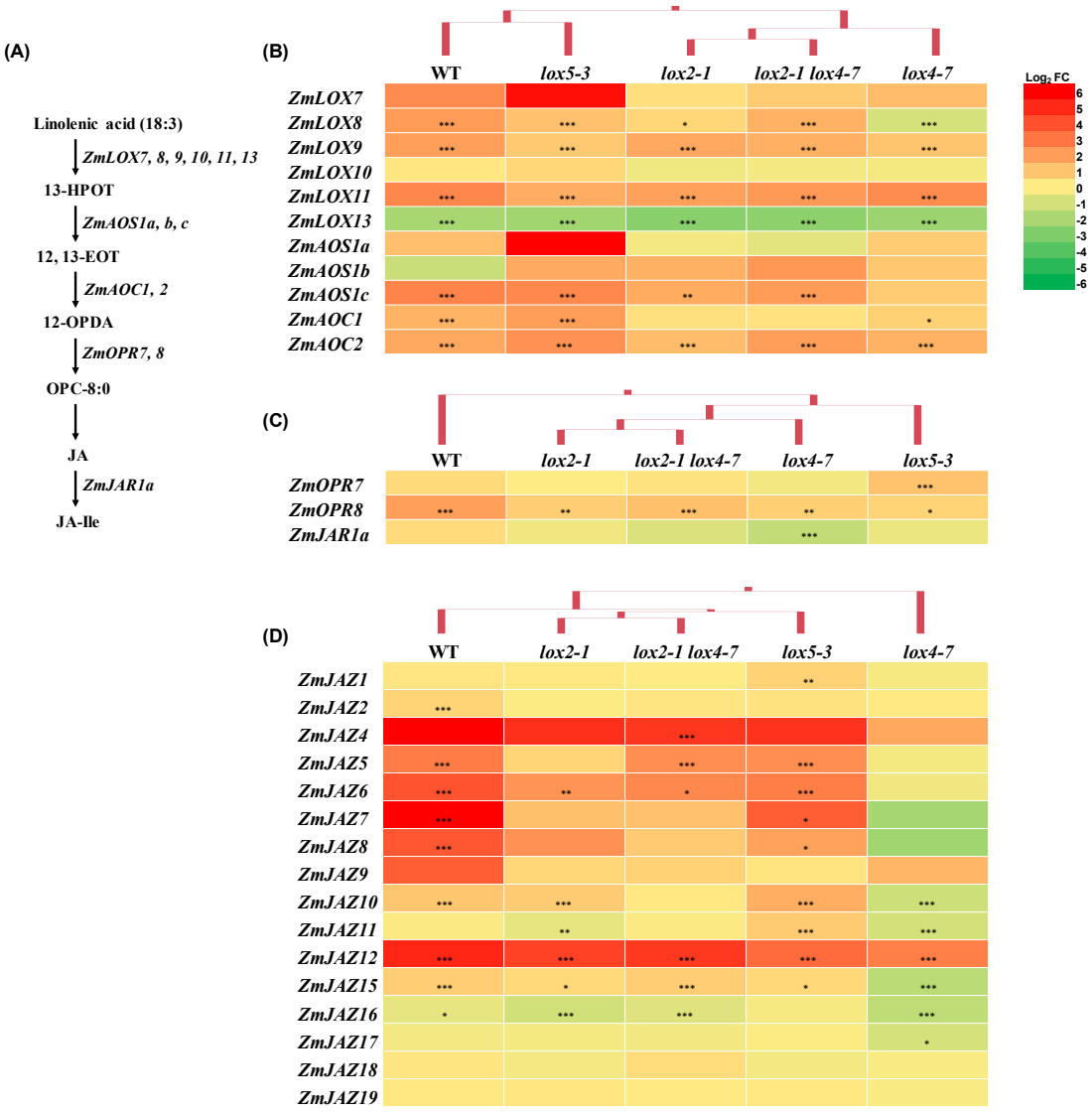


Figure 25. Expression of genes involved in JA biosynthesis pathway in response to drought in leaves. Maize genes predicted to be involved in JA biosynthesis pathway as described in (Borrego and Kolomiets, 2016) are listed in (A). (B) shows expression of the genes involved in JA-precursor 12-OPDA biosynthesis. (C) shows the genes required for conversion of 12-OPDA into JA and JA-Ile, and (D) shows *JAZ* isoforms. Hierarchical clustering of the genotypes was conducted by $\log_2$ (fold change) of the genes. Asterisks represent statistically significant differences based on the adjusted *p*-value (* $0.01 < p < 0.05$, ** $0.001 < p < 0.01$, *** $p < 0.001$).

**Expression of potassium channels in guard cell correlates with transpirational water loss**

Potassium channels expressed in guard cells have been reported to be important regulators of stomatal movement. Outward-rectifying $K^+$ channel GORK in *Arabidopsis thaliana* guard cells enhances stomatal closure by mediating $K^+$ efflux (Ache et al., 2000; Hosy et al., 2003). Several inward-rectifying $K^+$ channel proteins have been found in *Arabidopsis thaliana* guard cells involved in promoting stomatal opening via mediating $K^+$ uptake (Dietrich et al., 2001; Szyroki et al., 2001). To examine the expression of maize $K^+$ channels, the genes identified as $K^+$ channels expressed in maize guard cells and subsidiary cells as described in (Buchsenschutz et al., 2005) are listed here and their expression was examined in RNA-seq datasets from leaf samples (Figure 26). Interestingly, one of the inward-rectifying $K^+$ channels that promotes stomatal opening, KZM1, was significantly up-regulated in *lox2-1* in response to drought stress while down-regulated in WT and *lox4-7* mutant. ZORK, the outward-rectifying $K^+$ channel enhancing stomatal closure, was down-regulated in *lox2-1* but up-regulated in the *lox2-1 lox4-7* mutant. Collectively, mis-regulation of specific $K^+$ channels correlated with increased transpirational water loss in the *lox2-1* mutant.

To validate the RNA-seq results, qRT-PCR was conducted to confirm the expression of a group of LOX and OPR isoforms in our analysis. In total, 30 qRT-PCR reactions were conducted and the correlation of $\log_2$ (fold change) under WW and DS conditions between qRT-PCR and RNA-seq are shown in Figure 27.

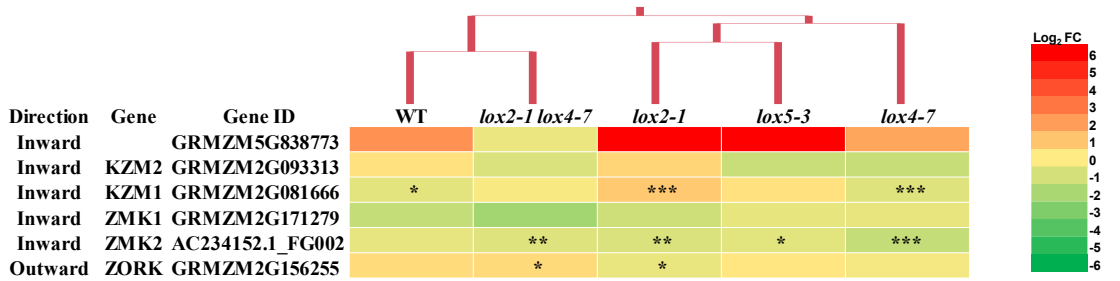


Figure 26. Expression of potassium channel proteins specific to guard cells and subsidiary cells. List of genes of potassium channels between guard cells and subsidiary cells as described in (Buchsenschutz et al., 2005) are shown here and gene IDs were identified from maizeGDB. Expression of these genes were examined from the RNA-seq results of leaf samples in response to drought stress and hierarchical clustering of the genotypes was conducted by $\log_2$ (fold change) of the genes. Expression results in white background mean data not available due to lack of expression under well-watered condition. Asterisks represent statistically significant differences based on the adjusted *p*-value (* $0.01 < p < 0.05$, ** $0.001 < p < 0.01$, *** $p < 0.001$).

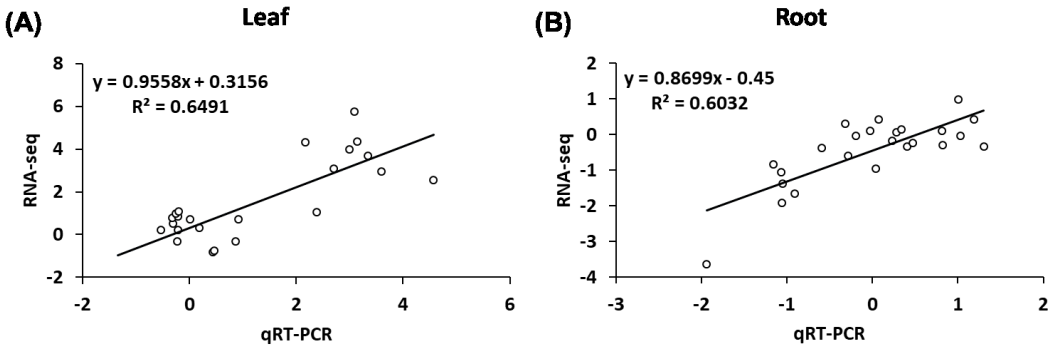


Figure 27. Validation of RNA-seq expression through qRT-PCR. Validation of RNA-seq was performed in both leaf (A) and root (B) samples from each genotype submitted for RNA-seq profiling. The plots demonstrate the gene expression ratio between well-watered and drought-stressed conditions in log scale with base of two.

**Exogenous 12-OPDA application restored *lox2-1* water loss**

12-OPDA has been recently reported to promote stomatal closure (Montillet et al., 2013; Savchenko et al., 2014). To test whether the lack of 12-OPDA is responsible for the decreased *lox2-1* drought tolerance, water loss measurement was conducted on WT and *lox2-1* mutants with or without exogenous 12-OPDA treatment. Seedlings of WT and *lox2-1* mutant were exogenously treated with either 2 ml of mock (0.003% ethanol) or 10 μM 12-OPDA per day after weights were recorded. Although no clear effect was observed on WT, transpirational water loss of *lox2-1* was reduced to WT level after 12-OPDA treatment (Figure 28). This result suggests that *ZmLOX2* serves to regulate transpirational water loss via mediating the balance between 12-OPDA and JA/JA-Ile.

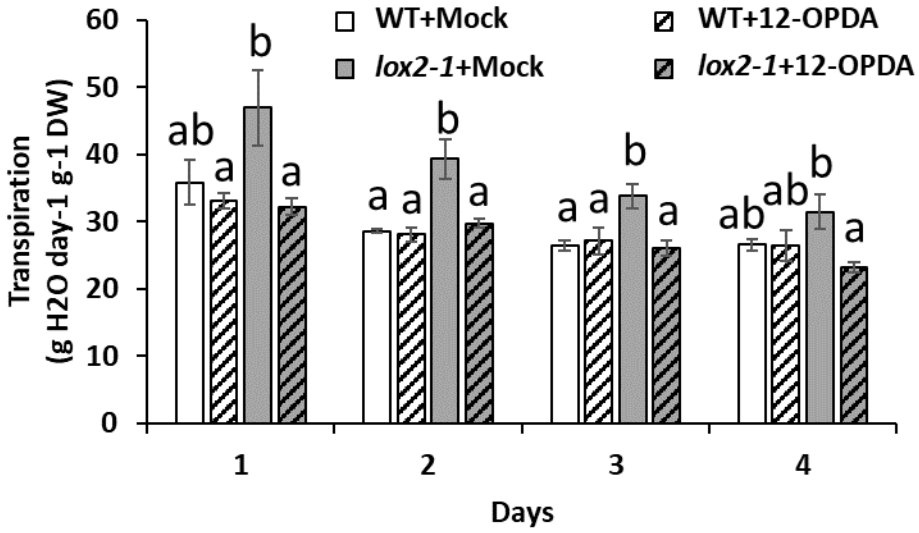


Figure 28. Exogenous 12-OPDA application restored *lox2-1* transpirational water loss to WT level. Two-weeks old maize seedlings were soaked in water to reach 100% water content and then withheld water. Starting at day 0 after weight was recorded, these seedlings were either sprayed with 2 milliliters of mock (0.03% ethanol) or 10 µM 12-OPDA per plant per day. The Y-axis represents transpirational water loss (g $H_2O$ $day^{-1}$ $g^{-1}$ DW) and the X-axis represents the days after withholding water. The white bar depicts WT sprayed with mock; the white bar shaded in a striped pattern depicts WT sprayed with 12-OPDA; the gray bar depicts *lox2-1* mutant sprayed with mock; the gray bar shaded in a striped pattern depicts *lox2-1* mutant sprayed with 12-OPDA. Bars are means ± SE. Unconnected letters indicate statistically significant differences among the samples within the same time-point (ANOVA followed by post hoc of Student's *t*-test, $p < 0.05$).

**JA promotes stomatal opening**

To test the hypothesis that JA functions in opening stomata, transpirational water loss measurement was conducted on the JA-deficient B73 *opr7-5 opr8-2* mutant and WT (B73 inbred line). *opr7-5 opr8-2* mutant had significantly less water lost through transpiration compared to WT during water deprivation for seven days (Figure 29A). To further test the effect of JA in the regulation of stomata functions, water loss via transpiration of *opr7-5 opr8-2* and WT was measured with or without exogenous MeJA treatment. Three milliliters of mock (0.004% ethanol) or 100 μM methyl jasmonic acid (MeJA) was sprayed onto each control or MeJA-treated plant every day right after weight measurement. Exogenous MeJA spray only slightly increased transpirational water loss of WT plants but significantly increased transpirational water loss of *opr7-5 opr8-2* mutant to similar levels as WT during water deprivation (Figure 29B). To confirm that JA serves to open stomata, stomatal aperture of leaf epidermal peels of both WT and *opr7-5 opr8-2* was measured with mock or 100 μM MeJA treatment. The result showed *opr7-5 opr8-2* had slightly smaller aperture under mock control condition but MeJA treatment significantly increased stomatal aperture to a wider level than that of WT while MeJA only slightly impacted WT (Figure 29C). These results strongly indicate that JA increases transpirational water loss through promoting stomatal opening.

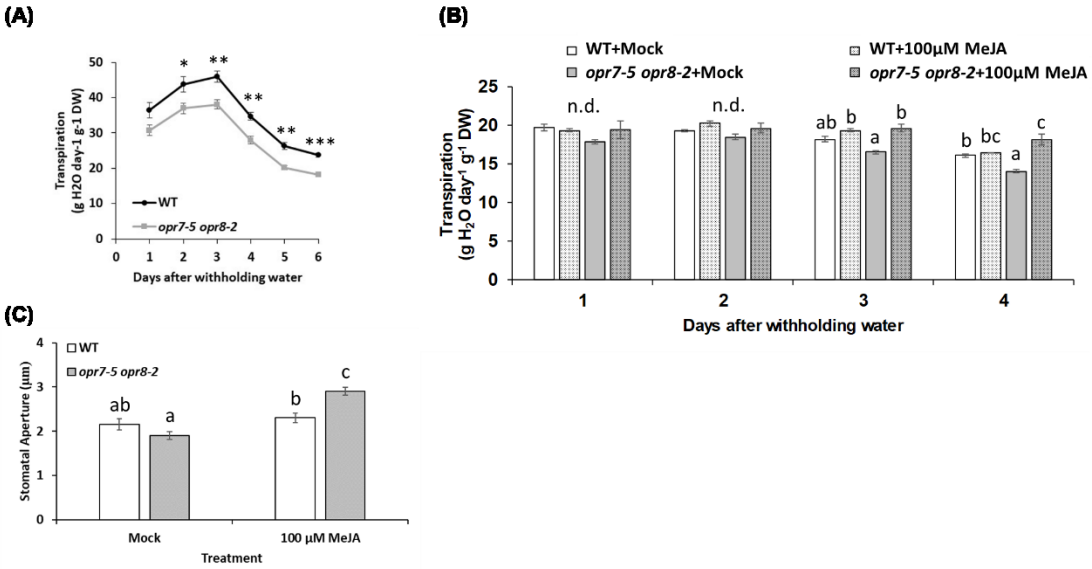


Figure 29. JA promotes stomatal opening. (A) Transpirational water loss of JA-deficient *opr7-5 opr8-2* mutant and WT during water deprivation. The Y-axis represents transpirational water loss (g $H_2O$ $day^{-1}$ $g^{-1}$ DW) and the X-axis represents the days after withholding water. Bars are means ± SE. Black line depicts WT and gray line depicts the *opr7-5 opr8-2* mutant. Asterisks represent statistically significant differences between WT and the *opr7-5 opr8-2* mutant within the same time-point (Student's *t*-test, * $0.01 < p < 0.05$, ** $0.001 < p < 0.01$, *** $p < 0.001$) (B) Transpirational water loss of JA-deficient *opr7-5 opr8-2* mutant and WT sprayed with 3 mls of mock (0.004% ethylene) or 100 µM MeJA solutions during water deprivation. (C) Stomatal aperture of WT and *opr7-5 opr8-2* mutants from leaf epidermal peels with mock or 100 µM MeJA treatment. The Y-axis represents transpirational water loss (g $H_2O$ $day^{-1}$ $g^{-1}$ DW) and the X-axis represents the days after withholding water. Bars are means ± SE. Unconnected letters indicate statistically significant differences among the samples within the same time-point (ANOVA followed by post hoc of Student's *t*-test, $p < 0.05$).

**Ethylene enhances stomatal closure**

Ethylene (ET) and JA interact with each other synergistically or antagonistically depending on the stresses. Previously, ethylene-deficient *acs6* mutant was reported to increase transpiration under drought conditions (Young et al., 2004), but no evidence connecting JA with ET under drought have been reported. To investigate the role of ET in the regulation of transpirational water loss in JA-deficient *opr7-5 opr8-2* mutant, ET production was measured in *opr7-5 opr8-2* mutant and WT under well-watered (WW) or 6 days after imposition of drought stress (DS). ET production was slightly increased in *opr7-5 opr8-2* under WW condition but increased to a significantly higher level in mutant compared to WT in response to DS (Figure 30A), suggesting that increased ET production reduced transpirational water loss. To test this hypothesis, ET-deficient mutant *acs2 acs6* mutant and WT (B73 inbred line) were utilized for water loss measurement. The results showed that the ET-deficient *acs2 acs6* mutant had significantly higher water loss through transpiration compared to WT during water deprivation (Figure 30B). Together, these results suggest that increased ET production is responsible for reduced transpirational water loss via enhancing stomatal closure, and that ET biosynthesis is antagonized by JA signaling.

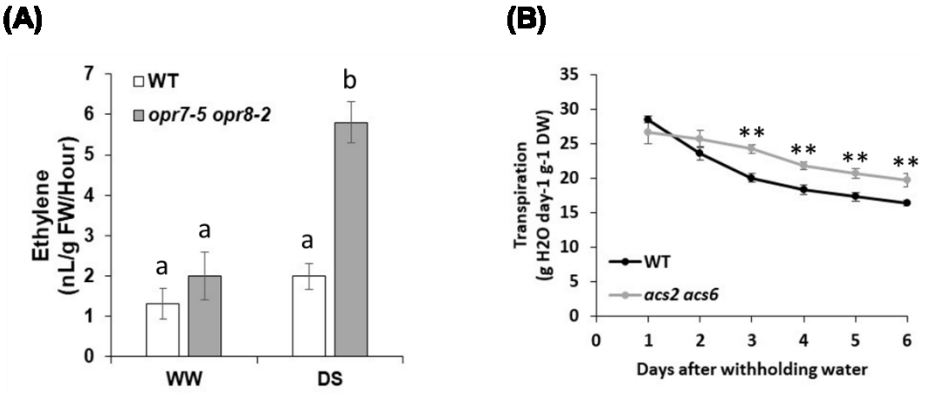


Figure 30. Ethylene enhances stomatal closure. (A) Ethylene production of fully developed 3rd leaves of JA-deficient *opr7-5 opr8-2* mutant and WT (B73 inbred) under well-watered (WW) or withholding water for six days (DS). The Y-axis represents ethylene production (nL ethylene/g FW/ hour) and the X-axis represents the genotypes. White bars are ethylene production under WW condition and gray bars are under drought stressed condition. Bars are means ± SE. Unconnected letters indicate statistically significant differences among the samples within the same time-point (ANOVA followed by post hoc of Student's *t*-test, $p < 0.05$). (B) Transpirational water loss of the ET-deficient *acs2 acs6* mutant and WT (B73 inbred) during water deprivation. The Y-axis represents transpirational water loss (g $H_2O$ $day^{-1}$ $g^{-1}$ DW) and the X-axis represents the days after withholding water. Bars are means ± SE. Black line depicts WT and gray line depicts *acs2 acs6* mutant. Asterisks represent statistically significant differences between WT and mutant within the same time-point (Student's *t*-test, ** $0.001 < p < 0.01$).

### *ZmLOX1* promotes salt stress tolerance via mediating SA and 10-OPEA biosynthesis in maize

To understand whether LOXs are required for salt stress tolerance in maize, WT, *lox1-3*, *lox2-1*, *lox4-7*, and *lox5-3* mutant seedlings in B73 genetic backgrounds were utilized to test salt stress tolerance. Maize seeds were grown in conical pots (20.5 by 4 cm). Five days after sowing, each conical pot with seedlings was given either 10 ml of sterile deionized water ($H_2O$) or 200 mM NaCl (salt stress) per day. Fourteen days after treatment, the soil was gently rinsed away and growth phenotypes including shoot length, shoot dry weight, root length, and root dry weight were recorded. Among the LOX mutants, *lox1-3* showed the most increased sensitivity to salt stress and salinity induced tissue senescence or degradation was more severe on both shoots and roots compared to WT and *lox2-1* (Figure 31A). Salinity severely impacted *lox1-3* shoot length (66% reduction), shoot dry weight (76% reduction), root length (43% reduction), and root dry weight (47% reduction) (Figure 31B). Reduced shoot length was observed on the *lox2-1* mutant while no further significant impact of salt stress on the roots of this mutant was observed. *lox4-7* and *lox5-3* mutants showed only mild growth reduction in response to salinity compared to WT. To test whether different *lox1* mutant allele also increases sensitivity to salinity, the same experiment was conducted using *lox1-4* knockdown allele (Figure 3). Milder but increased sensitivity to salinity was observed on *lox1-4* mutant in response to salt stress treatment with 48% reduction of shoot dry weight while only 27% reduction was observed on WT (Figure 31C). These results indicate that *ZmLOX1* enhances salt tolerance in B73 seedlings.

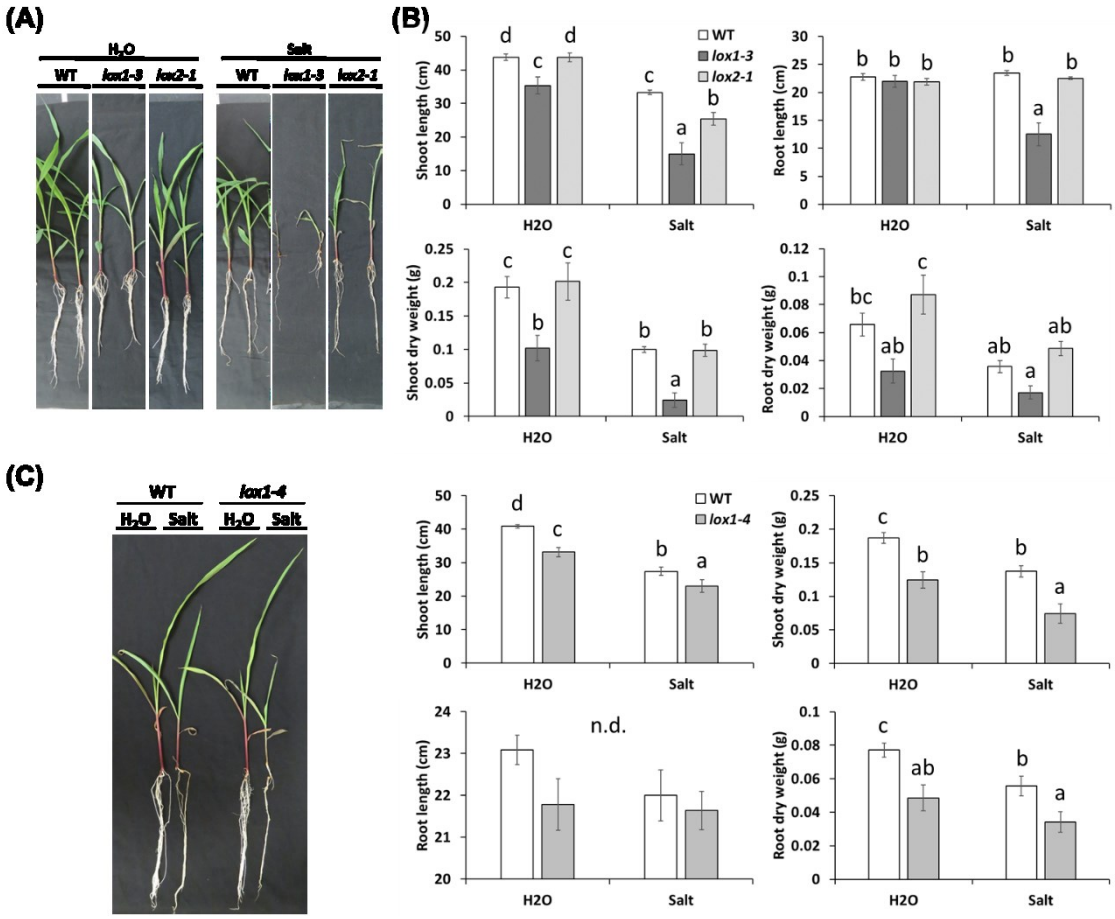


Figure 31. *ZmLOX1* promotes salt stress tolerance. Seedlings were grown in conical pots (20.5 by 4 cm). Photos of seedlings of WT, *lox1-3*, and *lox2-1* mutants were taken 14 days after treatment (A) and phenotypes were recorded (B). Results of alt stress experiment for *lox1-4* mutant allele are in (C). Bars are means ± SE. Unconnected letters indicate statistically significant differences among the samples within the same time-point (ANOVA followed by post hoc of Student's *t*-test, $p < 0.05$). n.d. (not statistically different).

To investigate the mechanism behind ZmLOX1-mediated salt stress tolerance, shoot and root tissues were collected for phytohormone and oxylipin profiling from both WT and *lox1-3* seedlings supplied with water or salt solution at 0 (control), 2, 4, and 8 days after treatment. ABA content was significantly lower in *lox1-3* shoots compared to WT but no difference was found in roots 8 days after salt stress treatment (Figure 32). SA content was significantly higher in *lox1-3* shoots and roots after salt stress treatment compared to WT. Overall, lower jasmonate contents including 12-OPDA, JA, and JA-Ile was observed in *lox1-3* leaves while a higher JA-Ile amount accumulated in roots after 8 days of salt treatment (Figure 33). WT seedlings accumulated elevated levels of 9-HOT and 9-KOT in shoots at 4 and 8 days in response to salinity but significantly lower content of these two 9-oxylipins was found in the *lox1-3* shoot (Figure 34). Significantly lower accumulation of 9-HOD, 9-HOT, and 9-KOD was observed in *lox1-3* roots after 4 and 8 days of salt stress treatment. Interestingly, 10-OPEA, the 12-OPDA positional isomer downstream of 9-LOX pathway, which can promote programmed cell death upon biotic stress (Christensen et al., 2015), accumulated to a significantly higher level in *lox1-3* roots in response to salt stress treatment as early as two days and maintained higher level at 4 and 8 days. Overall, lower 13-HOD, 13-HOT, and 13-KOD contents were observed in both shoot and root tissues of *lox1-3* in response to salt stress (Figure 35). Collectively, excessive amounts of SA and 10-OPEA correlated with increased salt sensitivity of *lox1-3*, suggesting *ZmLOX1* is required for maize salt tolerance via reducing excessive SA and 10-OPEA biosynthesis to reduce cell death processes.

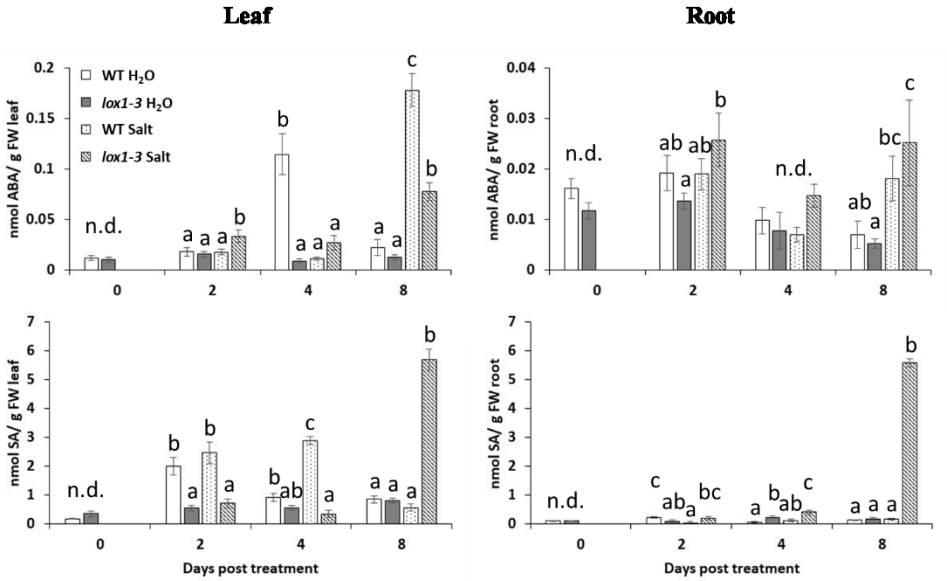


Figure 32. Accumulation of ABA and SA in leaves and roots of WT and *lox1-3* mutant in response salt stress. The leaves and roots were harvested at 0 (control), 2, 4, and 8 days after supplied with 10 ml of water or 200 mM NaCl per day for metabolite and hormone measurement. Bars are means ± SE. Unconnected letters indicate statistically significant differences among the samples within the same time-point (ANOVA followed by post hoc of Student's *t*-test, $p < 0.05$). n.d. (not statistically different).

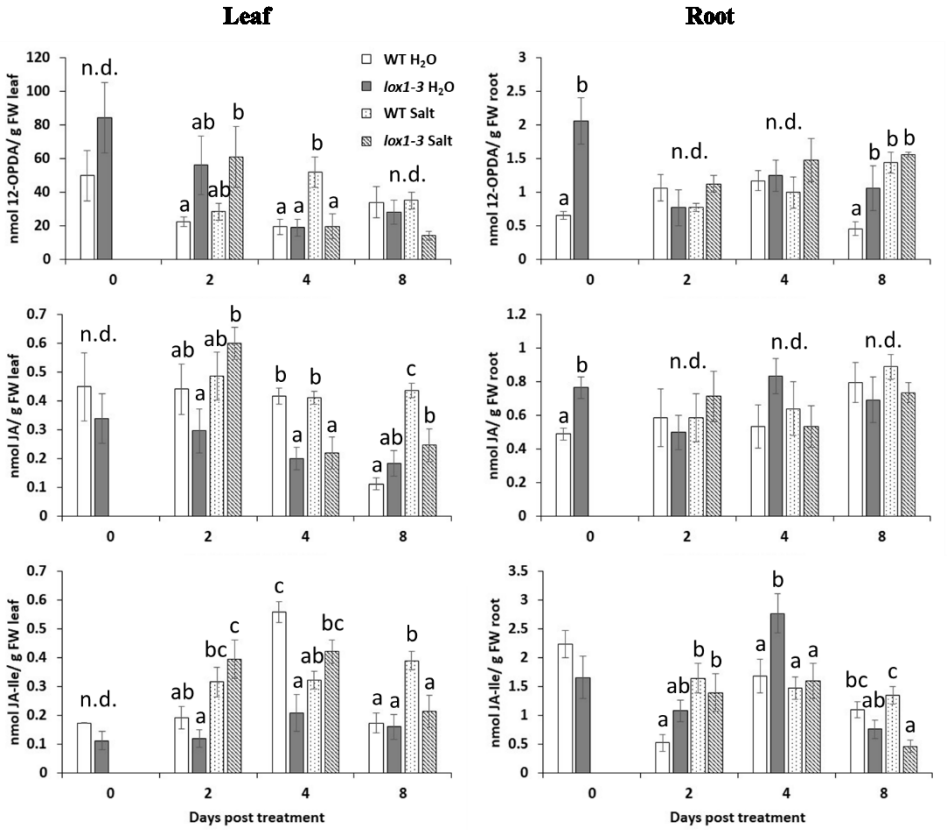


Figure 33. Accumulation of 12-OPDA, JA and JA-Ile in leaves and roots of WT and *lox1-3* mutant in response salt stress. The leaves and roots were harvested at 0 (control), 2, 4, and 8 days after supplied with 10 ml of water or 200 mM NaCl per day for metabolite and hormone measurements. Bars are means ± SE. Unconnected letters indicate statistically significant differences among the samples within the same time-point (ANOVA followed by post hoc of Student's *t*-test, $p < 0.05$). n.d. (not statistically different).

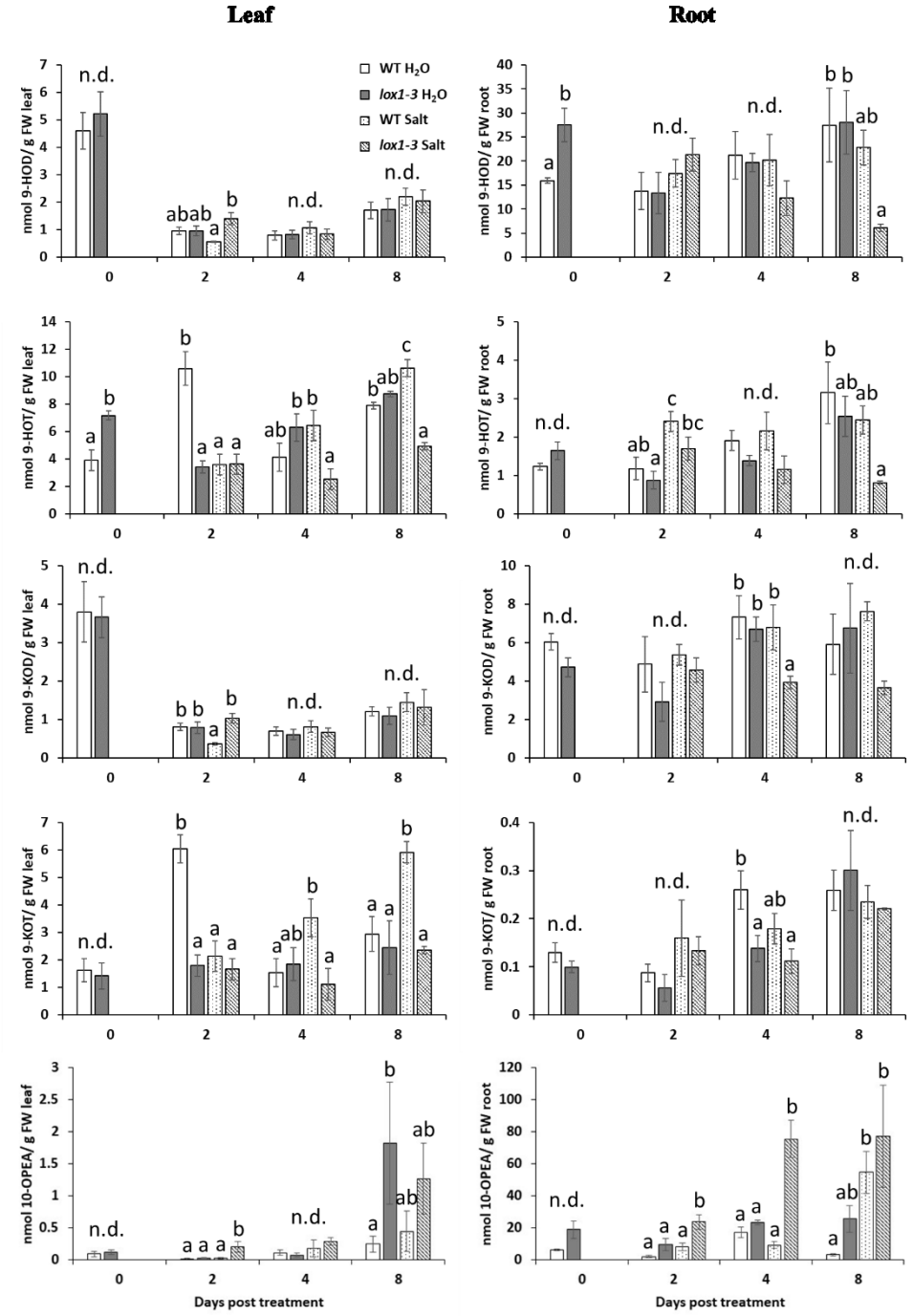


Figure 34. Accumulation of 9-oxylipins in leaves and roots of WT and *lox1-3* mutant in response salt stress. The leaves and roots were harvested at 0 (control), 2, 4, and 8 days after supplied with 10 ml of water or 200 mM NaCl per day for metabolite and hormone measurements. Bars are means ± SE. Unconnected letters indicate statistically significant differences among the samples within the same time-point (ANOVA followed by post hoc of Student's *t*-test, $p < 0.05$). n.d. (not statistically different).

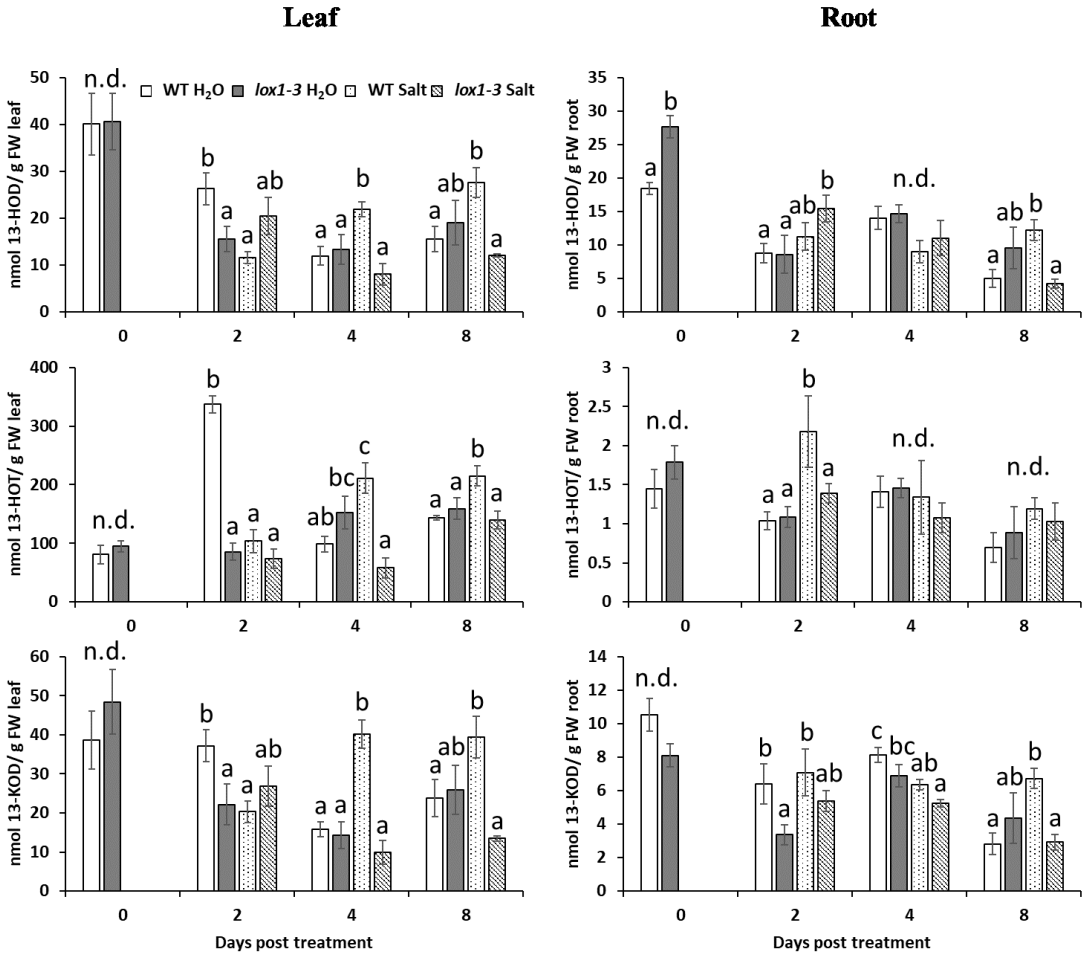


Figure 35. Accumulation of 13-oxylipins in leaves and roots of WT and *lox1-3* mutant in response salt stress. The leaves and roots were harvested at 0 (control), 2, 4, and 8 days after supplied with 10 ml of water or 200 mM NaCl per day for metabolite and hormone measurements. Bars are means ± SE. Unconnected letters indicate statistically significant differences among the samples within the same time-point (ANOVA followed by post hoc of Student's *t*-test, $p < 0.05$). n.d. (not statistically different).

## DISCUSSION

### Phytohormones cross talk during water deprivation

Plants produce an array of signals upon dehydration and hormones are the major molecules regulating drought responses. ABA, ET and JA have been shown to play important roles in drought stress response. Among these hormones, ABA plays the central role in closing stomata under water stress conditions. ABA in maize not only promotes stomatal closure but also maintains primary root growth via reducing ET production at low water potentials (Saab et al., 1990; Spollen et al., 2000; Sharp and LeNoble, 2002). However, the role of JA in regulating stomatal movement remains controversial. Activation and cross-talk between ABA- and JA-signaling during the first, but not repeated, water deficit was reported recently to be controlled through regulation of MYC2 transcription factor (Liu and Avramova, 2016; Avramova, 2017). In agreement with this, ABA and JA contents increased in maize leaves in response to withholding water. Many studies have reported that SA and JA function antagonistically in response to pathogen infection and insect attack (Mur et al., 2006; Spoel et al., 2007; Goodspeed et al., 2012; Chung et al., 2013), both SA and JA contents in maize leaves increased simultaneously in response to withholding water. These results suggest antagonism between SA and JA may be stress-specific.

### Oxylipin signals control drought stress responses in maize

In this study, we tested how specific *LOX* isoforms in maize B73 inbred line respond to drought stress and used reverse genetic approaches to investigate the role of different *LOX* isoforms in the regulation of transpirational water loss and drought

tolerance in maize. Gene expression of different *LOX* isoforms informed us which individual LOXs may potentially function in maize drought response. Disruption of ZmLOX2, ZmLOX3, and ZmLOX6 resulted in increased transpirational water loss, whereas *lox4* mutant alleles displayed reduced water loss. These results suggest that oxylipin signals produced by some LOX isoforms affect either positively or negatively transpirational water loss in maize. Recently, several studies have reported that oxylipins control stomatal movement in Arabidopsis and are required for resistance to abiotic stresses (Grebner et al., 2013; Montillet et al., 2013; Savchenko et al., 2014; Lim et al., 2015). Collectively, our findings and these recent reports indicate oxylipin signals are important in drought stress tolerance.

**JA promotes stomatal opening**

Exogenous MeJA treatment has been shown to promote stomatal closure by increasing ROS and NO production in an ABA-dependent manner (Suhita et al., 2004; Munemasa et al., 2007; Hossain et al., 2011). However, there are some inconsistent effects of exogenous treatment of MeJA on stomatal closure (de Ollas and Dodd, 2016). Exogenous MeJA has been reported to close stomata at low concentrations (10-20 μM) in Arabidopsis epidermal cells (Suhita et al., 2004). However, another study showed only 200 μM MeJA or higher concentration induced stomatal closure in the same plant species (Savchenko et al., 2014). In contrast, it was reported that JA-precursor, 12-OPDA, but not JA, promotes stomatal closure (Montillet et al., 2013). In addition, the phytotoxin coronatine secreted by bacterial pathogen *Pseudomonas syringae,* re-opens stomata via functionally and biochemically mimicking bioactive JA-Ile upon infection

(Zheng et al., 2012; Wasternack, 2017). Therefore, the authentic biological function of endogenous JA in controlling stomatal movement remains elusive. In this study, oxylipin and transcriptome profiling suggests that the JA biosynthesis pathway was regulated differentially by 9- and/or 13-oxylipns resulting in pronounced differences on transpirational water loss. We provided strong genetic evidence that that JA serves to open stomata by showing that JA-deficient *opr7-5 opr8-2* mutant had significantly reduced transpirational water loss during water deprivation and smaller stomatal aperture and that exogenous MeJA treatment restored these phenotypes to WT level.

**ET enhances stomatal closure**

Ethylene (ET) is another plant hormone regulating various plant processes including promoting fruit ripening, senescence, and stress responses (Bleecker and Kende, 2000) and its role in stomatal regulation is also controversial. Although ET has been suggested to induce $H_2O_2$ production in guard cells resulting in stomatal closure (Desikan et al., 2006; Ge et al., 2015), ABA-induced stomatal closure is impaired by exogenous ET treatment and an ET-overproducing mutant (*eto1*) delayed stomatal closure under drought stress (Tanaka et al., 2005). ET and JA function synergistically in resistance to necrotrophic fungal pathogen via regulating interaction between JAZ proteins and EIN3/EIL1 (Zhu et al., 2011; Zhang et al., 2014). However, ET and JA act antagonistically in the regulation of plant development and insect defense by modulating interactions between MYC2 and EIN3/EIL1 (Verhage et al., 2011; Zhang et al., 2014). However, ET and JA cross-talk under drought stress has not been clearly described. In this study, increased ET production was found in the JA-deficient *opr7-5 opr8-2* under

water stress and the ET-deficient *acs2 acs6* mutant lost more water through transpiration indicating that ET enhances stomatal closure and functions antagonistically to JA in controlling stomatal aperture in response to drought stress. These data are consistent with the observation that the *acs6* single mutant maintained higher transpiration under drought stress condition while no difference was observed under normal conditions (Young et al., 2004).

**Potassium channels and JAZ proteins control stomatal movement**

Plants regulate stomatal aperture in response to different stresses by modulating various ion flows in guard cells, especially potassium. Plants open stomata by increasing $K^+$ uptake through inward-rectifying $K^+$ channels into guard cells upon various stimuli including light, auxin, and low $CO_2$ condition (Szyroki et al., 2001). In contrast to this, $K^+$ efflux leads to stomatal closure in response to ABA or high $CO_2$ concentration (Ache et al., 2000; Hosy et al., 2003). Regulating expression of $K^+$ channel proteins and activity may be one of the mechanisms of drought tolerance. In rice, it has been reported recently that *OsKAT2* encodes an inward-rectifying $K^+$ channel specifically in guard cells and overexpression of a dominant negative form of OsKAT2(T235R) in rice improved drought tolerance without yield penalty by delaying stomatal opening in response to light (Moon et al., 2017). *KZM1* is the closest homolog gene of *OsKAT2* in the maize genome and its expression is significantly up-regulated in *lox2-1* under drought stressed conditions. It is therefore possible that such misexpression of this protein may lead to increased $K^+$ uptake and wider stomatal aperture eventually resulting in an increased transpirational water loss observed in *lox2-1* mutant.

JAZ proteins belong to the TIFY super-family of proteins and function as key regulators of JA-induced physiological, transcriptional and metabolic responses. JAZ proteins interact with COI1 in the Skp1/Cullin/F-box ($SCF^{COI1}$) ubiquitin complex that is formed in response to increase JA-Ile concentrations resulting ubiquitin-mediated degradation of JAZ proteins and activation of JA-regulated processes (Thines et al., 2007; Wasternack, 2017). Bacterial pathogen *P. syringae* secretes a functional and structural mimic of JA-Ile, coronatine, to hijack JA signaling to re-open stomata for penetration and infection via degrading JAZ proteins (Zheng et al., 2012; Gimenez-Ibanez et al., 2017). Recently, JAZ and TIFY gene families have been identified in several plant species of economic and agricultural importance such as rice, cotton, and tomato (Ye et al., 2009; Zhao et al., 2016; Chini et al., 2017). Overexpression of stress-inducible *OsTIFY11a* improved salt and osmotic stress tolerance in rice (Ye et al., 2009) and overexpression of *GaJAZ5* in *Arabidopsis thaliana* improved drought tolerance through reducing stomatal opening and transpirational water loss and increasing $H_2O_2$ accumulation (Zhao et al., 2016). However, how JAZ proteins regulate stomatal aperture in maize during drought stress remains unknown. In this study, transcriptome analyses revealed that several *ZmJAZ* genes such as *ZmJAZ5*, *ZmJAZ7*, and *ZmJAZ11* were differentially regulated in genotypes with contrasting drought responses implicating that these JAZ proteins function in regulating stomatal aperture. Further studies are required to characterize these *JAZ* genes in controlling stomatal dynamics.

### *ZmLOX1, ZmLOX2* and *ZmLOX6* localized in QTLs for drought-related traits

Quantitative trait loci (QTL)-based breeding approaches are not only more cost-effective in some cases but can also allow scientists to understand the genetic basis of plant development and crop yield, especially under water stress conditions (Collins et al., 2008). To date, many QTLs for drought-related traits have been reported. Interestingly, we found that *ZmLOX1* and *ZmLOX2* are within one of the QTL region responsible for anthesis-silking interval (ASI) identified by evaluation of the tropical populations under water-stress and well-watered conditions in Mexico, Kenya, and Zimbabwe (Almeida et al., 2013). In line with this finding, *lox2-1* mutant has greater anthesis-silking intervals (personal observation in TAMU research farm). Several maize germplasms have been identified to contain two copies of *ZmLOX2* in their genome by Southern blotting analysis (Huang and Kolomiets, unpublished data). More efforts are needed to test whether these two copies of *ZmLOX2* affect ASI and other drought-related traits after introgressing them into elite inbred germplasms. *ZmLOX6* localizes in the middle of a small QTL region on chromosome 2, which was identified for grain yield and anthesis-silking interval evaluated under water-stressed and well-watered environments (Semagn et al., 2013). In line with this result, we found *lox6-2* had significantly higher transpirational water loss than WT, suggesting *ZmLOX6* is involved in drought tolerance. *ZmLOX6* is a unique lipoxygenase in the maize genome possessing a fatty acid hydroperoxide lyase (HPL) activity by being able to cleave 13-HPOT into C13 and C5 products (Gao et al., 2008a). In the same study, it has been suggested that ZmLOX6 metabolizes the 13-hydroperoxides catalyzed by ZmLOX10 since they both co-localize

in the mesophyll chloroplasts (Nemchenko et al., 2006). ZmLOX10 is the sole lipoxygenase providing substrate for green leafy volatiles (GLVs) synthesized by HPL and GLVs regulates wound-induced JA biosynthesis pathway (Christensen et al., 2013). In addition, *cis*-3-hexenal, one of the GLV molecular species, has been shown to induce stomatal closure at 50 μM or higher concentration (Savchenko et al., 2014). In this study, we did not observe any difference between *lox10-3* mutant and WT, however this might be due to volatile communication within the same growth chamber space. Unlike GLVs, the function of downstream products of ZmLOX6 has not yet been identified. Further studies are needed to characterize the products of ZmLOX6 and the roles of these unique oxylipins in drought tolerance.

### ***ZmLOX1*** **is required for salt stress tolerance**

Salinity is one of the major threats to agricultural practice and accumulating evidence suggest lipid signals are also involved in salt stress tolerance. In this study, we provided strong genetic evidence that ZmLOX1 is important in the regulation of salt tolerance by mediating SA and 10-OPEA biosynthesis. SA was shown to increase abiotic stress tolerance when applied at low concentration but high level of exogenous application induced oxidative stress (Miura and Tada, 2014). After salt treatment, *lox1-3* had higher levels of SA accumulation at 2 and 4 days yet increased sensitivity to salinity suggesting SA enhances salt tolerance via *ZmLOX1*. Excessive amounts of SA accumulation at 8 days in both shoot and root of *lox1-3* could cause oxidative damage leading to cell death. 10-OPEA, the 12-OPDA positional isomer, has recently been reported to accumulate at necrotic tissue and functions to inhibit growth of fungi and

herbivores (Christensen et al., 2015). However, it is still not clear whether abiotic stress increases 10-OPEA accumulation. Under salt stress treatment, significantly higher levels of 10-OPEA content correlated with increased sensitivity of *lox1-3*. To my knowledge, this is the first study showing increased 10-OPEA accumulated following salt stress and its association with increased sensitivity.

In summary, this study provided strong genetic evidence that oxylipins mediated normal maize response to abiotic stresses. The role of 9-LOXs in this regulation through the control of JA-biosynthesis may be a universal mechanisms plant uses to promote increased drought tolerance (Figure 36A). In addition, *ZmLOX1* was found to regulates salt tolerance by mediating 10-OPEA biosynthesis (Figure 36B).

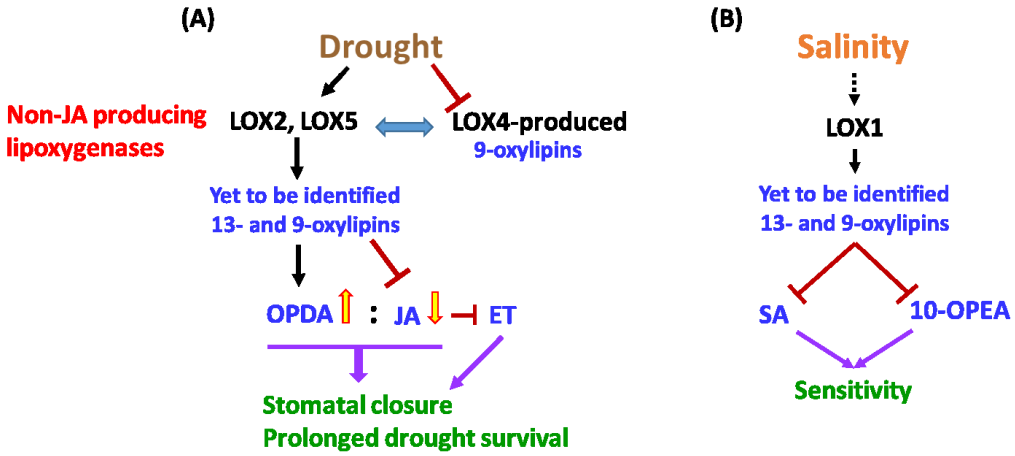


Figure 36. Proposed model of oxylipin signals mediated drought and salt stress responses in maize. (A) Metabolite profiling and RNA sequencing results suggest that *ZmLOX2* and *ZmLOX4* regulate maize drought responses in opposite manners by mediating the JA biosynthesis pathway and JA signaling to regulate stomatal aperture. ET acts antagonistically against JA to enhance stomatal closure. (B) *ZmLOX1* was found to regulates salt tolerance by mediating SA and 10-OPEA biosynthesis.

# CHAPTER V

# CONCLUSION

Plants generate various small signaling molecules to mediate responses upon pathogen infection and abiotic stresses. Oxylipins are a large group of lipid-derived molecular signals governing various biological process such as growth and development, abiotic stress responses, and microbe- and herbivore-induced defense responses. This study determined the biological function of two nontypical 13/9-LOXs, *ZmLOX1* and *ZmLOX2*, which possess dual positional specificity, and identified their roles in the interactions of maize with the hemi-biotrophic fungal pathogen *C. graminicola* in leaf and stalk. The second objective was to decipher the functions of oxylipins in mediating drought and salt stress tolerance in maize.

Recombinant ZmLOX1 protein contains approximately 70% 13-LOX and 30% 9-LOX activity *in vitro* at neutral pH conditions. ZmLOX1 and ZmLOX2 are not directly involved in wound-induced JA biosynthesis. Expression of *ZmLOX1* and *ZmLOX2* is significantly up-regulated by stress-related phytohormones including JA, ET, and ABA and mechanical wounding and treatment with GLV. Disruption of *ZmLOX1* and *ZmLOX2* caused significantly decreased resistance to *C. graminicola* in leaves associated with low levels of BA and SA accumulation. In contrast to that, in stalks, both *lox1-3* and *lox2-1* mutants were significantly more resistant to *C. graminicola* accompanied by significantly higher SA but lower 10-OPEA accumulation upon infection. These findings provide strong genetic evidence that dual positional

specific LOXs functions in the regulation of SA biosynthesis upon *C. graminicola* infection in an organ-specific manner by as-yet unknown mechanisms.

Other than plant-pathogen interactions, lipid signals also regulate plant abiotic stress responses. *lox2-1* had significantly higher transpirational water loss and failed to recover from prolonged drought stress. In contrast, *lox4* mutants exhibited reduced water loss and greater ability to recover from prolonged drought stress. Oxylipin and phytohormone profiling and transcriptome analysis suggest that the JA biosynthesis pathway was regulated by oxylipin signals produced by non-JA producing LOXs and that JA serves to open stomata. We provided strong genetic evidence that JA-deficient mutant *opr7-5 opr8-2* has smaller stomatal aperture and less transpirational water loss that can be restored by exogenous MeJA treatment. Increased ET production by *opr7-5 opr8-2* in response to drought stress is in agreement with higher transpirational water loss observed for ET-deficient *acs2 acs6* mutant suggesting ET enhances stomatal closure. Excessive amounts of SA and 10-OPEA accumulation in *lox1-3* is the most likely reason behind increased sensitivity to salt stress. This study shed new light on understanding the role of underexplored oxylipins produced by non-JA-producing LOXs in signaling maize responses to drought and salt stress.

Overall, the results from this study suggest that the rare LOXs possessing dual positional specificity have previously unknown function in regulating SA biosynthesis during plant-pathogen interaction in an organ-specific manner. In addition, this study also provides evidence that oxylipins are key regulators of abiotic stress tolerance.

## REFERENCES


**Ache, P., Becker, D., Ivashikina, N., Dietrich, P., Roelfsema, M.R., and Hedrich, R.** (2000). GORK, a delayed outward rectifier expressed in guard cells of *Arabidopsis thaliana*, is a K(+)-selective, K(+)-sensing ion channel. FEBS Lett **486,** 93-98.

**Acosta, I.F., Laparra, H., Romero, S.P., Schmelz, E., Hamberg, M., Mottinger, J.P., Moreno, M.A., and Dellaporta, S.L.** (2009). *tasselseed1* is a lipoxygenase affecting jasmonic acid signaling in sex determination of maize. Science **323,** 262-265.

**Almeida, G.D., Makumbi, D., Magorokosho, C., Nair, S., Borem, A., Ribaut, J.M., Banziger, M., Prasanna, B.M., Crossa, J., and Babu, R.** (2013). QTL mapping in three tropical maize populations reveals a set of constitutive and adaptive genomic regions for drought tolerance. Theor Appl Genet **126,** 583-600.

**Andreou, A., and Feussner, I.** (2009). Lipoxygenases - structure and reaction mechanism. Phytochemistry **70,** 1504-1510.

**Anjum, S.A., Tanveer, M., Ashraf, U., Hussain, S., Shahzad, B., Khan, I., and Wang, L.** (2016). Effect of progressive drought stress on growth, leaf gas exchange, and antioxidant production in two maize cultivars. Environ Sci Pollut Res Int **23,** 17132-17141.

**Avramova, Z.** (2017). The jasmonic acid-signalling and abscisic acid-signalling pathways cross talk during one, but not repeated, dehydration stress: a non-specific 'panicky' or a meaningful response? Plant Cell Environ **40,** 1704-1710.

**Balmer, D., de Papajewski, D.V., Planchamp, C., Glauser, G., and Mauch-Mani, B.** (2013). Induced resistance in maize is based on organ-specific defence responses. Plant J **74,** 213-225.

**Bergstrom, G.C. and .Nichilson, .R.L.** (1999). The biology of corn anthracnose: knowledge to exploit for improved management. Plant Disease **83,** 596-608.

**Bleecker, A.B., and Kende, H.** (2000). Ethylene: a gaseous signal molecule in plants. Annu Rev Cell Dev Biol **16,** 1-18.

**Boatwright, J.L., and Pajerowska-Mukhtar, K.** (2013). Salicylic acid: an old hormone up to new tricks. Molecular Plant Pathology **14,** 623-634.

**Borrego, E.J., and Kolomiets, M.V.** (2016). Synthesis and functions of jasmonates in maize. Plants (Basel) **5**, 1-25.

**Brenner, S., Johnson, M., Bridgham, J., Golda, G., Lloyd, D.H., Johnson, D., Luo, S., McCurdy, S., Foy, M., Ewan, M., Roth, R., George, D., Eletr, S., Albrecht, G., Vermaas, E., Williams, S.R., Moon, K., Burcham, T., Pallas, M., DuBridge, R.B., Kirchner, J., Fearon, K., Mao, J., and Corcoran, K.** (2000). Gene expression analysis by massively parallel signature sequencing (MPSS) on microbead arrays. Nat Biotechnol **18,** 630-634.

**Buchsenschutz, K., Marten, I., Becker, D., Philippar, K., Ache, P., and Hedrich, R.** (2005). Differential expression of K+ channels between guard cells and subsidiary cells within the maize stomatal complex. Planta **222,** 968-976.

**Chini, A., Ben-Romdhane, W., Hassairi, A., and Aboul-Soud, M.A.M.** (2017). Identification of TIFY/JAZ family genes in *Solanum lycopersicum* and their regulation in response to abiotic stresses. PLoS One **12,** e0177381.

**Cho, K., Kim, Y.C., Woo, J.C., Rakwal, R., Agrawal, G.K., Yoeun, S., and Han, O.** (2012). Transgenic expression of dual positional maize lipoxygenase-1 leads to the regulation of defense-related signaling molecules and activation of the antioxidative enzyme system in rice. Plant Sci **185-186,** 238-245.

**Cho, K., Han, Y., Woo, J.C., Baudisch, B., Klosgen, R.B., Oh, S., Han, J., and Han, O.** (2011). Cellular localization of dual positional specific maize lipoxygenase-1 in transgenic rice and calcium-mediated membrane association. Plant Sci **181,** 242-248.

**Christensen, S.A., Nemchenko, A., Park, Y.S., Borrego, E., Huang, P.C., Schmelz, E.A., Kunze, S., Feussner, I., Yalpani, N., Meeley, R., and Kolomiets, M.V.** (2014). The novel monocot-specific 9-lipoxygenase ZmLOX12 is required to mount an effective jasmonate-mediated defense against *Fusarium verticillioides* in maize. Mol Plant Microbe Interact **27,** 1263-1276.

**Christensen, S.A., Huffaker, A., Kaplan, F., Sims, J., Ziemann, S., Doehlemann, G., Ji, L., Schmitz, R.J., Kolomiets, M.V., Alborn, H.T., Mori, N., Jander, G., Ni, X., Sartor, R.C., Byers, S., Abdo, Z., and Schmelz, E.A.** (2015). Maize death acids, 9-lipoxygenase-derived cyclopente(a)nones, display activity as cytotoxic phytoalexins and transcriptional mediators. Proc Natl Acad Sci U S A **112,** 11407-11412.

**Christensen, S.A., Nemchenko, A., Borrego, E., Murray, I., Sobhy, I.S., Bosak, L., DeBlasio, S., Erb, M., Robert, C.A., Vaughn, K.A., Herrfurth, C., Tumlinson, J., Feussner, I., Jackson, D., Turlings, T.C., Engelberth, J., Nansen, C., Meeley, R., and Kolomiets, M.V.** (2013). The maize lipoxygenase, *ZmLOX10*, mediates green leaf volatile, jasmonate and herbivore-induced plant volatile production for defense against insect attack. Plant J **74,** 59-73.

**Chung, S.H., Rosa, C., Scully, E.D., Peiffer, M., Tooker, J.F., Hoover, K., Luthe, D.S., and Felton, G.W.** (2013). Herbivore exploits orally secreted bacteria to suppress plant defenses. Proc Natl Acad Sci U S A **110,** 15728-15733.

**Collins, N.C., Tardieu, F., and Tuberosa, R.** (2008). Quantitative trait loci and crop performance under abiotic stress: where do we stand? Plant Physiol **147,** 469-486.

**Constantino, N.N., Mastouri, F., Damarwinasis, R., Borrego, E.J., Moran-Diez, M.E., Kenerley, C.M., Gao, X., and Kolomiets, M.V.** (2013). Root-expressed maize lipoxygenase 3 negatively regulates induced systemic resistance to *Colletotrichum graminicola* in shoots. Front Plant Sci **4,** 510-521.

**Cruz de Carvalho, M.H.** (2008). Drought stress and reactive oxygen species: Production, scavenging and signaling. Plant Signal Behav **3,** 156-165.

**Daryanto, S., Wang, L., and Jacinthe, P.A.** (2016). Global synthesis of drought effects on maize and wheat production. PLoS One **11,** e0156362.

**de Ollas, C., and Dodd, I.C.** (2016). Physiological impacts of ABA-JA interactions under water-limitation. Plant Mol Biol **91,** 641-650.

**Dean, R., Van Kan, J.A., Pretorius, Z.A., Hammond-Kosack, K.E., Di Pietro, A., Spanu, P.D., Rudd, J.J., Dickman, M., Kahmann, R., Ellis, J., and Foster, G.D.** (2012). The Top 10 fungal pathogens in molecular plant pathology. Molecular Plant Pathology **13,** 414-430.

**Desikan, R., Last, K., Harrett-Williams, R., Tagliavia, C., Harter, K., Hooley, R., Hancock, J.T., and Neill, S.J.** (2006). Ethylene-induced stomatal closure in *Arabidopsis* occurs via AtrbohF-mediated hydrogen peroxide synthesis. Plant J **47,** 907-916.

**Dietrich, P., Sanders, D., and Hedrich, R.** (2001). The role of ion channels in light-dependent stomatal opening. J Exp Bot **52,** 1959-1967.

**Droillard, M.J., Rouet-Mayer, M.A., Bureau, J.M., and Lauriere, C.** (1993). Membrane-associated and soluble lipoxygenase isoforms in tomato pericarp (characterization and involvement in membrane alterations). Plant Physiol **103,** 1211-1219.

**Fahad, S., Bajwa, A.A., Nazir, U., Anjum, S.A., Farooq, A., Zohaib, A., Sadia, S., Nasim, W., Adkins, S., Saud, S., Ihsan, M.Z., Alharby, H., Wu, C., Wang, D., and Huang, J.** (2017). Crop production under drought and heat stress: plant responses and management options. Front Plant Sci **8,** 1147-1162.

**Feussner, I., and Wasternack, C.** (2002). The lipoxygenase pathway. Annu Rev Plant Biol **53,** 275-297.

**Fischer, G., Shah, M., Tubiello, F.N., and van Velhuizen, H.** (2005). Socio-economic and climate change impacts on agriculture: an integrated assessment, 1990-2080. Philos Trans R Soc Lond B Biol Sci **360,** 2067-2083.

**Fita, A., Rodriguez-Burruezo, A., Boscaiu, M., Prohens, J., and Vicente, O.** (2015). Breeding and domesticating crops adapted to drought and salinity: a new paradigm for increasing food production. Front Plant Sci **6,** 978-990.

**Flowers, T.J.** (2004). Improving crop salt tolerance. J Exp Bot **55,** 307-319.

**Frey, T.J., Weldekidan, T., Colbert, T., Wolters, P.J.C.C., and Hawk, J.A. .** (2011). Fitness evaluation of *Rcg1*, a locus that confers resistance to *Colletotrichum graminicola* (Ces.) G.W. Wils. using near-isogenic maize hybrids. CROP SCIENCE **2011,** 13.

**Funk, C.D.** (2001). Prostaglandins and leukotrienes: advances in eicosanoid biology. Science **294,** 1871-1875.

**Gao, X., Stumpe, M., Feussner, I., and Kolomiets, M.** (2008a). A novel plastidial lipoxygenase of maize (*Zea mays*) *ZmLOX6* encodes for a fatty acid hydroperoxide lyase and is uniquely regulated by phytohormones and pathogen infection. Planta **227,** 491-503.

**Gao, X., Starr, J., Gobel, C., Engelberth, J., Feussner, I., Tumlinson, J., and Kolomiets, M.** (2008b). Maize 9-lipoxygenase ZmLOX3 controls development, root-specific expression of defense genes, and resistance to root-knot nematodes. Mol Plant Microbe Interact **21,** 98-109.

**Gao, X., Shim, W.B., Gobel, C., Kunze, S., Feussner, I., Meeley, R., Balint-Kurti, P., and Kolomiets, M.** (2007). Disruption of a maize 9-lipoxygenase results in increased resistance to fungal pathogens and reduced levels of contamination with mycotoxin fumonisin. Mol Plant Microbe Interact **20,** 922-933.

**Gao, X., Brodhagen, M., Isakeit, T., Brown, S.H., Gobel, C., Betran, J., Feussner, I., Keller, N.P., and Kolomiets, M.V.** (2009). Inactivation of the lipoxygenase *ZmLOX3* increases susceptibility of maize to *Aspergillus* spp. Mol Plant Microbe Interact **22,** 222-231.

**Ge, X.M., Cai, H.L., Lei, X., Zhou, X., Yue, M., and He, J.M.** (2015). Heterotrimeric G protein mediates ethylene-induced stomatal closure via hydrogen peroxide synthesis in *Arabidopsis*. Plant J **82,** 138-150.

**Gimenez-Ibanez, S., Boter, M., Ortigosa, A., Garcia-Casado, G., Chini, A., Lewsey, M.G., Ecker, J.R., Ntoukakis, V., and Solano, R.** (2017). JAZ2 controls stomata dynamics during bacterial invasion. New Phytol **213,** 1378-1392.

**Glazebrook, J.** (2005). Contrasting mechanisms of defense against biotrophic and necrotrophic pathogens. Annu Rev Phytopathol **43,** 205-227.

**Goodspeed, D., Chehab, E.W., Min-Venditti, A., Braam, J., and Covington, M.F.** (2012). *Arabidopsis* synchronizes jasmonate-mediated defense with insect circadian behavior. Proc Natl Acad Sci U S A **109,** 4674-4677.

**Gou, W., Zheng, P., Tian, L., Gao, M., Zhang, L., Akram, N.A., and Ashraf, M.** (2017). Exogenous application of urea and a urease inhibitor improves drought stress tolerance in maize (*Zea mays* L.). J Plant Res **130,** 599-609.

**Grebner, W., Stingl, N.E., Oenel, A., Mueller, M.J., and Berger, S.** (2013). Lipoxygenase6-dependent oxylipin synthesis in roots is required for abiotic and biotic stress resistance of *Arabidopsis*. Plant Physiol **161,** 2159-2170.

**Hanin, M., Ebel, C., Ngom, M., Laplaze, L., and Masmoudi, K.** (2016). New insights on plant salt tolerance mechanisms and their potential use for breeding. Front Plant Sci **7,** 1787-1803.

**Hossain, M.A., Munemasa, S., Uraji, M., Nakamura, Y., Mori, I.C., and Murata, Y.** (2011). Involvement of endogenous abscisic acid in methyl jasmonate-induced stomatal closure in *Arabidopsis*. Plant Physiol **156,** 430-438.

**Hosy, E., Vavasseur, A., Mouline, K., Dreyer, I., Gaymard, F., Poree, F., Boucherez, J., Lebaudy, A., Bouchez, D., Very, A.A., Simonneau, T., Thibaud, J.B., and Sentenac, H.** (2003). The *Arabidopsis* outward K+ channel *GORK* is involved in regulation of stomatal movements and plant transpiration. Proc Natl Acad Sci U S A **100,** 5549-5554.

**Howe, G.A., and Schilmiller, A.L.** (2002). Oxylipin metabolism in response to stress. Curr Opin Plant Biol **5,** 230-236.

**Hwang, I.S., and Hwang, B.K.** (2010). The pepper 9-lipoxygenase gene *CaLOX1* functions in defense and cell death responses to microbial pathogens. Plant Physiol **152,** 948-967.

**Kilaru, A., Herrfurth, C., Keereetaweep, J., Hornung, E., Venables, B.J., Feussner, I., and Chapman, K.D.** (2011). Lipoxygenase-mediated oxidation of polyunsaturated *N*-acylethanolamines in *Arabidopsis*. J Biol Chem **286,** 15205-15214.

**Kim, E.S., Choi, E., Kim, Y., Cho, K., Lee, A., Shim, J., Rakwal, R., Agrawal, G.K., and Han, O.** (2003). Dual positional specificity and expression of non-traditional lipoxygenase induced by wounding and methyl jasmonate in maize seedlings. Plant Mol Biol **52,** 1203-1213.

**Kumar, D.** (2014). Salicylic acid signaling in disease resistance. Plant Sci **228,** 127-134.

**Leon, J., Shulaev, V., Yalpani, N., Lawton, M.A., and Raskin, I.** (1995). Benzoic acid 2-hydroxylase, a soluble oxygenase from tobacco, catalyzes salicylic acid biosynthesis. Proc Natl Acad Sci U S A **92,** 10413-10417.

**Lim, C.W., Han, S.W., Hwang, I.S., Kim, D.S., Hwang, B.K., and Lee, S.C.** (2015). The pepper lipoxygenase CaLOX1 plays a role in osmotic, drought and high salinity stress response. Plant Cell Physiol **56,** 930-942.

**Liu, N., and Avramova, Z.** (2016). Molecular mechanism of the priming by jasmonic acid of specific dehydration stress response genes in *Arabidopsis*. Epigenetics Chromatin **9,** 8-30.

**Lu, Y., Li, Y., Zhang, J., Xiao, Y., Yue, Y., Duan, L., Zhang, M., and Li, Z.** (2013). Overexpression of *Arabidopsis* molybdenum cofactor sulfurase gene confers drought tolerance in maize (*Zea mays* L.). PLoS One **8,** e52126.

**Marcos, R., Izquierdo, Y., Vellosillo, T., Kulasekaran, S., Cascon, T., Hamberg, M., and Castresana, C.** (2015). 9-Lipoxygenase-derived oxylipins activate brassinosteroid signaling to promote cell wall-based defense and limit pathogen infection. Plant Physiol **169,** 2324-2334.

**McKersie, B.** (2015). Planning for food security in a changing climate. J Exp Bot **66,** 3435-3450.

**Meeks, M., Murray, S., Hague, S., and Hays, D.** (2013). Measuring maize seedling drought response in search of tolerant germplasm. Agronomy **3,** 135-147.

**Meeley, R.B., and Briggs, S.P.** (1995). Reverse genetics for maize. Maize Genet. Coop. Newsl. **69,** 67-82.

**Miranda, V.J., Porto, W.F., Fernandes, G.D.R., Pogue, R., Nolasco, D.O., Araujo, A.C.G., Cota, L.V., Freitas, C.G., Dias, S.C., and Franco, O.L.** (2017). Comparative transcriptomic analysis indicates genes associated with local and systemic resistance to *Colletotrichum graminicola* in maize. Sci Rep **7,** 2483-2496.

**Miura, K., and Tada, Y.** (2014). Regulation of water, salinity, and cold stress responses by salicylic acid. Front Plant Sci **5,** 4-15.

**Montillet, J.L., Leonhardt, N., Mondy, S., Tranchimand, S., Rumeau, D., Boudsocq, M., Garcia, A.V., Douki, T., Bigeard, J., Lauriere, C., Chevalier, A., Castresana, C., and Hirt, H.** (2013). An abscisic acid-independent oxylipin pathway controls stomatal closure and immune defense in *Arabidopsis*. PLoS Biol **11,** e1001513.

**Moon, S.J., Kim, H.Y., Hwang, H., Kim, J.A., Lee, Y., Min, M.K., Yoon, I.S., Kwon, T.R., and Kim, B.G.** (2017). A dominant negative OsKAT2 mutant delays light-induced stomatal opening and improves drought tolerance without yield penalty in rice. Front Plant Sci **8,** 772-780.

**Munemasa, S., Oda, K., Watanabe-Sugimoto, M., Nakamura, Y., Shimoishi, Y., and Murata, Y.** (2007). The *coronatine-insensitive 1* mutation reveals the hormonal signaling interaction between abscisic acid and methyl jasmonate in *Arabidopsis* guard cells. Specific impairment of ion channel activation and second messenger production. Plant Physiol **143,** 1398-1407.

**Mur, L.A., Kenton, P., Atzorn, R., Miersch, O., and Wasternack, C.** (2006). The outcomes of concentration-specific interactions between salicylate and jasmonate signaling include synergy, antagonism, and oxidative stress leading to cell death. Plant Physiol **140,** 249-262.

**Nalam, V.J., Alam, S., Keereetaweep, J., Venables, B., Burdan, D., Lee, H., Trick, H.N., Sarowar, S., Makandar, R., and Shah, J.** (2015). Facilitation of *Fusarium graminearum* infection by 9-lipoxygenases in *Arabidopsis* and wheat. Mol Plant Microbe Interact **28,** 1142-1152.

**Nemchenko, A., Kunze, S., Feussner, I., and Kolomiets, M.** (2006). Duplicate maize 13-lipoxygenase genes are differentially regulated by circadian rhythm, cold stress, wounding, pathogen infection, and hormonal treatments. J Exp Bot **57,** 3767-3779.

**Owens, S.** (2001). Salt of the earth. Genetic engineering may help to reclaim agricultural land lost due to salinisation. EMBO Rep **2,** 877-879.

**Park, Y.S., Kunze, S., Ni, X., Feussner, I., and Kolomiets, M.V.** (2010). Comparative molecular and biochemical characterization of segmentally duplicated 9-lipoxygenase genes *ZmLOX4* and *ZmLOX5* of maize. Planta **231,** 1425-1437.

**Porta, H., and Rocha-Sosa, M.** (2002). Plant lipoxygenases. Physiological and molecular features. Plant Physiol **130,** 15-21.

**Ranum, P., Pena-Rosas, J.P., and Garcia-Casal, M.N.** (2014). Global maize production, utilization, and consumption. Annals of the New York Academy of Sciences **1312,** 105-112.

**Ruggiero, B., Koiwa, H., Manabe, Y., Quist, T.M., Inan, G., Saccardo, F., Joly, R.J., Hasegawa, P.M., Bressan, R.A., and Maggio, A.** (2004). Uncoupling the effects of abscisic acid on plant growth and water relations. Analysis of *sto1*/*nced3*, an abscisic acid-deficient but salt stress-tolerant mutant in *Arabidopsis*. Plant Physiol **136,** 3134-3147.

**Saab, I.N., Sharp, R.E., Pritchard, J., and Voetberg, G.S.** (1990). Increased endogenous abscisic acid maintains primary root growth and inhibits shoot growth of maize seedlings at low water potentials. Plant Physiol **93,** 1329-1336.

**Savchenko, T., Kolla, V.A., Wang, C.Q., Nasafi, Z., Hicks, D.R., Phadungchob, B., Chehab, W.E., Brandizzi, F., Froehlich, J., and Dehesh, K.** (2014). Functional convergence of oxylipin and abscisic acid pathways controls stomatal closure in response to drought. Plant Physiol **164,** 1151-1160.

**Schiller, D., Contreras, C., Vogt, J., Dunemann, F., Defilippi, B.G., Beaudry, R., and Schwab, W.** (2015). A dual positional specific lipoxygenase functions in the generation of flavor compounds during climacteric ripening of apple. Hortic Res **2,** 15003.

**Schnable, P.S., Ware, D., Fulton, R.S., Stein, J.C., Wei, F., Pasternak, S., Liang, C., Zhang, J., Fulton, L., Graves, T.A., Minx, P., Reily, A.D., Courtney, L., Kruchowski, S.S., Tomlinson, C., Strong, C., Delehaunty, K., Fronick, C., Courtney, B., Rock, S.M., Belter, E., Du, F., Kim, K., Abbott, R.M., Cotton, M., Levy, A., Marchetto, P., Ochoa, K., Jackson, S.M., Gillam, B., Chen, W., Yan, L., Higginbotham, J., Cardenas, M., Waligorski, J., Applebaum, E., Phelps, L., Falcone, J., Kanchi, K., Thane, T., Scimone, A., Thane, N., Henke, J., Wang, T., Ruppert, J., Shah, N., Rotter, K., Hodges, J., Ingenthron, E., Cordes, M., Kohlberg, S., Sgro, J., Delgado, B., Mead, K., Chinwalla, A., Leonard, S., Crouse, K., Collura, K., Kudrna, D., Currie, J., He, R., Angelova, A., Rajasekar, S., Mueller, T., Lomeli, R., Scara, G., Ko, A., Delaney, K., Wissotski, M., Lopez, G., Campos, D., Braidotti, M., Ashley, E., Golser, W., Kim, H., Lee, S., Lin, J., Dujmic, Z., Kim, W., Talag, J., Zuccolo, A., Fan, C., Sebastian, A., Kramer, M., Spiegel, L., Nascimento, L., Zutavern, T., Miller, B., Ambroise, C., Muller, S., Spooner, W., Narechania, A., Ren, L., Wei, S., Kumari, S., Faga, B., Levy, M.J., McMahan, L., Van Buren, P., Vaughn, M.W., Ying, K., Yeh, C.T., Emrich, S.J., Jia, Y., Kalyanaraman, A., Hsia, A.P., Barbazuk, W.B., Baucom, R.S., Brutnell, T.P., Carpita, N.C., Chaparro, C., Chia, J.M., Deragon, J.M., Estill, J.C., Fu, Y., Jeddeloh, J.A., Han, Y., Lee, H., Li, P., Lisch, D.R., Liu, S., Liu, Z., Nagel, D.H., McCann, M.C., SanMiguel, P., Myers, A.M., Nettleton, D., Nguyen, J., Penning, B.W., Ponnala, L., Schneider, K.L., Schwartz, D.C., Sharma, A., Soderlund, C., Springer, N.M., Sun, Q., Wang, H., Waterman, M., Westerman, R., Wolfgruber, T.K., Yang, L., Yu, Y., Zhang, L., Zhou, S.,**

**Zhu, Q., Bennetzen, J.L., Dawe, R.K., Jiang, J., Jiang, N., Presting, G.G., Wessler, S.R., Aluru, S., Martienssen, R.A., Clifton, S.W., McCombie, W.R., Wing, R.A., and Wilson, R.K.** (2009). The B73 maize genome: complexity, diversity, and dynamics. Science **326,** 1112-1115.

**Semagn, K., Beyene, Y., Warburton, M.L., Tarekegne, A., Mugo, S., Meisel, B., Sehabiague, P., and Prasanna, B.M.** (2013). Meta-analyses of QTL for grain yield and anthesis silking interval in 18 maize populations evaluated under water-stressed and well-watered environments. BMC Genomics **14,** 313-328.

**Sharp, R.E., and LeNoble, M.E.** (2002). ABA, ethylene and the control of shoot and root growth under water stress. J Exp Bot **53,** 33-37.

**Shrestha, R., Noordermeer, M.A., van der Stelt, M., Veldink, G.A., and Chapman, K.D.** (2002). *N*-acylethanolamines are metabolized by lipoxygenase and amidohydrolase in competing pathways during cottonseed imbibition. Plant Physiol **130,** 391-401.

**Shrivastava, P., and Kumar, R.** (2015). Soil salinity: a serious environmental issue and plant growth promoting bacteria as one of the tools for its alleviation. Saudi J Biol Sci **22,** 123-131.

**Skibbe, D.S., Doehlemann, G., Fernandes, J., and Walbot, V.** (2010). Maize tumors caused by *Ustilago maydis* require organ-specific genes in host and pathogen. Science **328,** 89-92.

**Smith, P., and Gregory, P.J.** (2013). Climate change and sustainable food production. Proc Nutr Soc **72,** 21-28.

**Sofo, A., Dichio, B., Xiloyannis, C., and Masia, A.** (2004). Lipoxygenase activity and proline accumulation in leaves and roots of olive trees in response to drought stress. Physiol Plant **121,** 58-65.

**Spoel, S.H., Johnson, J.S., and Dong, X.** (2007). Regulation of tradeoffs between plant defenses against pathogens with different lifestyles. Proc Natl Acad Sci U S A **104,** 18842-18847.

**Spollen, W.G., LeNoble, M.E., Samuels, T.D., Bernstein, N., and Sharp, R.E.** (2000). Abscisic acid accumulation maintains maize primary root elongation at low water potentials by restricting ethylene production. Plant Physiol **122,** 967-976.

**Suhita, D., Raghavendra, A.S., Kwak, J.M., and Vavasseur, A.** (2004). Cytoplasmic alkalization precedes reactive oxygen species production during methyl

jasmonate- and abscisic acid-induced stomatal closure. Plant Physiol **134,** 1536-1545.

**Szyroki, A., Ivashikina, N., Dietrich, P., Roelfsema, M.R., Ache, P., Reintanz, B., Deeken, R., Godde, M., Felle, H., Steinmeyer, R., Palme, K., and Hedrich, R.** (2001). KAT1 is not essential for stomatal opening. Proc Natl Acad Sci U S A **98,** 2917-2921.

**Tanaka, Y., Sano, T., Tamaoki, M., Nakajima, N., Kondo, N., and Hasezawa, S.** (2005). Ethylene inhibits abscisic acid-induced stomatal closure in *Arabidopsis*. Plant Physiol **138,** 2337-2343.

**Thines, B., Katsir, L., Melotto, M., Niu, Y., Mandaokar, A., Liu, G., Nomura, K., He, S.Y., Howe, G.A., and Browse, J.** (2007). JAZ repressor proteins are targets of the SCF(COI1) complex during jasmonate signalling. Nature **448,** 661-665.

**Vellosillo, T., Martinez, M., Lopez, M.A., Vicente, J., Cascon, T., Dolan, L., Hamberg, M., and Castresana, C.** (2007). Oxylipins produced by the 9-lipoxygenase pathway in *Arabidopsis* regulate lateral root development and defense responses through a specific signaling cascade. Plant Cell **19,** 831-846.

**Verhage, A., Vlaardingerbroek, I., Raaymakers, C., Van Dam, N.M., Dicke, M., Van Wees, S.C., and Pieterse, C.M.** (2011). Rewiring of the jasmonate signaling pathway in *Arabidopsis* during insect herbivory. Front Plant Sci **2,** 47-58.

**Wasternack, C.** (2007). Jasmonates: an update on biosynthesis, signal transduction and action in plant stress response, growth and development. Ann Bot **100,** 681-697.

**Wasternack, C.** (2017). The Trojan horse coronatine: the COI1-JAZ2-MYC2,3,4-ANAC019,055,072 module in stomata dynamics upon bacterial infection. New Phytol **213,** 972-975.

**Woodward, G., Bonada, N., Brown, L.E., Death, R.G., Durance, I., Gray, C., Hladyz, S., Ledger, M.E., Milner, A.M., Ormerod, S.J., Thompson, R.M., and Pawar, S.** (2016). The effects of climatic fluctuations and extreme events on running water ecosystems. Philos Trans R Soc Lond B Biol Sci **371**, 1-15.

**Yalpani, N., Leon, J., Lawton, M.A., and Raskin, I.** (1993). Pathway of salicylic acid biosynthesis in healthy and virus-inoculated tobacco. Plant Physiol **103,** 315-321.

**Yan, Y., Huang, P.C., Borrego, E., and Kolomiets, M.** (2014). New perspectives into jasmonate roles in maize. Plant Signal Behav **9,** e970442.

**Yan, Y., Christensen, S., Isakeit, T., Engelberth, J., Meeley, R., Hayward, A., Emery, R.J., and Kolomiets, M.V.** (2012). Disruption of *OPR7* and *OPR8* reveals the versatile functions of jasmonic acid in maize development and defense. Plant Cell **24,** 1420-1436.

**Ye, H., Du, H., Tang, N., Li, X., and Xiong, L.** (2009). Identification and expression profiling analysis of *TIFY* family genes involved in stress and phytohormone responses in rice. Plant Mol Biol **71,** 291-305.

**Young, T.E., Meeley, R.B., and Gallie, D.R.** (2004). ACC synthase expression regulates leaf performance and drought tolerance in maize. Plant J **40,** 813-825.

**Zhang, J., Simmons, C., Yalpani, N., Crane, V., Wilkinson, H., and Kolomiets, M.** (2005). Genomic analysis of the 12-oxo-phytodienoic acid reductase gene family of *Zea mays*. Plant Mol Biol **59,** 323-343.

**Zhang, X., Zhu, Z., An, F., Hao, D., Li, P., Song, J., Yi, C., and Guo, H.** (2014). Jasmonate-activated MYC2 represses ETHYLENE INSENSITIVE3 activity to antagonize ethylene-promoted apical hook formation in *Arabidopsis*. Plant Cell **26,** 1105-1117.

**Zhao, G., Song, Y., Wang, C., Butt, H.I., Wang, Q., Zhang, C., Yang, Z., Liu, Z., Chen, E., Zhang, X., and Li, F.** (2016). Genome-wide identification and functional analysis of the *TIFY* gene family in response to drought in cotton. Molecular genetics and genomics : MGG **291,** 2173-2187.

**Zheng, X.Y., Spivey, N.W., Zeng, W., Liu, P.P., Fu, Z.Q., Klessig, D.F., He, S.Y., and Dong, X.** (2012). Coronatine promotes *Pseudomonas syringae* virulence in plants by activating a signaling cascade that inhibits salicylic acid accumulation. Cell Host Microbe **11,** 587-596.

**Zhu, Z., An, F., Feng, Y., Li, P., Xue, L., A, M., Jiang, Z., Kim, J.M., To, T.K., Li, W., Zhang, X., Yu, Q., Dong, Z., Chen, W.Q., Seki, M., Zhou, J.M., and Guo, H.** (2011). Derepression of ethylene-stabilized transcription factors (EIN3/EIL1) mediates jasmonate and ethylene signaling synergy in *Arabidopsis*. Proc Natl Acad Sci U S A **108,** 12539-12544.